



저작자표시-비영리-동일조건변경허락 2.0 대한민국

이용자는 아래의 조건을 따르는 경우에 한하여 자유롭게

- 이 저작물을 복제, 배포, 전송, 전시, 공연 및 방송할 수 있습니다.
- 이차적 저작물을 작성할 수 있습니다.

다음과 같은 조건을 따라야 합니다:



저작자표시. 귀하는 원 저작자를 표시하여야 합니다.



비영리. 귀하는 이 저작물을 영리 목적으로 이용할 수 없습니다.



동일조건변경허락. 귀하가 이 저작물을 개작, 변형 또는 가공했을 경우에는, 이 저작물과 동일한 이용허락조건하에서만 배포할 수 있습니다.

- 귀하는, 이 저작물의 재이용이나 배포의 경우, 이 저작물에 적용된 이용허락조건을 명확하게 나타내어야 합니다.
- 저작권자로부터 별도의 허가를 받으면 이러한 조건들은 적용되지 않습니다.

저작권법에 따른 이용자의 권리는 위의 내용에 의하여 영향을 받지 않습니다.

이것은 [이용허락규약\(Legal Code\)](#)을 이해하기 쉽게 요약한 것입니다.

[Disclaimer](#)



공학박사학위논문

**An Experimental Study of  
Horizontal Behavior of Group  
Suction Piles in Sand**

사질토 지반에 근입된 그룹형 석션파일의  
수평방향 거동에 대한 실험적 고찰

2014년 8월

서울대학교 대학원  
건설환경공학부  
이주형

# An Experimental Study of Horizontal Behavior of Group Suction Piles in Sand

지도 교수 김명모

이 논문을 공학박사 학위논문으로 제출함

2014년 7월

서울대학교 대학원  
건설환경공학부  
이주형

이주형의 공학박사 학위논문을 인준함

2014년 6월

위원장 정충기 (인)

부위원장 김명모 (인)

위원 박준범 (인)

위원 조성원 (인)

위원 김정환 (인)

## **ABSTRACT**

# **An Experimental Study of Horizontal Behavior of Group Suction Piles in Sand**

Lee, Ju Hyung

Department of Civil & Environmental Engineering  
The Graduate School  
Seoul National University

In this study, a new type of suction pile as foundations of recently-developed massive and hybrid types of floating structures, group suction piles were proposed to improve the shortcomings of conventional single suction piles. Small scaled model tests were performed to investigate the better performance of the newly developed group suction piles and to estimate its horizontal behavior. To minimize the inherent limitation of small-scale model tests, the model suction piles were manufactured considering the similarity in their geometries, equivalent flexural and axial rigidities, and interface problems (in terms of relative roughness between model pile and sands). Furthermore, for more accurate component behavior analysis (in terms of vertical and horizontal movement as well as rotation) of large-displacement suction pile behavior, Particle Image Velocimetry (PIV) analysis is implemented.

To secure repeatability of the experimental method and to verify the efficiency of the group suction piles, preliminary single suction pile

tests were performed under various loading conditions. For the single suction pile, the effect of suction installation method on its ultimate horizontal capacity was evaluated from the model tests and the change of its ultimate horizontal capacity under various combinations of loading location and load inclination was analyzed. The test results of single suction piles were compared with the estimations based on the typically-used equations proposed by other researcher.

From the group suction piles model tests, their horizontal behavior was examined for various loading locations, load inclinations, and component pile spacings. In addition, the effect of cyclic loading on the ultimate and residual horizontal resistances was analyzed. The group effect of group suction piles was assessed by measuring load distribution ratios of component piles.

Strong linear relationship between ultimate horizontal capacity and pile rotation was identified for both single and group suction piles. The rotations of suction piles against horizontal loads were much smaller for group type than for single type. The horizontal resistances of single suction piles rapidly decrease and converge to zero after their ultimate capacities, while considerable residual horizontal resistances were identified for the group suction piles. The residual resistances of group suction piles range from 40% ~ 75% of their ultimate capacities. From the results of the load distributions of component piles, the horizontal resistance for group suction piles increased with an increasing component pile spacing. Moreover, it is expected the group effect on the ultimate horizontal resistance is not significant for the group suction piles with pile spacing larger than 4 times their pile diameters.

As results, the newly proposed group suction piles in this study effectively resists against horizontal loading regardless of loading location and load inclination (0 and 20 degrees with respect to the

horizontal direction) without significant rotation, compared to the case of a single suction pile. Therefore, under horizontal loading conditions, the group suction piles can be considered a more favorable foundation type as a foundation of floating structures compared to the conventional single suction piles.

**Keywords : suction pile, group suction piles, horizontal behavior, model test, PIV analysis, group effect**

*Student Number : 2010-31010*

## **TABLE OF CONTENTS**

<b>ABSTRACT .....</b>	<b>i</b>
<b>TABLE OF CONTENTS .....</b>	<b>iv</b>
<b>LIST OF TABLES .....</b>	<b>viii</b>
<b>LIST OF FIGURES .....</b>	<b>x</b>
<b>LIST OF SYMBOLS .....</b>	<b>xv</b>
<b>Chapter 1 Introduction .....</b>	<b>1</b>
1.1 Overview .....	1
1.2 Suction pile .....	4
1.2.1 Definition .....	4
1.2.2 Installation mechanism .....	6
1.3 Group suction piles .....	10
1.3.1 Definition .....	10
1.3.2 Installation method .....	12
1.3.3 Weakness and limitation of group suction piles .....	13
1.4 Objectives .....	15
1.5 Organization of dissertation .....	17
<b>Chapter 2 Literature review .....</b>	<b>19</b>
2.1 History of field applications .....	19

2.2 History of research studies .....	21
2.3 Recent research on horizontally loaded single suction pile .....	24
2.4 Recent research on horizontally loaded group pile .....	34

## **Chapter 3 Experimental setup ..... 41**

3.1 Introduction .....	41
3.2 Test equipment .....	42
3.2.1 Soil chamber .....	42
3.2.2 Horizontal loading system .....	45
3.2.3 Vibrating compaction system .....	47
3.2.4 Micro-cone penetration test .....	49
3.2.5 PIV method .....	54
3.3 Model pile on the test .....	57
3.3.1 Design and instrumentation .....	57
3.3.2 Surface roughness of model pile .....	69
3.4 Soil conditions .....	72
3.4.1 Engineering properties of the test sand .....	72
3.4.2 Size effect .....	75
3.4.3 Internal scale effect .....	80
3.4.4 Target relative density .....	81

## **Chapter 4 Model tests on single suction pile ..... 83**

4.1 Introduction .....	83
4.2 Test program .....	86
4.3 Test results and discussion .....	88

4.3.1 Reliability of the test results .....	88
4.3.2 Effect of installation method .....	92
4.3.3 Effect of loading conditions .....	95
4.4 Summary .....	104

## **Chapter 5 Model tests on group suction piles ..... 105**

5.1 Introduction .....	105
5.2 Test program .....	105
5.3 Test results and discussion .....	107
5.3.1 Effect of loading conditions .....	107
5.3.2 Effect of pile spacing .....	128
5.3.3 Group effect .....	131
5.4 Summary .....	133

## **Chapter 6 Interpretation of model test results ..... 135**

6.1 Introduction .....	135
6.2 Ultimate horizontal resistance .....	136
6.2.1 Ultimate horizontal bearing capacity of rigid pile .....	136
6.2.2 Single suction pile .....	144
6.2.3 Group suction piles .....	147
6.2.4 Group effect .....	150
6.3 Comparison of single and group pile .....	152
6.3.1 Effect of loading conditions .....	152
6.3.2 Effect of pile spacing .....	156
6.4 Cost analysis .....	158

6.5 Summary .....	164
-------------------	-----

**Chapter 7 Summary and conclusions ..... 167**

7.1 Summary .....	167
7.2 Conclusions and recommendations .....	171
7.2.1 Conclusions .....	171
7.2.2 Recommendations .....	174

**References ..... 177**

**초 록 ..... 195**

## LIST OF TABLES

Table 2.1 Horizontal resistance according to various loading locations from previous research .....	32
Table 2.2 Horizontal resistance according to various loading angles from previous research .....	33
Table 2.3 P-multiplier values of group pile .....	37
Table 3.1 Classification of Broms' method .....	58
Table 3.2 Material properties of iron and aluminum .....	58
Table 3.3 Test result of surface roughness .....	70
Table 3.4 Soil properties .....	73
Table 3.5 Internal friction angle ( $^{\circ}$ ) of Joomunjin Standard Sand .....	73
Table 3.6 Input properties .....	78
Table 4.1 Loading angle and loading location of suction piles in Catenary mooring system .....	85
Table 4.2 Test program for single suction pile .....	87
Table 4.3 Ultimate horizontal earth pressure by pressure sensor and Broms' equation .....	91
Table 5.1 Test program for group suction piles .....	106
Table 5.2 Cyclic testing program .....	126
Table 5.3 Load distribution factor for 2D spacing .....	131
Table 5.4 Load distribution factor for 3D spacing .....	131
Table 5.5 Load distribution factor for 4D spacing .....	131
Table 6.1 Comparison of the measured ultimate horizontal resistances with the calculated resistances of block-assumed group suction piles .....	149
Table 6.2 Calculation procedure for estimating group effect .....	151
Table 6.3 Calculation results of group effect .....	151
Table 6.4 Summarized comparison results of ultimate horizontal	

resistance .....	157
Table 6.5 Equivalent number of piles based on the comparison of the ultimate horizontal capacities .....	158
Table 6.6 Calculation table of economic analysis .....	161
Table 6.7 Calculation procedure of economic analysis .....	162

## LIST OF FIGURES

Fig. 1.1 Definition of the suction pile components .....	4
Fig. 1.2 Installation procedure of the suction pile .....	6
Fig. 1.3 Installation mechanism of suction pile .....	7
Fig. 1.4 Optimum design pressure difference (Bang and Cho, 2003) .....	9
Fig. 1.5 Scheme of group suction piles .....	10
Fig. 1.6 An example of the installation of $3 \times 3$ group suction piles .....	12
Fig. 2.1 Three-dimensional soil failure wedge (Bang et al., 2001) .....	25
Fig. 2.2 Stresses along pile circumference (Bang et al., 2001) .....	26
Fig. 2.3 Caisson capacity measured in horizontal load tests (Coffman et al., 2004) .....	28
Fig. 2.4 Measured model suction pile pullout loading capacity .....	29
Fig. 2.5 The distribution of excess pore pressure along depth under different amplitudes (Lu et al., 2007) .....	31
Fig. 2.6 Illustration of reduction in the lateral pile resistance due to interference with trailing row shear zones (Broms et al., 1988) .....	34
Fig. 2.7 P-multiplier concept for pile group effects (McVay et al., 1995) .....	35
Fig. 2.8 Scheme of Hybrid foundation concept (Biene et al., 2012) .....	38
Fig. 2.9 Suction hybrid foundation (Jee et al., 2013) .....	39
Fig. 3.1 Scheme of testing system .....	42
Fig. 3.2 Soil chamber .....	43
Fig. 3.3 Soil chamber located away from the upper plate .....	44
Fig. 3.4 Soil chamber located under the upper plate .....	44
Fig. 3.5 Load actuator .....	45
Fig. 3.6 Submerged load cell .....	46
Fig. 3.7 Scheme of vibrating system .....	47

Fig. 3.8	Vibrator .....	47
Fig. 3.9	Installed vibrator on the upper plate .....	48
Fig. 3.10	Micro strain gauges of the cone .....	49
Fig. 3.11	Scheme of micro-cone .....	50
Fig. 3.12	Electric circuit of Wheaston Bridge .....	51
Fig. 3.13	Micro-cone and pushing rod .....	51
Fig. 3.14	Thrust mechanism .....	51
Fig. 3.15	Installed penetrometer (left) and connected micro-cone (right)	
	.....	52
Fig. 3.16	Power supply (E3630A model) .....	52
Fig. 3.17	Multimeter (34401A model) .....	53
Fig. 3.18	Data logger .....	53
Fig. 3.19	Scheme of PIV method .....	54
Fig. 3.20	Scheme of the two methods of PIV .....	55
Fig. 3.21	Observed image with tracking black points .....	56
Fig. 3.22	Scheme of initial plan .....	57
Fig. 3.23	Scheme of single suction model pile .....	59
Fig. 3.24	Initial version of the model pile .....	60
Fig. 3.25	Installing problem on initial version of model pile .....	61
Fig. 3.26	Install wire (First) .....	62
Fig. 3.27	Penetrate model pile (Second) .....	62
Fig. 3.28	Draw model pile by wire (Third) .....	63
Fig. 3.29	Second version of model pile and inducing jig .....	63
Fig. 3.30	Scheme of the final version of model pile .....	64
Fig. 3.31	Final version of model pile .....	64
Fig. 3.32	Group suction piles (3D) .....	65
Fig. 3.33	Scheme of installed group suction piles (4D) .....	65
Fig. 3.34	Scheme of side view of group suction piles .....	66
Fig. 3.35	Scheme of plain view of group suction piles .....	66
Fig. 3.36	Attached earth pressure cell .....	67
Fig. 3.37	Attached inducing jig on third row .....	67

Fig. 3.38 Schematic expression of surface roughness (Leland and Kraft, 1991) .....	69
Fig. 3.39 Original model pile .....	71
Fig. 3.40 Sand blasted model pile .....	71
Fig. 3.41 Grain size distribution curve .....	72
Fig. 3.42 Axial and volumetric strain Dr 70% .....	74
Fig. 3.43 Axial strain and deviatoric stress Dr 70% .....	74
Fig. 3.44 Scheme of installed model pile .....	76
Fig. 3.45 FE meshes and boundary conditions .....	77
Fig. 3.46 Horizontal load-movement curves at the top of the foundation .....	79
Fig. 4.1 Effect of seepage gradient on soil effective stress (Manh, 2005) .....	84
Fig. 4.2 Loading conditions of suction piles in Catenary mooring system .....	85
Fig. 4.3 Results of horizontal pull-out tests of a single suction pile ..	89
Fig. 4.4 Horizontal resistance-displacement curves of suction piles installed by suction pressure and jacking force .....	92
Fig. 4.5 CPT results of inside and outside on suction pile by different installations .....	93
Fig. 4.6 Horizontal resistances and normalized displacements of single suction pile with different loading locations .....	95
Fig. 4.7 Summarized ultimate resistances with different loading locations .....	96
Fig. 4.8 The PIV analysis results of horizontal behavior on single suction pile with different loading locations with no inclination .....	98
Fig. 4.9 Scheme of behavior on single suction pile .....	100
Fig. 4.10 Horizontal resistance and normalized displacement with different loading locations with 20° inclined .....	101
Fig. 4.11 Comparisons of the ultimate pull-out resistances of single	

suction piles with 0° and 20° .....	102
Fig. 5.1 Horizontal resistance of normalized displacement on 2D with no inclination .....	107
Fig. 5.2 Summarized horizontal resistance on different loading locations (2D) .....	108
Fig. 5.3 Horizontal resistance of normalized displacement on 3D with no inclination .....	109
Fig. 5.4 Summarized horizontal resistance on different loading locations (3D) .....	109
Fig. 5.5 Horizontal resistance of normalized displacement on 4D with no inclination .....	110
Fig. 5.6 Summarized horizontal resistance on different loading locations (4D) .....	111
Fig. 5.7 PIV analysis on 2D .....	113
Fig. 5.8 PIV analysis on 3D .....	115
Fig. 5.9 PIV analysis on 4D .....	116
Fig. 5.10 Scheme of horizontal behavior on 2D spacing .....	118
Fig. 5.11 Scheme of horizontal behavior on 3D spacing .....	120
Fig. 5.12 Scheme of horizontal behavior on 4D spacing .....	122
Fig. 5.13 Summarized ultimate horizontal resistance on different loading locations (3D and 4D) with 0° and 20° .....	123
Fig. 5.14 Summarized residual horizontal resistance on different loading locations (3D and 4D) with 0° and 20° .....	124
Fig. 5.15 Horizontal resistance and normalized displacement under diverse cyclic loadings .....	127
Fig. 5.16 Cyclic loadings and variations of stiffness .....	127
Fig. 5.17 Horizontal behavior of group suction piles with different pile spacings .....	129
Fig. 5.18 Arrangement of piles .....	132
Fig. 6.1 Scheme of horizontal resistance of pile .....	137
Fig. 6.2 Distribution of ultimate unit horizontal bearing capacity .....	138

Fig. 6.3 Distribution of ultimate unit horizontal bearing capacity (Petrasovits and Award, 1972) .....	140
Fig. 6.4 Distribution of the ultimate unit horizontal bearing capacity .....	141
Fig. 6.5 initial ground response coefficient .....	143
Fig. 6.6 C <sub>1</sub> , C <sub>2</sub> , C <sub>3</sub> .....	143
Fig. 6.7 Comparison of estimated Hu and measured Hu .....	145
Fig. 6.8 Rotation of single suction pile at ultimate horizontal resistance .....	146
Fig. 6.9 Rotation of group suction piles at ultimate horizontal resistance .....	147
Fig. 6.10 Block resistance of group suction piles against sliding .....	149
Fig. 6.11 Summarized ultimate horizontal resistance of single and group suction piles with different loading .....	152
Fig. 6.12 Normalized residual resistance of single and group suction piles with different loading locations .....	153
Fig. 6.13 Summarized ultimate horizontal resistance of single and group suction piles with 20° inclination .....	154
Fig. 6.14 Comparison on the ultimate horizontal resistance of single and group suction piles .....	156
Fig. 6.15 Scheme of top cap using H beam .....	159
Fig. 6.16 Construction cost analysis results with respect to horizontal resistance .....	163

## LIST OF SYMBOLS

$A$	Coefficient of frequency or static loading
$A_s$	Cross-section area of suction pile
$\alpha$	Loading angle
$c$	Cohesion of soil
$C_c$	Coefficient of curvature
$C_u$	Uniformity coefficient
$C_1, C_2, C_3$	Function of internal friction angle
$D$	Internal diameter of pile
$\delta$	Displacement of pile
$D_{10}$	Effective particle size, 10 passing percent
$D_{30}$	Particle size of 30 passing percent
$D_{50}$	Mean particle size, 50 passing percent
$D_{60}$	Particle size of 60 passing percent
$D_f$	Embedded pile length
$\delta_f$	Interface friction angle between pile shaft and soil
$\delta'$	Developed interface friction angle between pile and soil
$D_r$	Relative density
$E$	Elastic modulus
$e$	distance from loading location to soil surface
$e_{\max}$	Maximum void ratio
$e_{\min}$	Minimum void ratio
$f_m$	P-multiplier factor of group pile
$F_p$	Penetration force
$F_r$	Resistance force
$\gamma_{d\max}$	Maximum unit weight of soil
$\gamma_{d\min}$	Minimum unit weight of soil
$\gamma'$	Buoyant unit weight of soil
$G-OL-O^\circ$	Group pile - loading point - loading angle
$G_s$	Specific gravity
$H_u$	ultimate horizontal bearing capacity

$I$	Moment of inertia
$k$	Initial ground response coefficient
$K_a$	Active earth pressure coefficient
$K_o$	At-rest lateral earth pressure coefficient
$K_p$	Passive earth pressure coefficient
$L$	Embedded pile length
$L_{\max}$	Maximum wall length
$M$	Mobilization factor ( $< 1$ )
$\eta$	Pile rotation factor
$N$	SPT value
$N_1$	SPT value under effective overburden pressure $1 \text{ kg/cm}^2$
$(N_1)_{60}$	SPT value having 60% of the blow energy
$\phi$	Soil internal friction angle
$\phi'$	Drained friction angle
$P_i$	i th trailing row of group pile
$P_s$	Net suction pressure (outside - inside pressure)
$P_u$	Ultimate horizontal resistance of single pile
$p_u$	ultimate unit bearing capacity of pile
$Q_{inside}$	Inside interface frictional resistance
$Q_{outside}$	Outside interface frictional resistance
$Q_{tip}$	Resistance of tip of pile
$\sigma_3$	Minimum principle stress
$\sigma_r$	Maximum normal stress along r-direction
$\sigma_v$	Vertical effective stress
$\sigma_{v,0.6x}'$	Effective vertical stress at $0.6x$ depth for soil surface
$R_a$	Average surface roughness of model pile
$R_n$	Relative roughness
$R_{res}$	Residual resistance of pile
$R_{ult}$	Ultimate horizontal resistance of pile
$s$	Cross section coefficient (circular=0.8, rectangular=1.0)
$S - OL - O^\circ$	Single pile - loading point - loading angle
$t$	Wall thickness
$\tau_d$	shear stress along r-direction
$\tau_f$	Skin resistance of pile

$\tau_{r\theta}$	$\tau_d \sin\theta$
$\tau_{rz}$	$\tau_d \cos\theta$
$\theta$	Rotation in degree
W	Self weight of pile
$\xi$	Failure wedge inclination angle at pile tip
$x_r$	distance from the soil surface to rotation point of pile
$z$	Loading point

(Page intentionally left blank)

# **CHAPTER I INTRODUCTION**

## **1.1 Overview**

Fast growing industrialization worldwide has accelerated the use of more available ground space and civic complaint has constrained land uses; therefore, the need for effective use of marine space is more emphasized recently. More and more marine structures have been under construction domestically following the increasing need for using marine space and developing offshore wind power. In addition, many projects regarding the development of marine resource and offshore infrastructure, valued billions of dollars, are expected in the coming years. The previous market of marine space development in Korea was heavily dependent on landfill methods, such as dredging work. However, the previous offshore landfill projects, requiring high construction cost and inducing marine pollution, are being replaced with many cost efficient and eco-friendly projects including development of floating structures and their foundations. But, limited study on the foundations of floating structures has been conducted domestically, and therefore, securing independent foundation design technology of floating structures is urgent task.

The floating structure is generally built at relatively deeper sea, and because of the limits in required equipment and cost efficiency, the foundation is designed with a combined system that incorporates an anchor and mooring system instead of driven pile or drilled shaft. Currently, several types of anchors and foundations are used at deep

sea, and among them, a drag anchor or suction pile is more commonly used because of its great constructability and cost efficiency. And the suction pile is more popular than the drag anchor which is uncertain in estimating the bearing capacity and construction efficiency (Colliat et al., 1996).

Suction piles, as foundations of floating structures, have been usually used to resist mainly horizontal loadings. Moreover, loads inducing the maximum pull-out capacities vary according to the loading locations or loading inclinations with diverse field conditions and hydraulic conditions. The maximum pull-out capacities are also influenced by installation methods. Due to the many influential factors involving suction pile capacities, it is difficult to determine the optimal loading locations producing the maximum pull-out capacities.

The suction piles have many advantages over other types of anchors, such as (a) precise positioning in deepwater, (b) ease of removal and relocation, (c) less dependency on heavy installation equipment, and (d) large diameter that can develop considerable resistance against significant lateral and torsional loads generated by the environmental loads and loads transferred from the superstructure. However, the potential for reinstallation of the suction piles has always been an issue for engineers. Successful installation of offshore foundations is more difficult over onshore foundations due to limited available operative time under harsh environmental conditions, such as wind, wave, and tide. Moreover, expansive offshore equipment, such as jack-up barge or offshore crane, are required and the cost required for offshore foundation installation could be significant because of the slow equipment operation from their limited available operative time.

Retrieval and reinstallation of the suction pile may be necessary if one of the following scenarios is encountered: (a) The installation bias

in terms of verticality exceed the permitted tolerance; or (b) Unexpected local soil conditions are encountered during and after the suction pile installation (Li and Zhang, 2012). For example, the soil is found weaker than expected that the pile will not be able to develop adequate in-place capacity; or the stronger layer is present, causing the early refusal to the suction pile embedment. Carefully planned and executed geotechnical and geophysical surveys may minimize the occurrence of the latter case.

Recently, many studies on the suction pile implementation are underway to reduce the suction pile installation cost. The studies focus on the development of supplementary equipment improving installation efficiency by implementing percussion system or water jet to increase the penetration capacity of the suction pile (Allersma et al., 2001a; Bang et al., 2005). However, such approaches proved not to be the fundamental solution because of additional costs for their implementation and limited applications for particular soil conditions. Thus it is necessary to develop another type of the suction pile, which installs easily and has improved and stable bearing capacity.

In this study, a new type of suction pile as foundations of floating structures, group suction piles were proposed to improve the shortcomings of conventional single suction piles. Small-scale model tests were performed to estimate horizontal behavior of group suction piles. The horizontal behavior of single suction pile and group suction piles with different spacings (2, 3 and 4 times of the pile diameter) was analyzed varying loading location and load inclination. In addition, load distributions of component piles in group suction piles were evaluated based on the earth pressures measured from pressure meters attached on the component piles.

## 1.2 Suction pile

### 1.2.1 Definition

A suction pile is a hollow circular tube closed by a lid at the upper end. Literally, it resembles a reversed can. The pile lid can be a stiffened flat plate or a dome. Illustrations of the typical suction piles can be seen in Fig. 1.1.

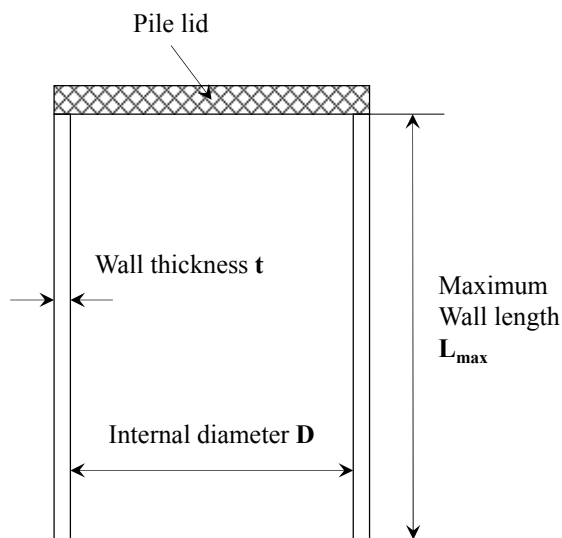


Fig. 1.1 Definition of the suction pile components

The maximum wall length, the length of the pile wall measured from the lower lid surface to the wall tip, to diameter ratio (aspect ratio) is smaller than in a pipe pile, normally less than 10. The wall thickness to diameter ratio is also smaller, generally in the range of 0.3% ~ 0.6%. In the long piles, stiffeners are often added along the

internal perimeter (ring stiffeners) or longitudinally to prevent them from buckling during installation. Stiffeners are commonly used in the suction piles with clay, where the maximum wall length to diameter ratio can be as high as 9 (Tjelta, 2001), but generally less common in the piles placed in sand due to a much lower ratio, often smaller than 1.

The suction piles are also known for a number of different names, such as, bucket foundations, skirted foundations, suction anchors, suction caissons, suction piles etc (Tjelta, 2001). The bucket foundation, a term which is primarily used when the suction pile is attached to the structure, for example, a jacket structure or a sub-sea structure, forms an integrated part of this structure. The individual bucket foundations, often 3 or 4 per structure, have a geometry which often resembles an inverted bucket, hence the name and aspect ratios are often less than one ( $L/D < 1$ ). Skirted foundation, a general term used when skirts are attached to the foundations to increase the bearing capacity and/or provide the scour protection. The skirts may be shallow or deep forming a circular, square or irregular geometry. The bucket foundation is a special case of the general term for ‘skirted foundation.’ The suction anchor is most frequently used with the same definition as the suction pile. So far, the suction anchor is mostly used to provide an anchor point for horizontal loads in a mooring system. The suction caisson is defining a suction anchor that is circular and otherwise as defined above. The suction pile is generally given the same definition as suction caisson, and, if the aspect ratio becomes less than unity, the similarity to a pile is not obvious. Despite the name differences, they all share the same installation mechanism, which will be described below. In this thesis, the term of ‘suction pile’ will be used.

### 1.2.2 Installation mechanism

The suction pile installation requires a simple process as illustrated in Fig. 1.2. After placing the suction piles on a seabed using crane, the suction piles are installed to the desired depth by first allowing them to penetrate into the soil under their self-weight. Then water is pumped out of the pile interior, which creates lower inner pressure that penetrates the piles into the soil for the targeted depth. The suction pump is removed and returned after the pile penetration is completed.

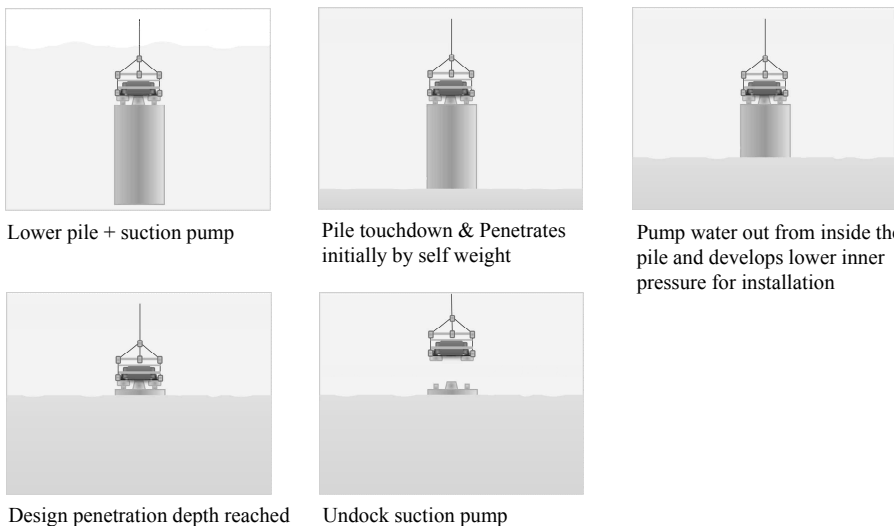


Fig. 1.2 Installation procedure of the suction pile

The force generated during the penetration of the suction pile is illustrated in Fig. 1.3. When the suction pile is placed on the seabed, the tip of the pile is penetrated into the soft ground to certain depth by self-load ( $W$ ). When the intrusive force by the self-load, end bearing capacity at the tip, skin friction force and self-load are in equilibrium, the water inside the pile is discharged by the pump, and

the pile is penetrated by the pressure difference. To cope with the difference in pressure inside and outside the pipe, the sea water needs to flow into the pile or suction pile to penetrate into the ground, but the sea water can hardly flow into the pipe at the un-drained clay layer or on the sea-bed with low permeability, and thus penetration force is generated to the extent of the pressure difference multiplied by the area. Equation to calculate the penetration force and penetration resistance force of the suction pile is shown as Eq. (1.1) and (1.2)

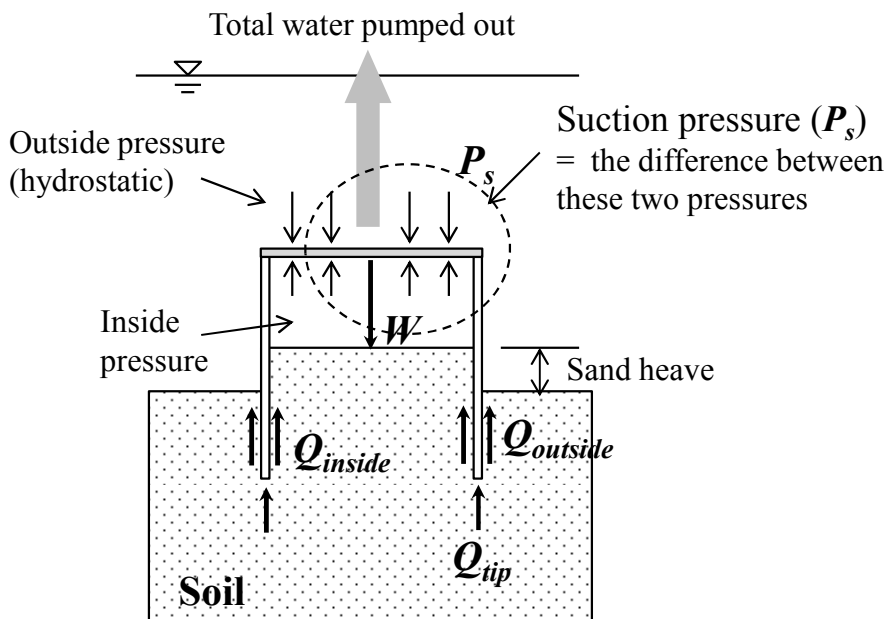


Fig. 1.3 Installation mechanism of suction pile

$$F_p = W + P_s \times A_s \quad (1.1)$$

Where,  $F_p$ : Penetration force

$W$ : Self weight of pile

$P_s$ : Net suction pressure (outside - inside pressure)

$A_s$ : Cross-section area of suction pile

$$F_r = M \times (Q_{outside} + Q_{inside} + Q_{tip}) \quad (1.2)$$

Where,  $F_r$ : Resistance force

$M$ : Mobilization factor ( $< 1$ )

$Q_{outside}$ : Outside interface frictional resistance

$Q_{inside}$ : Inside interface frictional resistance

$Q_{tip}$ : Resistance of tip of pile

As indicated in the above Equation, the penetration force is proportional to the cross-sectional area of the pile or square of the diameter while the penetration resistance force is proportional to the circumference or diameter of the pile, and this is to indicate that, the larger the diameter of the pile, the greater the penetration force. Another advantage of the suction pile is easy pull-out, in addition to easy installation since it allows the water to flow into the pile in reverse order, comparing to the case of penetration (Bang and Cho, 2003).

When the suction pressure difference is too small, causing the penetration force to be less than the penetration resistance, the suction pile is not penetrated into the ground. On the contrary, when the suction pressure is too high, the water is rapidly absorbed into the pile on sand layer, causing the boiling phenomenon or uplift seepage, which enables to install the pile. On the clay layer, the soil inside the pile is isolated from the ground and comes up to the top of the pile, causing the plugging phenomenon which also makes it impossible to install the pile. Minimum suction pressure that is needed to penetrate the suction

pile is dubbed while the lower bound and suction pressure that the pile cannot be installed due to boiling or plugging is dubbed for the upper bound. So the optimal design pressure difference for stable installation of the suction pile shall be determined with the range between the lower bound and upper bound as indicated in Fig. 1.4 (Bang and Cho, 2003).

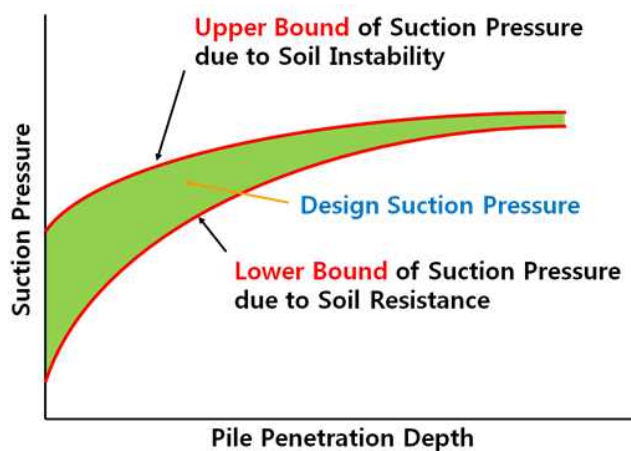


Fig. 1.4 Optimum design pressure difference (Bang and Cho, 2003)

Though the suction pile was installed on the sandy soil with the appropriate suction pressure, what noteworthy is the amount of sand heave, a difference between the soil surface level inside the pile compartment, and the surrounding soil outside the pile is unavoidable as shown in Fig. 1.3 (Manh, 2005).

## 1.3 Group suction piles

### 1.3.1 Definition

In this study, group suction piles have been proposed newly for foundation of floating structure. The group suction piles are similar form to a general group pile, and the structure is combined form of a top cap and several single suction piles as shown in Fig. 1.5.

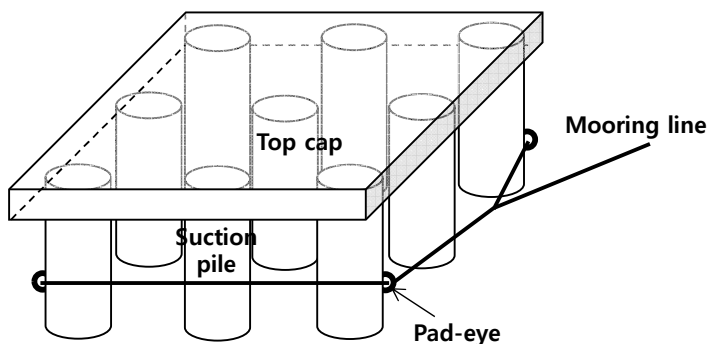


Fig. 1.5 Scheme of group suction piles

This group suction piles are favorable structure to support massive loading, and it can be expected to be shown the improvement of horizontal bearing capacity because top cap can restrain a rotation in horizontal loading by combining single suction piles strongly.

The group suction piles also have diverse advantages, especially in installation. When the suction pile is penetrated into the ground, it is possible to adjust the degree of horizontality by controlling the individual suction piles, and the top cap can role as guide to allow vertical installation in inclined ground. In aspect of practice, the most

advantage is that group suction piles can modularize in construction. In other words, individual suction pile can be manufactured on factory or land shore, and rearrange the number of suction piles in construction site. Therefore, since the piles can be installed flexibly in unexpected field or hydraulic conditions, construction time can be reduced significantly.

The group suction piles can be used to combine single suction piles, a large diameter single suction pile can be replaced by several single suction piles.

### 1.3.2 Installation method

The installation method of group suction piles is same with existing method for single suction pile, but it can be different according to the number of single suction piles. Provided group suction piles are isotropic that, if number of single suction piles are under four, group suction piles by prefabricated with top cap on land shore can be installed on offshore at once. Even if single suction piles are needed more than four, it is possible economically. As shown in Fig. 1.6; first, suction files can be installed at corners of the top cap, next, suction piles can be installed additionally into the holes of top cap pre-penetrated in advance. The installation method of group suction piles can be controlled as much as possible.

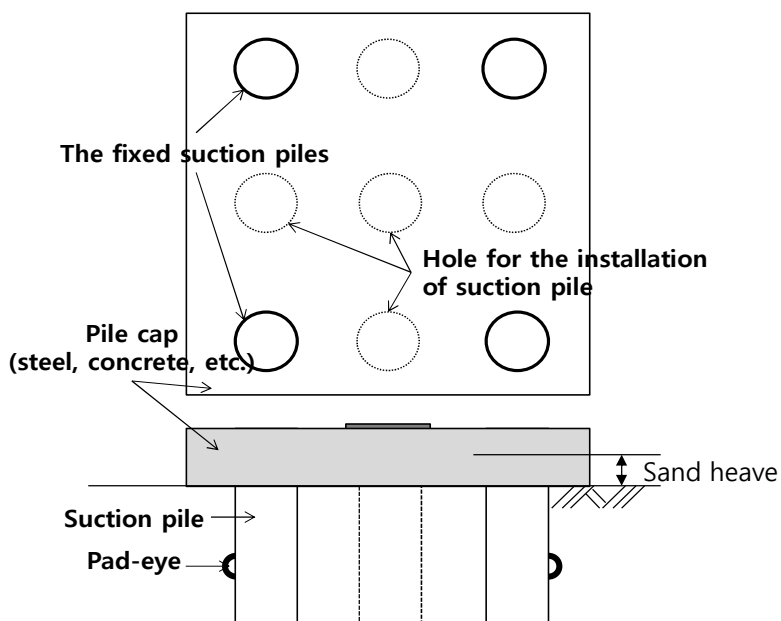


Fig. 1.6 An example of the installation of 3×3 group suction piles

Since the suction pressure can be adjusted under installation, the group suction piles are favorable in vertical installation compared to existing single suction pile. In addition, due to the weight of the top cap, the effective length of suction pile can be penetrated completely by eliminating the effect of sand heave, which occurs in sand necessarily as shown in Fig. 1.6, thus, top cap can be installed to adhere to the below of top cap with ground surface. So, piled raft effect can be anticipated additionally in vertical or moment load applied.

### **1.3.3 Weakness and limitations of group suction piles**

Special considerations are required for the use of the newly developed group suction piles due to the following limitations.

- (1) The applicability of the newly developed group suction piles should be tested in real fields due to the complexity of its structure. Lack of the verified design and construction methods, further research regarding establishment of design and construction methods is a priority for the reliable and successful implementation of the newly developed group suction piles.
- (2) The self-weight of top cap induces increasing skirt depth of component piles, which helps successful initiation of suction installation. However, at the same time, it increases the self-weight of foundation system. Particularly, if the diameters or spacing of component piles are large, an inevitably increased size of top cap results in increases of self-weight and construction cost of the foundation. Therefore, the dimension and installation method of

group pile and the materials of top cap should be determined after enough considerations of available construction equipment and conditions of the construction site.

- (3) Many component piles with narrow spacing of a group pile induces considerable densification of foundation around the piles; therefore, it should be noted that the densified soils will increase the penetration resistance of suction pile installation.
- (4) The suction installation force of a suction pile proportionally increases with an increasing pile's cross-sectional area (with an increasing square of pile diameter), while the penetration resistance against the pile installation proportionally increases with increasing perimeter of the suction pile (with increasing pile diameter). Therefore, in a given dense soil, the use of a group pile with small diameter component piles can be unfavorable, compared with that of a large-diameter single suction pile.
- (5) For a group pile with many component piles or large-diameter component piles used for a high-load carrying foundation, it may be difficult to install all the component piles simultaneously due to the limitation of suction pile installation equipment. In this case, staged installation of component piles may be implemented: A group pile with minimum component piles is installed first, followed by the installation of the rest of the component piles on the previously installed group pile. Under the deep sea, there might be a difficulty of locating the installation of companion piles in the staged installation of a group pile.

## 1.4 Objectives

The purpose of this study is to propose a novel and new type of group suction piles for their use as foundations of floating structures to improve the shortcomings of conventional single suction piles. Small-scale model tests were performed to estimate horizontal behavior of group suction piles.

TriPLICATE tests were performed for each test condition to ensure the repeatability and reliability of experimental system and methods of model tests of single suction piles. From the examination of the suction installation effect on the horizontal pull-out resistance of a single suction pile in sands, a decrease of effective stress inside the suction pile was identified for the suction piles installed using suction pressure. As jacked suction piles have higher effective stress inside of the suction piles, an estimation of the horizontal capacity of the single jacked suction pile overestimates the real in-situ horizontal capacity of suction-installed pile. In addition, the change of its ultimate horizontal capacities of suction-installed suction piles under various combinations of loading location and load inclination was analyzed. The test results of single suction piles were compared with the estimations based on the typically-used prediction equations proposed by other researchers.

The horizontal behavior of group suction piles with different spacings (2D, 3D, and 4D) was analyzed varying loading location and load inclination. As suction piles are widely used as foundations of horizontally-moving floating structures under offshore environmental loads, the suction piles are also subjected to horizontal cyclic loadings. Therefore, a cyclic horizontal load test was performed to examine the cyclic loading effect on the horizontal group suction piles behavior. In

addition, load distributions of component piles were evaluated based on the earth pressures measured from pressure meters attached on the component piles.

## **1.5 Organization of dissertation**

The organization of this dissertation is as follows:

- Chapter 1 presents research background and objectives, and describes the basic concepts of a conventional suction pile and new type group suction piles.
- Chapter 2 includes the history of field applications, research studies of suction piles, literature review on recent research of horizontally loaded single suction piles and horizontally loaded group piles.
- Chapter 3 demonstrates the test equipment, instrumented model pile, and soil layer preparation. Test equipment is composed of large-scale soil chamber, horizontal loading system, vibrating compaction system, micro-cone penetrometer and Particle Image velocimetry (PIV) system.
- Chapter 4 describes the model test results on single suction piles. The effect of suction installation on ultimate horizontal capacity of suction pile was evaluated from the model tests, and the change of ultimate horizontal capacity under various combinations of loading location and load inclination was analyzed.
- Chapter 5 presents the model test results on group suction piles. The horizontal behavior of group suction piles was examined for different loading locations, load inclinations, and component pile spacings. In addition, the effect of cyclic loading on the ultimate and residual horizontal resistances was analyzed. The group effect of

group suction piles was assessed by measuring load distributions of component piles.

- Chapter 6 explains further interpretation of the model test results. The ultimate horizontal capacities of single suction piles measured from the model tests were compared with those estimated from the lateral capacity equations of rigid piles given by previous researchers. The group effect of group suction piles is examined based on the measured earth pressures attached on all the component piles. The efficiency of group suction piles were evaluated by examining horizontal behavior of group suction piles under different loading location, load inclinations, and pile spacings. Comparison has been made between single pile and group pile behavior. The comprehensive cost analysis of the group pile was performed considering manufacture, transportation, and installation cost.
- Chapter 7 presents summary, conclusions, and recommendations in future uses of the newly developed group pile.

## **CHAPTER II LITERATURE REVIEW**

### **2.1 History of field applications**

Although a suction caisson is still viewed as a relatively new concept in the offshore industry, its first use as a type of anchorage and foundation system dated back to the late 1950s. Since then, there have been numerous field applications of the suction caisson around the world. To limit this section to manageable length, only milestone applications has been discussed.

One of the earliest reported uses on this concept is probably the portable core sampler device by Mackereth (1958). The equipment was used to core samples in a lake bottom. It was later retrieved by supplying compressed air into the compartment. In 1972, Shell Inc. developed a self-operating unit to conduct cone tests in the North Sea (North Sea Report, 1972). In 1980, the suction caisson was first used commercially at large scale in the Gorm field, North Sea (Senpere and Auvergne, 1982). The first field observations of installation problems, where excessive sand heave was formed inside the caisson, were also recorded in this project.

The suction concept was applied to a permanent foundation system in the Gullfaks C gravity platform in 1989 firstly (Tjelta et al., 1990). The foundation wall was able to penetrate into the final depth of 22 m with the assistance of the suction pressure, created by water pumped out from the concrete cells. This foundation system led to further applications for the Snorre Tension Leg Platform (TLP) (Fines et al.,

1991; Stove et al., 1992; Dyvik et al., 1993), and later the Draupner E (previously Europipe 16/11E) and Sleipner T platforms (Bye et al., 1995; Tjelta, 1995), all in the North Sea. It is worth noting here that the Draupner E and Sleipner T platforms marked for the first time that the suction caisson alone was used as a permanent foundation in sand. They also demonstrated that, with the use of such suction, the wall penetration in very dense sand was possible.

The success of the above projects has led to a rapid increase in the use of the suction caisson in the offshore industries over the past decade. It is estimated that, at present, there are nearly 500 suction caissons installed in more than 50 locations around the world (Andersen et al., 2005). Today, the suction caisson is used virtually in all five continents (Europe, Africa, Asia, America, and Australia), with water depths varying from shallow water ( $20\text{ m} \sim 40\text{ m}$ ) to the real deep areas (over 1000 m). The device has also been considered for military use (Bang et al., 1999) and as a foundation system for future offshore wind turbines (Feld et al., 1999; Houldby and Byrne, 2000; Feld, 2001). The way the suction caisson is put together in operation also varies, from a single unit as in most cases to single units with multiple compartments (Masui et al., 2001) and cluster units, i.e. many caissons are placed together as a unit, such as, those in the Hanze project (Aas et al., 2002; Sparrevik, 2002).

## **2.2 History of research studies**

Planning and design of the suction caisson for field applications have been possible only because the knowledge had been gained from researches. Experimental tests have been conducted to disclose the behavior of the suction pile on the horizontal and vertical moment performed by the University of Oxford, the University of Western Australia, the University of Aalborg, and many other institutions (Yoon et al, 2010). To date, there have been many studies on various aspects of the suction caisson in both clay and sand.

First of all, in the early 1960s, Goodman et al. (1961), in a feasibility study that included perhaps some of the earliest published research results on suction caisson, proposed the wider use of the “vacuum” concept for marine anchoring purposes. During that time, it was common practice to use gravity anchors because their holding capacity could be easily calculated (Brown and Nacci, 1971).

Following these initial researches, there have been a number of other studies that investigated the behavior of the suction caisson in soil. Brown and Nacci (1971) explored the caisson pullout performance in granular soil and reported a high force of weight ratio and a conical failure surface. Wang et al. (1975, 1977) investigated the holding capacity in a wider range of soils, including sand, silt and clay, and developed a breakout capacity equation by using the Mohr-Coulomb failure theory.

A similar study was conducted for caisson in sand by Helfrich et al. (1976) and it showed that a Mohr-Coulomb criterion could predict failure loads within 13% of the measured values. The required caisson size in a field application was also predicted by extrapolating the model

test data. Wilson and Sohota (1980) and Sohota and Wilson (1982) presented studies that used modified suction anchors that were installed by water jetting, and buried at some depth below the surface.

Most researches during this early period were focused on simple monotonic pullout (short-term). Since the late 1980s, researches on the suction caisson have increased significantly. Apart from continuing studies on monotonic breakout capacity (Steensen-Bach, 1992), initial investigations on the caisson cyclic behavior (Larsen, 1989) and computer modelling (Christensen and Haahr, 1992) were also conducted. Systematic field tests were also conducted through large scale field trials from as early as the 1970s (Hogervorst, 1980) and it lasted until recent days (Stevenson, 2003; Fakharian and Rismanchian, 2004).

Recently, as attributable to the advanced technology, the geo-centrifuge test was performed in this field (Bang et al., 2001; Allersma et al., 2003; Bang et al., 2006; Jang et al., 2013). Also, behavior under both monotonic and cyclic loading has been considered for experimental modelling, numerical analysis and centrifuge tests (Deng and Carter, 2000; Zdravkovic et al., 2001; Cao et al., 2002; Deng and Carter, 2002; Supachawarote et al., 2004; Lu et al., 2007).

Additionally, the soil types considered by the studies were diverse, including sand (Byrne, 2000; Iskander et al. 2002; Byrne and Houlsby, 2002; Byrne and Houlsby, 2004), clay (Fuglsang and Stensen-Bach, 1991; Andersen and Jostad, 1999; House, 2002; Iskander et al. 2002; Clukey et al., 2004), layered sand-clay (Allersma et al., 2001b), and calcareous soils (Watson and Randolph, 1997; Randolph et al., 1998; Watson, 1999).

Different installation studies in clay involved investigations on limiting the caisson phase ratio to prevent the plug upheaval (House et al., 1999), variations in soil stress along the caisson wall and set-up

effects (Rauch et al., 2003; Andersen et al. 2004; Masui et al., 2004; Chen and Randolph, 2004), penetration and upheaval in soft clay (El-Gharbawy et al., 1999; Andersen et al., 2005), and penetration prediction (Andersen and Jostad, 1999; Houslsby and Byrne, 2005).

There was an interesting study among installation of the suction pile that was related to the relocation distance on the suction pile. In general, during the installation process or after the pile is installed, if the suction pile must be retrieved and reinstalled, the common practice is often to relocate or reinstall the pile for three diameters (3D) to five diameters (5D) away from the center-to-center. Li et al. (2012) investigated the pile relocation over shorter distance in order to overcome the potential challenges associated with the common practice. Li et al. indicated that the minimum relocation distance could be reduced to 2D without any change to the suction pile design and the relocation distance affects the pile movement more significantly than the capacities.

The installation is, however, more complex due to the seepage flow in the soil, which may create excessive sand heave inside the caisson and piping failure. It is well known that the seepage flow plays a key role in assisting the suction installation of caisson in sand (Manh et al., 2005). By loosening sand along the caisson's inner wall and at the wall tip, the flow significantly reduces the soil resistance. At the same time, this may also help create the plug loosening and upward movement of the sand column inside the caisson. Despite widely observed in both field tests and small-scale experimental studies, the behavior of the seepage flow and the extent of sand plug loosening during the suction installation are not well understood. Hence, understanding is still limited, and more researches are prudent to investigate the associated issues.

## 2.3 Recent research on horizontally loaded single suction pile

There are several pre-studies on the horizontally loaded suction piles. These are the basis for this thesis.

Allersma et al. (2000) carried out small-scale geo-technical centrifuge testing to investigate the horizontal bearing capacity of the suction piles in sand and clay. The influence of several parameters was tested, such as, height/diameter ratio, attachment point of the cable and loading angle. The test results were compared with the API standard and 3-dimensional finite element calculations. Allersma et al. indicated that the attachment angle influences the bearing capacity significantly and the optimum attachment height would appear to be  $z=3L/5$  ( $z$ : loading point,  $L$ : embedded pile length) with  $\alpha=15^\circ$ . Since the finite element calculations appeared to be in agreement with the measured tendencies of the test results, it is believed that a combination of numerical calculations and tests in a small centrifuge yields a powerful design tool.

In study of Bang et al. (2001), an analytical solution procedure that can estimate the resistance of the suction piles against horizontal loads was developed by considering the truly three-dimensional normal and shear stresses along the circumference of the pile surface as well as a tree-dimensional soil failure wedge (Fig. 2.1 ~ 2.2). In this paper, Bang et al. (2001) had been drawn passive lateral earth pressure  $P$  restrained by the soil weight and the friction angle. The developed passive thrust  $P$  is shown in Eq. (2.1).

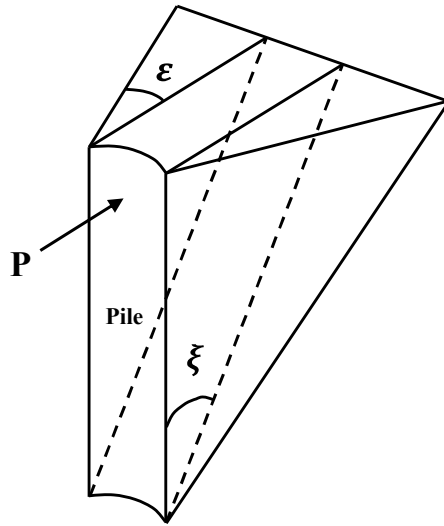


Fig. 2.1 Three-dimensional soil failure wedge (Bang et al., 2001)

$$P = \frac{D}{1 - \tan\delta' \tan\xi} \left( \frac{1}{2} \gamma' z^2 \tan^2 \xi + \frac{1}{3} \gamma' \frac{z^3}{D} \tan^3 \frac{\phi}{2} - \frac{1}{3} K_o \gamma' \frac{z^3}{D} \tan\xi \tan \frac{\phi}{2} + \frac{2}{3} K_o \gamma' \frac{z^3}{D} \tan\phi \tan\xi \sin\xi \right) \quad (2.1)$$

Where,  $\phi$ : Soil internal friction angle

$\gamma'$ : Buoyant unit weight of soil

$\delta'$ : Developed interface friction angle between pile and soil

$\xi$ : Failure wedge inclination angle at pile tip

$D$ : Pile diameter

$z$ : Depth from ground surface to point of interest

$K_o$ : At-rest lateral earth pressure coefficient

Moreover, Bang et al. (2001) had been presented horizontal force  $F$  (Eq. (2.2)) and vertical force  $V$  (Eq. (2.3), Fig. 2.2).

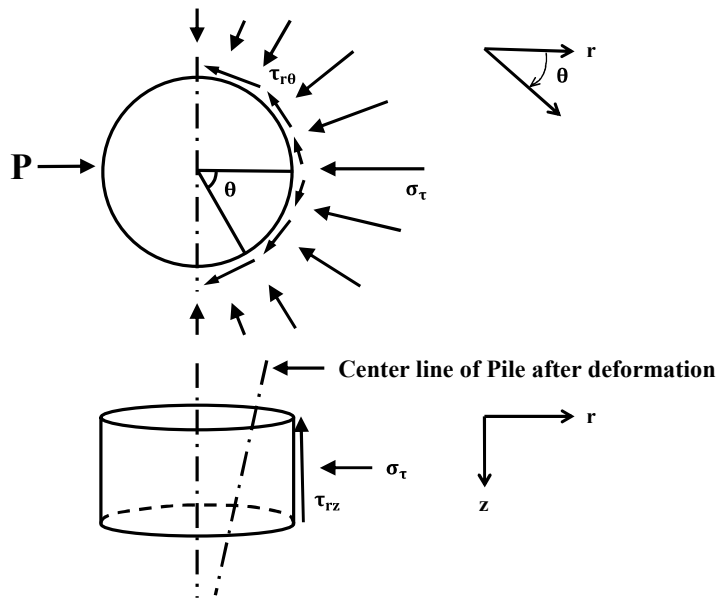


Fig. 2.2 Stresses along pile circumference (Bang et al., 2001)

$$F = 2 \int_0^{\eta H} \left( \int_0^{\pi/2} \sigma_r \cos\theta dA + \int_0^{\pi/2} \tau_r \sin\theta dA \right) dz \quad (2.2)$$

Where,  $\eta$ : Pile rotation factor

$\sigma_r$ : Maximum normal stress along r-direction

$\tau_{r\theta}$ :  $\tau_d \sin\theta$ ,  $\tau_d$  = shear stress along r-direction

$$V = 2 \int_0^{\eta H} \int_0^{\pi/2} \tau_{rz} dAdz \quad (2.2)$$

Where,  $\tau_{rz}$ :  $\tau_d \cos\theta$

In addition, the geo-centrifuge test results were analyzed and compared to validate the analytical solution of the ultimate horizontal loading capacity of the suction piles. Bang et al. concluded that the

loading point associated with the maximum ultimate horizontal loading capacity is  $0.55L$  ( $L$ : embedded pile length) for clay and approximately  $0.8L$  for sand. The analytical predictions compared very well with the experimental observations made through the geo-centrifuge model tests in sand. Bang et al. (2006) presented similar results. However, he concluded that validation of the analytical solution for soils with cohesion only or both cohesion and friction have yet to be made.

Randolph et al. (2002) conducted analysis of the suction caisson capacity in clay. A three-dimensional upper bound approach is described for caissons undergoing significant horizontal motion or rotation assessed by comparison with the independent semi-analytical three-dimensional finite element analyses. In this study, the major factors are the depth, maximum radial extent of the conical failure wedge and the velocity variation within the wedge. Chairat et al. (2004) also performed similar study in the NC clay. Chairat et al. concluded that optimal loading point is approximately  $0.7L$  for  $L/D=3$  ( $D$ : pile diameter). An increase in the loading angle by  $5^\circ$  results in a reduction in capacity for 10% as the combined effect of interaction and the rotation has a negative impact.

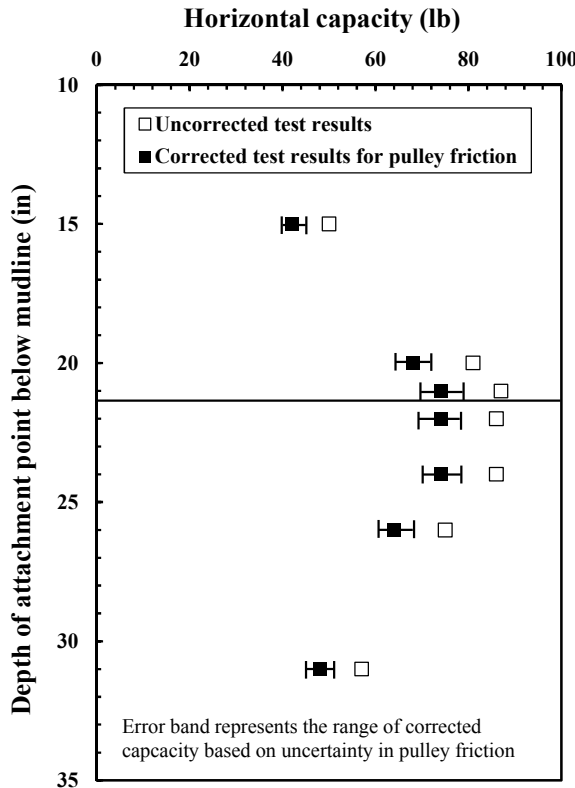


Fig. 2.3 Caisson capacity measured in horizontal load tests  
(Coffman et al., 2004)

There were horizontal load tests performed in a laboratory deposit of NC kaolinite (Coffman et al., 2004). Displacements of the caisson pad-eye at failure were 3 to 13% of the caisson diameter. After its failure, the lateral capacity dropped to a minimum level after movements of around 25% of the diameter. The optimum loading point was found between two-thirds and three-fourths of the caisson embedment depth below the mud line (Fig. 2.3 above). The measured capacities were in agreement with the predictions from a simplified limit equilibrium analysis and finite element simulation.

Jang et al. (2013) conducted a series of centrifugal tests modelling

the maximum horizontal pullout capacity of the suction pile embedded in sand by differentiating the diameter and the length of the pile. The loading point was located at 75% of the pile length from the top and the results were compared to the prediction equations of the suction piles. As a result, it is found that the horizontal pullout capacity of the suction pile was proportional to the diameter and square of length. The equation derived from the Rankine's passive earth pressure equation predicts the test results very well (Fig. 2.4). When pulling out the test pile from the left was apt to rotate clockwise, its rotational point at the maximum pullout capacity was found to be in the upper part of the pile. In addition, on the basis of the center of the suction pile, the vertical displacements for all cases appeared to develop toward the ground surface. This study concluded that the maximum pullout capacity has a linear relationship with the pile diameter within the range of aspect ratio from 2 to 3 for pile length of 60 mm. Also, there was no difference in the maximum pullout capacity in the tests with different g level, which means the model test may be appropriate regardless of the particle size.

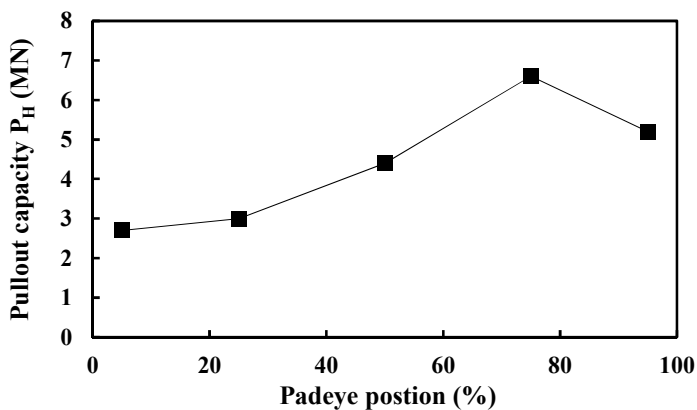


Fig. 2.4 Measured model suction pile pullout loading capacity  
(Jang et al., 2013)

There are some studies over horizontal dynamic loading. In one of the studies, Wang et al. (2006) carried out the experimental investigation on the response of the suction bucket foundation in a fine sand layer under horizontal dynamic loading. The developments of settlement and excess pore pressure of the sand foundation had been mainly studied. It was shown that the sand surrounding the bucket softens or even liquefies at the first stage if the loading amplitude is over the critical value. At a later stage, the bucket is settled and the sand layer is consolidated gradually. Wang et al. stated that, with the solidification of the liquefied sand layer and the settlement of the bucket, the movement of sand layer and the bucket reached a stable state.

In addition, Zhang et al. (2007) studied the centrifuge modelling of the suction bucket foundations for platforms (in the Bohai Bay, China) under the ice-sheet-induced cyclic lateral loadings (0.8 Hz ~ 1.0 Hz). The results indicated that the excess pore water pressures reached the highest values within a depth of 1.0 m ~ 1.5 m below the mud line. Two failure modes were observed: Liquefaction in early excitations and settlement-induced problems after long-term excitations.

In study of Lu et al. (2007), Lu et al. studied the dynamic loading by using liquefaction index. The liquefaction index is the ratio of the excess pore pressure for the initial vertical effective stress (Fig. 2.5).

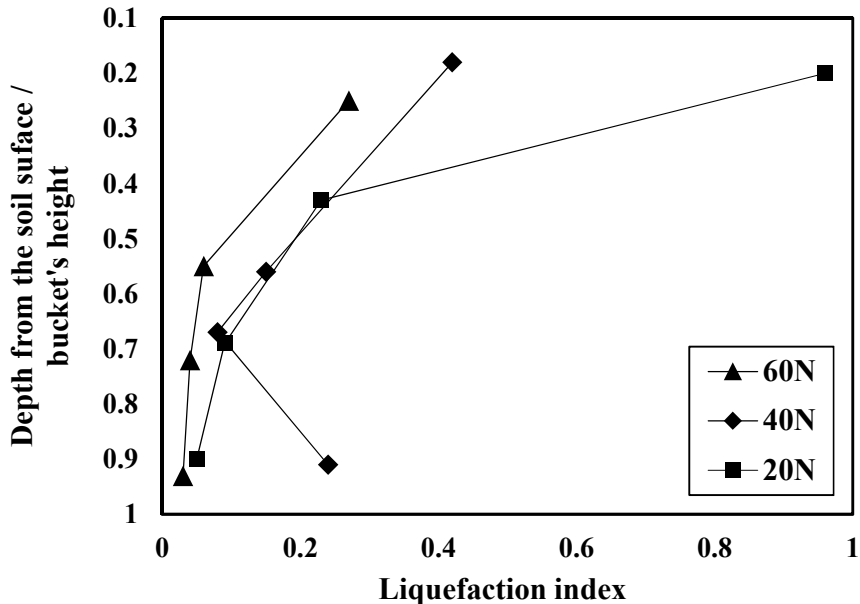


Fig. 2.5 The distribution of excess pore pressure along depth under different amplitudes (Lu et al., 2007)

The liquefaction index becomes smaller and smaller when the loading amplitude changes from 60 N (about 54% of the static bearing capacity) to 20 N (about 20% of the static bearing capacity). When the amplitude is 10 N (about 10% of the static bearing capacity), there is no building of the liquefaction index. It is shown that, when the loading amplitude is over a critical value (about 10% ~ 18% of the static bearing capacity), the sand layer at the upper part (40% of the bucket's height) around the bucket was softened or even liquefied under the horizontal dynamic loading while 100% of the bucket's height may be liquefied under the vertical dynamic loading.

The results on the loading location effect has been summarized in Table 2.1 and 2.2.

Table 2.1 Horizontal resistance according to various loading locations from previous research

Author z/L	Allersma et al. (2000)		Bang et al. (2001)		Supachawarote et al. (2004)	Coffman et al. (2004)	Kim and Jang (2011)
	Centri fuge (150g)	Nume rical	Analytic		Numerical	Model test	Centrifuge (100g)
			Clay	Sand			
0	47	46	38	19			
0.05							42
0.10			42	20			
0.20	53	55	49	11			
0.25							46
0.30			61	30			
0.40	60	61	75	39			
0.45						70	
0.50			90	48			65
0.55			100				
0.60	87	88	90	67	83		
0.65					93	100	
0.70		96	77	93	100	100	
0.75					96	100	100
0.80	100	100	64	100	92	84	
0.85					86		
0.90			51	56	75		
0.95							78
1.00			46	37		64	
Note	$\alpha = 15^\circ$ L/D = 17 Sand		D = 3m L = 6m		NC clay	NC clay	D = 3cm L = 6cm

Table 2.2 Horizontal resistance according to various loading angles from previous research

Author \ Angle	Allersma et al. (2000)		Zdravkovic et al. (2001)	Supachawarote et al. (2004)
	Centrifuge (150g)	Numerical	Analytic	Numerical
0		100	100	100
5		89	100	
10	100	83	98	100
15	93	78		
20	86	72	91	98
25	79	67		
30		61	81	89
Note	$h = 3L/5$ $L/D = 1.7$		$D = 5m$ $L = 30m$	NC clay

## 2.4 Recent research on horizontally loaded group pile

In the late 1980s, Brown et al. (1988) studied the lateral load behavior of the pile group in sand. A large-scale group of the steel pipe piles and isolated single pile were subjected to the two-way cyclic lateral loading. The tests were conducted in a submerged firm to dense sand that was placed and compacted around the piles. In this study, the deflection of the piles in the experimental group was significantly greater than the single pile under a load equal to the average load per pile. The reduced efficiency of the group under the lateral load was due principally to the effect of ‘shadowing’ (Fig. 2.6).

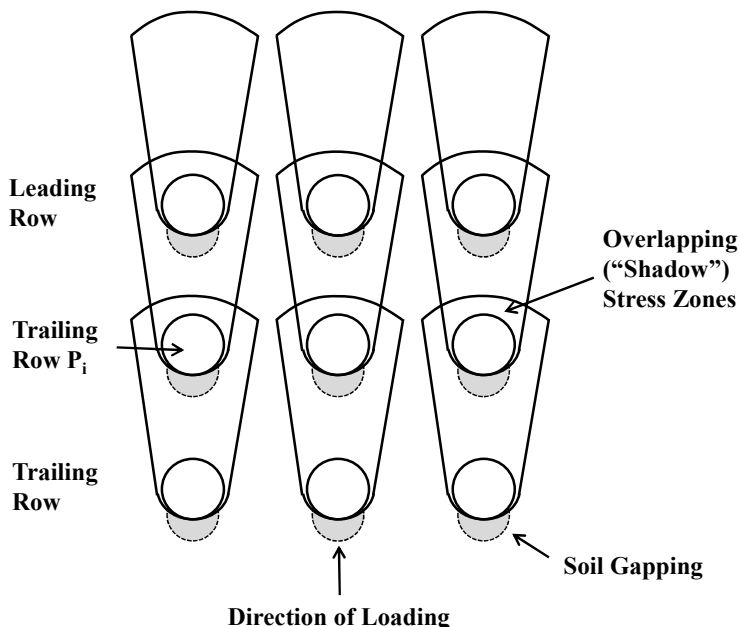


Fig. 2.6 Illustration of reduction in the lateral pile resistance due to interference with trailing row shear zones (Broms et al., 1988)

Piles in the trailing rows had a greatly reduced soil resistance because of the influence of the piles in the leading row. The soil resistance of the piles in the leading row was only slightly reduced below the isolated single pile. Brown et al. insisted that the key to design of pile groups for lateral loading appeared for the development of rational methods for predicting the loss of the soil resistance in piles within the trailing rows. A convenient way of expressing the loss in soil resistance due to group effect can be used as the ‘ $p$ -multiplier,’ a constant used to modify  $p-y$  curves for an isolated single pile (Fig. 2.7).

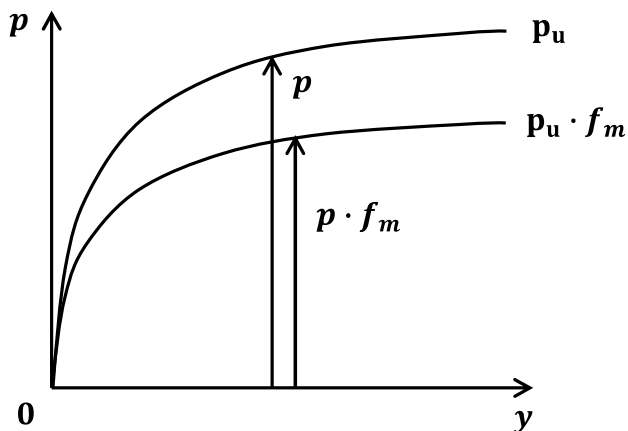


Fig. 2.7 P-multiplier concept for pile group effects (McVay et al., 1995)

In the research of McVay et al. (1995), a number of conclusions were reached on the basis of the works reported for three-row groups in sand. The shadowing effect appeared to be a function of the pile spacing and soil density. For a three-row pile group at 3D spacing, the group contribution varies from a high of 45%, 32%, and 23% for very sand, 41%, 32%, and 27% for medium dense sands, and 37%, 33%, and 30% for medium loose sands.

After three years, McVay et al. (1998) published the paper related to the centrifuge testing of the large laterally loaded pile groups ( $3 \times 3$  to  $7 \times 3$ ) in sands. The instrumentation allowed the determination of both bending moments and shear forces at the head of each pile in loose and medium dense sands. From the test results of variable size groups in loose and medium dense sands, it was found that an individual row's contribution to a group's lateral resistance did not change with size of the group, only with its row position. It was found that the percentage of load carried by an individual row did not change with the soil density, suggesting that the multipliers were independent of the latter.

Rollines et al. (1998) conducted tests of the full-scale pile group on a lateral load in clay. A static lateral load test was performed on the full-scale pile group to determine the resulting pile-soil-pile interaction effects. The  $3 \times 3$  pile group at three-diameter spacing was driven into a profile consisting of soft to medium-stiff clays and silts underlain by sand. Trailing rows carried less than the leading row and middle row piles carried the lowest loads. Maximum moments in the group piles were 50% ~ 100% higher than the single pile. Additionally, Rollines et al. indicated that the closely spaced pile group ( $\approx 3D$  spacing) deflected 2 ~ 2.5 times higher than the isolated single pile under the same average load.

In the later study (2005), Rollines et al. concluded that the group interaction effects can be adequately accounted for using p-multipliers in a lateral analysis program, such as, LPILE or GROUP. For the  $3 \times 3$  pile group with 3.3D spacing, back-calculated p-multipliers were found to be approximately 0.8, 0.4, and 0.4 for the front, middle, and back rows, respectively. These values were in agreement with the p-multipliers from other full-scale and centrifuge tests in sand. These

results suggested that the p-multipliers are not highly sensitive to the pile installation techniques or initial relative density of the sand.

In the recent study, Kim et al. (2011) performed extensive laboratory model pile tests to investigate the pile group interaction effects. Kim et al. showed that a pile spacing of more than six times the pile diameter in group seems to be large enough to eliminate the group effects of the pile for both medium and loose sand, and in such cases, the individual piles for the pile groups behaved the same as a single pile. For medium dense sand, however, the pile group behaved as a single pile at pile spacing of about eight times the pile diameter and beyond. The p-multipliers were estimated to be 0.84, 0.58, and 0.4, respectively.

The results on p-multiplier has been summarized in Table 2.3.

Table 2.3 P-multiplier values of group pile

Researchers	Soil Type	Spacing (D)	Pattern	Average p-multiplier			
				1 <sup>st</sup> row	2 <sup>nd</sup> row	3 <sup>rd</sup> row	4 <sup>th</sup> row
Brown et al. (1988)	Clean medium sand ( $\Phi=38^\circ$ )	3	$3 \times 3$	0.8	0.4	0.3	-
McVay et al. (1995)	Medium dense sand	3	$3 \times 3$	0.8	0.4	0.3	-
McVay et al. (1998)	Medium dense sand	3	$4 \times 3$	0.8	0.4	0.4	0.3
Rollins et al. (1998)	Clean medium sand ( $\Phi=38^\circ$ )	3	$3 \times 3$	0.8	0.4	0.3	-
Ruesta et al. (1997)	Loose fine sand ( $\Phi=32^\circ$ )	3	$4 \times 4$	0.8	0.7	0.3	0.3

Lastly, the type of hybrid foundation has been studied. Aiming for an optimum design, Bienen et al. (2012) investigated in details the soil failure mechanisms and resulting foundation capacity under un-drained vertical, horizontal, and moment (VHM) loading of the hybrid foundation concept by using numerical modelling. The hybrid foundation aims to provide additional horizontal and moment capacity by optimizing the amount of the steel required and minimizing structural design complexity associated with long and large diameter skirted foundation. Bienen et al. analyzed a skirted foundation with the additional internal skirts that exceeded the length of the external skirts (Fig. 2.8). This geometry resulted particularly in the horizontal capacity (with key influences for increased moment capacity identified as well). This was significant since it indicates the potential of this foundation concept as an economical foundation alternative, especially when compared with a large bucket foundation.

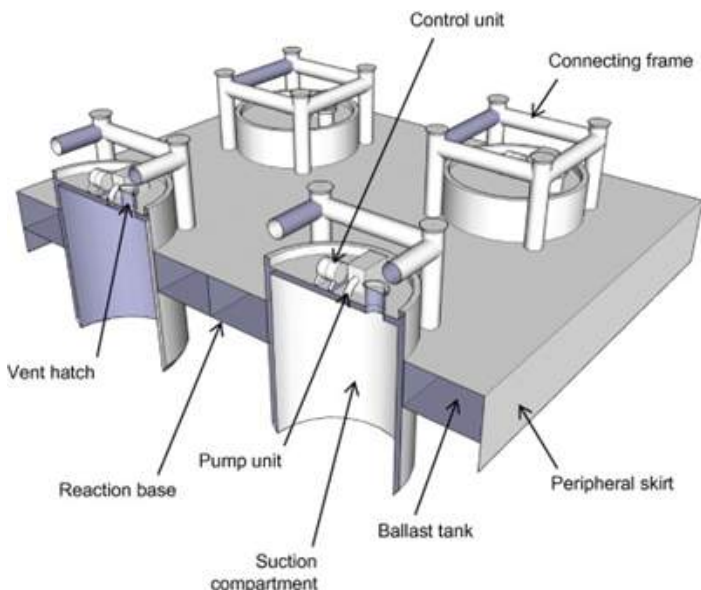


Fig. 2.8 Scheme of Hybrid foundation concept (Biene et al., 2012)

Kim et al. (2014) studied the behavior of the hybrid foundation in sand under the vertical and horizontal loading in the centrifuge. In case of the vertical loading on the hybrid suction foundation with circular mat, when displacement was induced by 20% of the diameter, the bearing capacity was 1.81 times larger than the single suction foundation. And in case of the horizontal loading with the same condition as above, when the displacement was induced by 9% of the diameter, it was found that the bearing capacity was 1.95 times larger than those of single suction foundation. Kim et al. concluded that, before and after contacting on ground with mat, the behavior was significant different from the single suction foundation.

In the present, a research group has been underway to develop to expand the market of offshore plant from 2012 by Ministry of Trade, Industry and Energy in Korea (Jee et al, 2013). This group aims to develop the technique for installation of offshore plant with deep sea such as more 3,000 m depth. The goal of the group includes techniques of foundations, stable lowering, dynamic positioning, and URF Installation. Based on these techniques, a suction hybrid foundation combined mat and blade has been under review to resist external forces effectively under various loadings (Fig. 2.9).

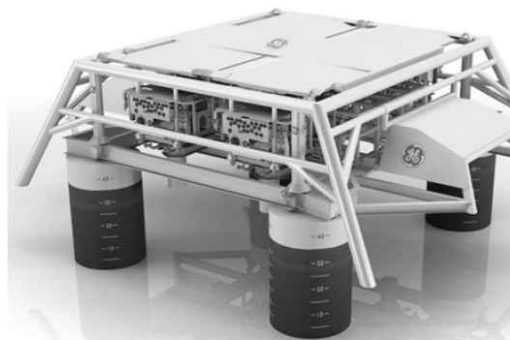


Fig. 2.9 Suction hybrid foundation (Jee et al., 2013)

(Page intentionally left blank)

## **CHAPTER III EXPERIMENTAL SETUP**

### **3.1 Introduction**

The relationship between soil and structure can be revealed by implementing a field test with similar scale. However, in most cases, a laboratory test is implemented because of practical problems; high cost, potential danger to human life (simulation of a slope failure, etc.). Especially, simulating offshore structures is more difficult.

Due to difficulties presented above, mostly a small-scale model test is conducted. At this time, the small-scale model tests have some disadvantages as follows; (a) soil stress difference (low confinement), (b) possible significant difference in soil-structure interaction problem, and (c) less accuracy in quantitative measures. Thus, the model test is typically used as qualitative approach in general. In other words, they are useful in providing information on generic behavior that can be expected in the prototype structure.

Therefore, to overcome these limitations, this study has been done its best as followings; (a) adapt consistent model scale (in Ch.3.2.1), (b) implement PIV method for accurate track of movement (in Ch.3.2.5), (c) use of equivalent flexural and axial stiffness (EI) (in Ch.3.3.1), (d) improve soil-structure interaction by relative roughness (in Ch.3.3.2), and (e) compare experimental results with analytical solutions (in Chapter VI).

## 3.2 Test equipment

### 3.2.1 Soil chamber

The soil chamber used in this study is a rectangular steel chamber. It was designed and manufactured at the Korea Institute of Construction Technology using 17 mm ~ 22 mm thick stiff steel plates. The chamber consists of several main parts as following: (a) a test box, (b) vibrating compaction system for making specific density, (c) load actuator for applying horizontal loading, (d) a wire and pulley system for connecting with load actuator and model pile, and (e) load and displacement measuring system (Fig. 3.1).

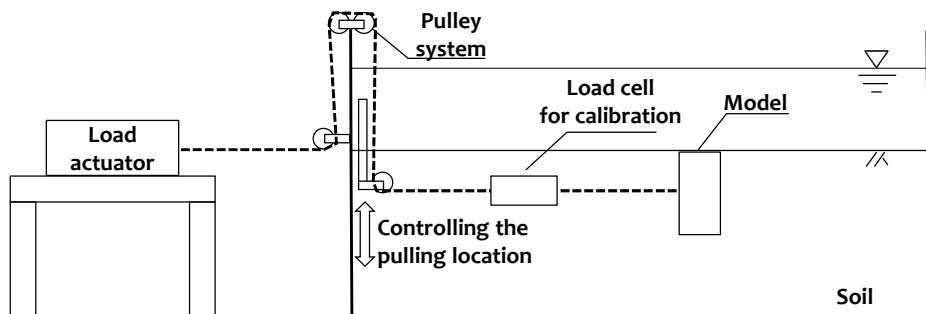


Fig. 3.1 Scheme of testing system

The soil chamber for model test cannot reproduce the infinite field condition but can produce only limited test condition. Consequently, different results from model test and field can be occurred due to this "chamber size effect." According to a large number of research results, however, if the ratio of pile diameter and soil chamber's distance is more than some constant value, it is well known that chamber size effect can be negligible (See 3.2.1 in detailed).

Based on the research results and the size of group suction piles used in this study, in this study, the size of the soil chamber had been decided as  $1.0\text{ m} \times 2.0\text{ m} \times 1.5\text{ m}$  (width  $\times$  length  $\times$  height) and made by steel to support the corresponding weight of used soil and water and upper confining load (Fig. 3.2).



Fig. 3.2 Soil chamber

One side of the soil chamber had been manufactured by special acrylate board to observe the condition of the specimen with the naked eye. Besides, two drainage pipes had been installed on the bottom and both sides of the soil chamber to drain the water in the soil chamber. To prevent plugging phenomenon between water supplying pipes and draining pipes, a porous ceramic filter had been inserted on the interface.

The soil chamber used in this study have been devised to move forwards and backwards by using pump for convenience to apply load and prepare test. Most preparatory works (i.e. installing wire, penetrating model pile, etc.) have been performed after the upper plate

translocate up and soil chamber move out (Fig. 3.3). While the vibrating compaction is needed, the soil chamber has been relocated to the location of the upper plate (Fig. 3.4).



Fig. 3.3 Soil chamber located away from the upper plate



Fig. 3.4 Soil chamber located under the upper plate

### **3.2.2 Horizontal loading system**

For analyzing the behavior of model pile, measuring the behavior of horizontal pullout is important. An actuator had been installed in outside of the soil chamber and a system have been suggested to apply horizontal load by compounding a wire and a pulley. In this study, improved horizontal loading system suggested above has been built. The load actuator has 1000kgf standard and displacement control as 0.1mm/min (Bongshin Co., Fig. 3.5).



Fig. 3.5 Load actuator

Total four pulleys have been installed to be able to vary the position of loading location. Although such compounded wire-pulley system can pull the model pile as various loading points and angles and have advantages such as no damage on the wall of the soil chamber and no loss of the soil, the problems, that applied load lessen, can happen because of diverse causes such as the friction between wire

and pulley, between particles and buried pulley, between wire and soil particles, etc. To solve this problems, submerged load cell has been set up in the soil between model pile and pulley to measure true value (Fig. 3.6).



Fig. 3.6 Submerged load cell

This submerged load cell is a product treated by triple waterproof so that the load can be measured as 0.01 kg accuracy in fully submerged state. Therefore, the reliability on the test has been improved by installing external load cell and submerged load cell simultaneously.

### 3.2.3 Vibrating compaction system

In general, when using soil chamber, raining method is wildly used. Raining method is using falling energy of sand particles when preparing the soil condition of model test. This method is usually useful in dry condition, but in case of submerged condition like this study, it is not suitable for the test, because the used sand has to be dry off after finishing the test.

Accordingly, in this study, new method has been contrived not raining method to establish the target relative density of model test. The steel plate (an upper plate) has been installed on the vertical loading actuator so that it can confine the surface of the sand, and high-generating power vibrator (EXEN Co., 550Wh, 120 Hz) has been installed on the upper plate (Fig. 3.7 ~ 3.9).

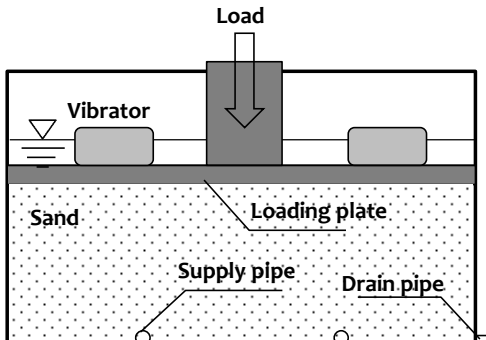


Fig. 3.7 Scheme of vibrating system



Fig. 3.8 Vibrator



Fig. 3.9 Installed vibrator on the upper plate

Hence, after saturating and disturbing the sand within the soil chamber, an upper confinement is applied on the surface of the soil, and compaction can be done by operating the vibrator. This is new method of model test to make the target density of the soil in terms of using the principle of liquefaction (Ishihara and Yoshimine, 1992; Lade and Yamamoto, 1997) which can cause the consolidation of the soil with dispersion of excessive pore water pressure.

### **3.2.4 Micro-cone penetration test**

#### **Micro-cone**

Estimating tip resistance using micro-cone can be evaluated by two micro strain gauges attached in inner wall of the cone and two strain gauges attached in back part of the cone. Strain gauges used in this micro-cone is the sensor of measuring electric resistance so that it can obtain the electric resistance from the amount of the strain caused by external force (Fig. 3.10 ~ 3.11).



Fig. 3.10 Micro strain gauges of the cone

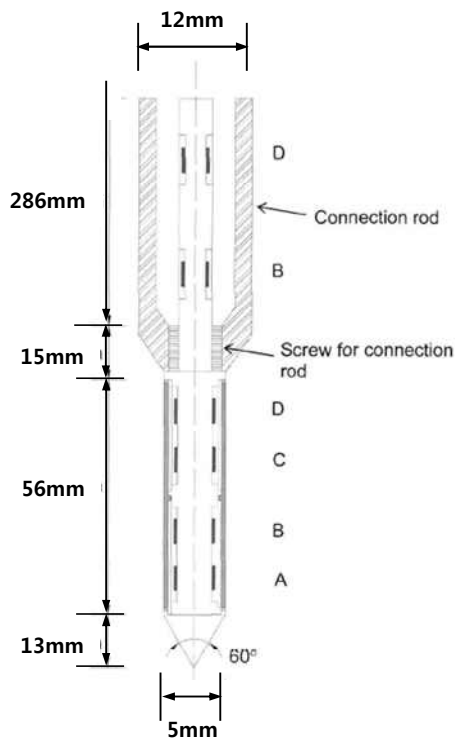


Fig. 3.11 Scheme of micro-cone

Most metal's original electric resistances are changed when mechanical tensile and compressive forces are applied. From this principle, the strain can be measured according to the change of resistance. However, general ohmmeter cannot measure the amount of change because the strain is too small. Thus, the micro change of resistance is measured by using electrical circuit of strain amplification called 'Wheatston Bridge' (Fig. 3.12).

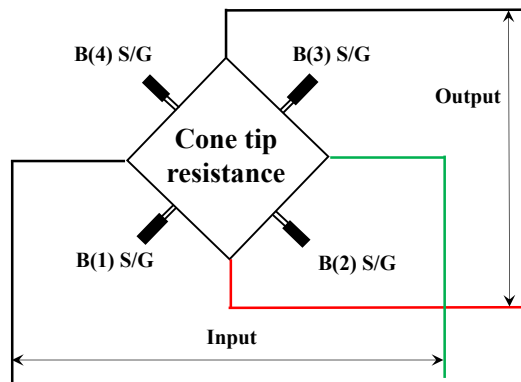


Fig. 3.12 Electric circuit of Wheaton Bridge

### Penetrometer

A penetrometer of micro-cone consists of two main parts: pushing rod (Fig. 3.13), and thrust mechanism (Fig. 3.14).

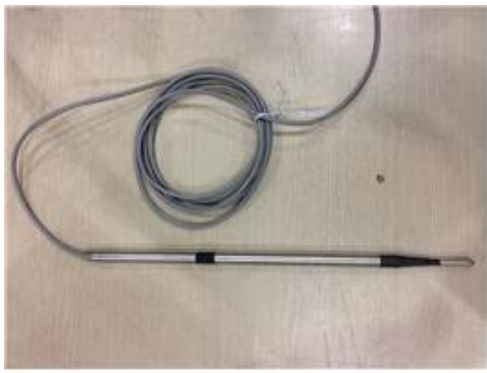


Fig. 3.13 Micro-cone and pushing rod



Fig. 3.14 Thrust mechanism

The pushing rod is used to protect the electric line connected to micro strain gauges and secure the location of the line. The thrust mechanism is located on outer side of cone rod. It consists of electric

motor to generate the rotation force for penetrating the micro cone, rod thrust bearing, and rod thrust transformer to transfer rotation force of electric motor to rod thrust bearing (Fig. 3.15). The rate of penetration is adjusted by an adjustable speed equipment.



Fig. 3.15 Installed penetrometer (left) and connected micro-cone (right)

### Measurement equipment

A constant input voltage (2.0V) is supplied to micro strain gauges attached on micro-cone tip through power supply (Fig. 3.16). The change of resistance when the micro-cone is penetrated into the soil is measured by multimeter (Fig. 3.17), so that the penetrating resistance of the soil can be estimated (Fig. 3.18).



Fig. 3.16 Power supply (E3630A model)



Fig. 3.17 Multimeter (34401A model)

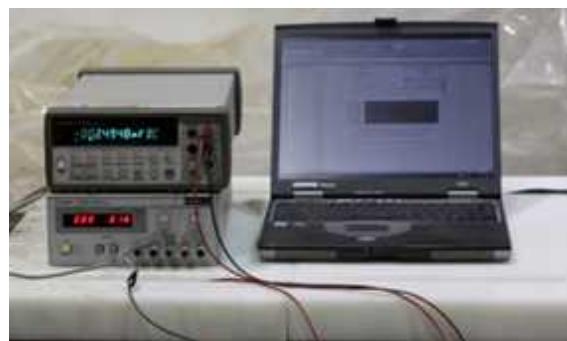


Fig. 3.18 Data logger

### 3.2.5 PIV method

Particle Image velocimetry (PIV) is an optical method of flow visualization used in education and research. Recently, it was used more and more in geotechnical engineering. The general idea of this method is explained in Fig. 3.19. A camera system and illumination system are set up in front of the measuring area. Photographs are taken at different time during test for analysis the movement of tracer particles.

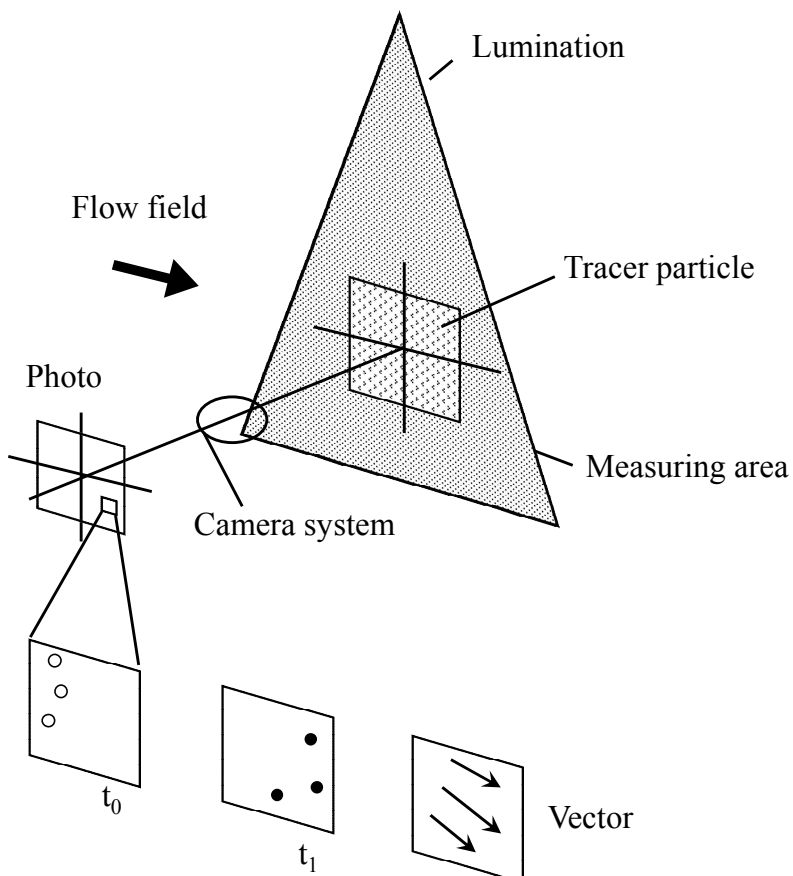


Fig. 3.19 Scheme of PIV method

Generally, PIV method can be divided into two kinds. One is called density correlation method where movement of local grey-scale pattern is measured, while another one is called particle tracking velocimetry method where movement of tracer particles is measured. The two are compared in the below Fig. 3.20.

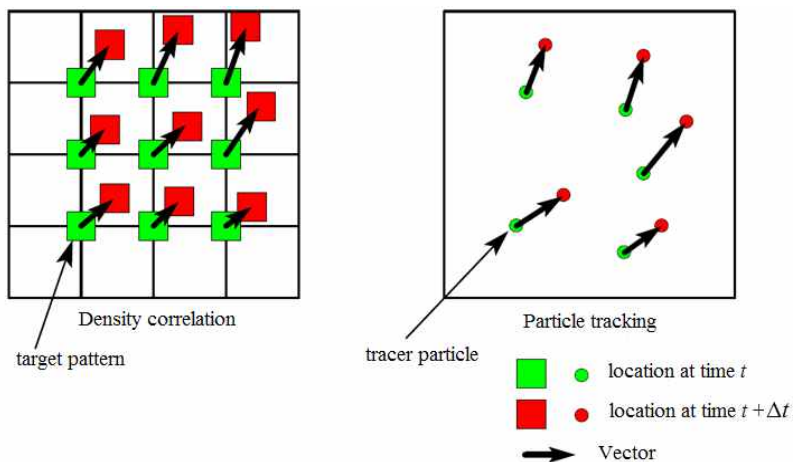


Fig. 3.20 Scheme of the two methods of PIV

For the density correlation method, it is also called digital image correlation (DIC) method in many publications. The image is first divided into random grids, then a target pattern is set up at each grid point. In the next image, the target pattern may move to another place. The new location of the target pattern will be calculated by an evaluation equation and then the movement can be calculated. Therefore, 2 images are needed for comparison analysis in this method and the target patterns in two images should have certain level of correlation. This method is suitable for small displacement, for example, progressive deformation of soils.

For the particle tracking method, tracer particles are set up in

observed object. They can be extracted by binary image or other method and locations of the tracer particles in each image can be known separately. Therefore, images at different time can be analyzed separately and there is no correlation requirement between images. This method is suitable for both small and large displacements, and especially for random arrangement of observed object (Fig. 3.21).

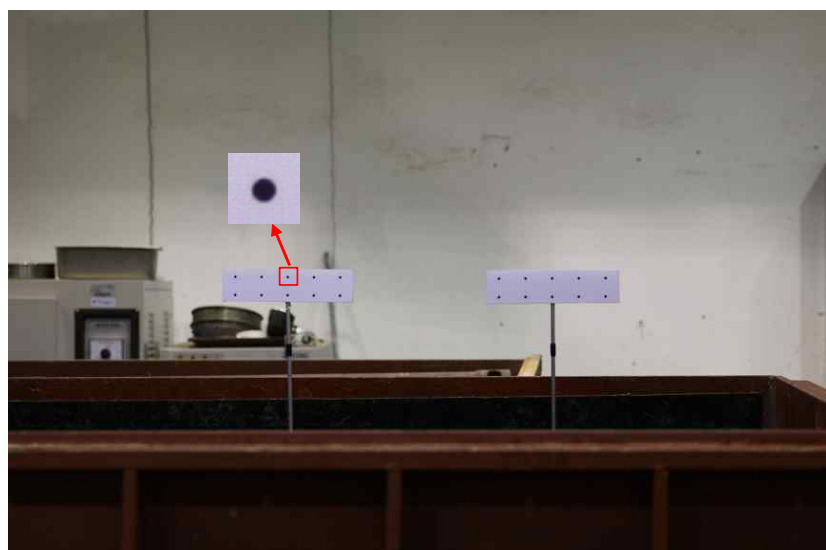


Fig. 3.21 Observed image with tracking black points

### 3.3 Model pile on the test

#### 3.3.1 Design and instrumentation

##### *Single suction pile*

In Korea, the maximum diameter of prefabricated pile is 3 m. Since the width of used soil chamber is 1 m, the scale of model pile had been considered based on this 1 m. The purpose of this study was for estimating the behavior of group suction piles having  $2D \sim 4D$  spacing. According to the results of Prakash (1962) and Chung & Jeong (2001), minimum distance to avoid the group size effect is about  $3D$ . Thus, the width had been decided as  $15D$  ( $3D + 9D + 3D$ ,  $15D = 1$  m,  $D = 66.7$  mm, Fig. 3.22), finally  $D$  had been decided as 60 mm diameter in practice. Thus, the scale has been confirmed as 1/50 (60 mm / 3 m).

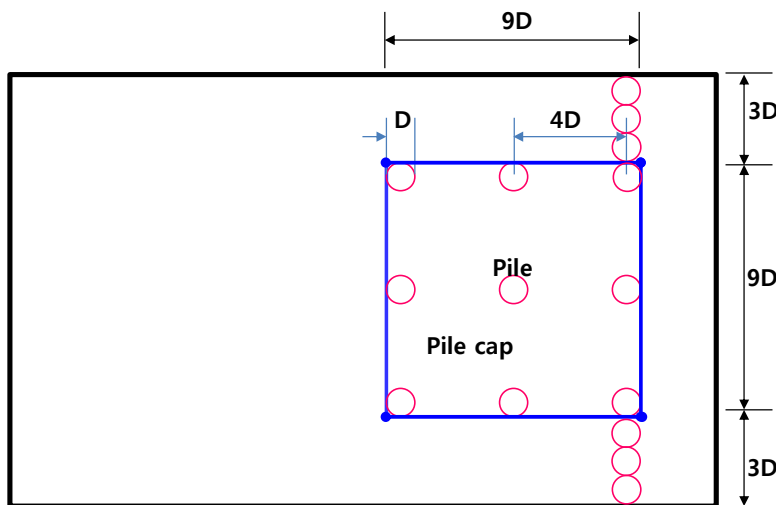


Fig. 3.22 Scheme of initial plan

Next, based on the classification of Broms' method, an aspect ratio (L/D; L: pile length, D: pile diameter) has been decided 3 as a short pile (Table 3.1).

Table 3.1 Classification of Broms' method

L/D	2	3	4	5	6	
Diameter (m)	3.0					
Length (m)	6.0	9.0	12.0	15.0	18.0	
Classification by Broms' method	Short pile		Medium pile			

The single suction pile consists of two main parts: (a) a pile cap, which is able to suck, and (b) pile wall, which will be penetrated into the soil. First of all, the pile cap had been processed by cutting 60 mm diameter of aluminum plate having 30 mm thickness to install a pump outlet on the center. Secondly, the pile wall was made by using manufactured aluminum pipe having 60 mm diameter and 1.2 mm thickness, and cut as 180 mm length (Table 3.2, Fig. 3.23). The aluminum was chosen to simulate the flexural stiffness (EI) of iron, which is prototype's material.

Table 3.2 Material properties of iron and aluminum

Materials	E (kgf/cm <sup>2</sup> × 10 <sup>3</sup> )	Diameter (cm)	Thickness (cm)	I (cm <sup>4</sup> )	EI (kgf • cm <sup>2</sup> × 10 <sup>3</sup> )
Iron	2.17	6.00	0.04	3386.14	7347.92
Aluminum	0.72	6.00	0.12	10117.85	7284.85

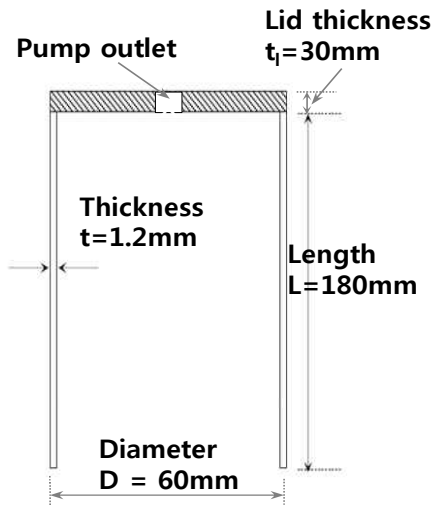


Fig. 3.23 Scheme of single suction model pile

In this study, a wire jig has been contrived for connecting with model pile to estimate horizontal pullout behavior of the pile. At the first stage of this study, the loading system was directly connecting the wire jig and the model pile using pad-eye (Fig. 3.24).



Fig. 3.24 Initial version of the model pile

Although this system had an advantage to apply load onto exactly target loading location, the wire jig had to be installed from outside of the surface to target loading location path by pressing the wire into the soil (Fig. 3.25). This method could not only check how exactly the wire had maintained the horizontality, but also could occur some problems such as the disturbance of the soil. Also, it could be considered as unintentional resistance while penetrating the model pile.

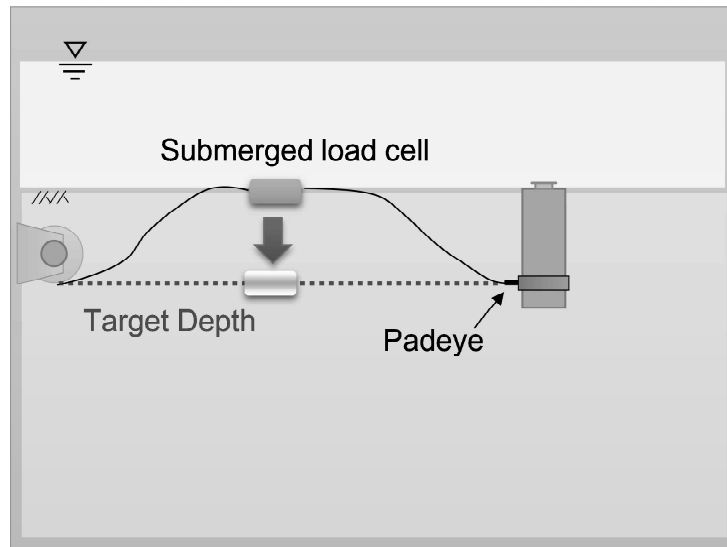


Fig. 3.25 Installing problem on initial version of model pile

To minimize such disturbance of the soil, the type of model pile had been changed from the initial version of one. Consequently, the testing method had been modified; first, the wire was installed and buried at the target loading depth in advance (Fig. 3.26). Next, model pile was penetrated into the center of installed wire (Fig. 3.27), and lastly, the wire was drawn horizontally to connect the target loading location on the model pile (Fig. 3.28).

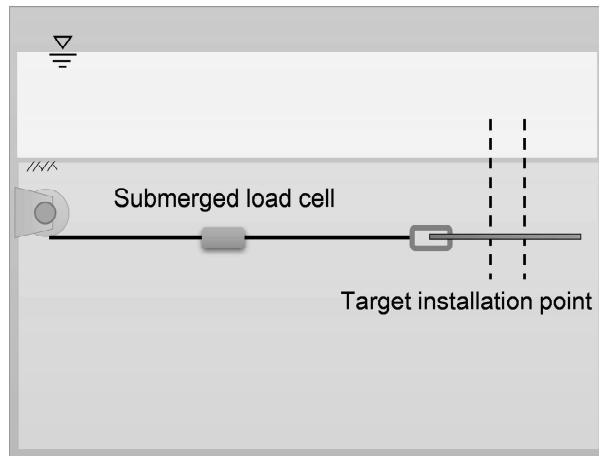


Fig. 3.26 Install wire (First)

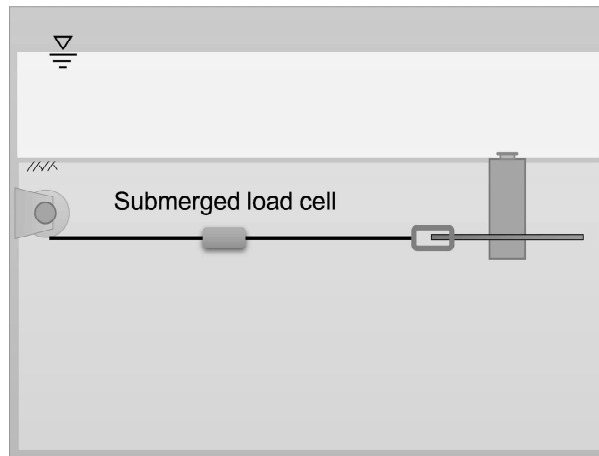


Fig. 3.27 Penetrate model pile (Second)

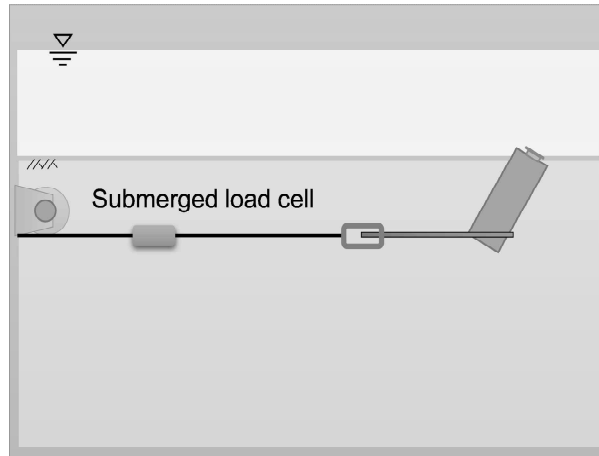


Fig. 3.28 Draw model pile by wire (Third)

Thus, inducing jig in shape of ribbon had been contrived newly to connect with model pile well (Fig. 3.29). This inducing jig had 70 mm height, 40 mm width, and 5 mm thickness. Although this type of model pile had excellent efficiency without disturbance of the soil when locating the wire and model pile, It still had some disadvantages such as an increase of model pile's weight and penetration resistance, and change of model pile's centroid, etc.



Fig. 3.29 Second version of model pile and inducing jig

At the end of several trials and errors, finally inducing jig has been contrived to minimize the penetration resistance, and to vary the loading location on the model pile (Fig. 3.30 ~ 3.31).

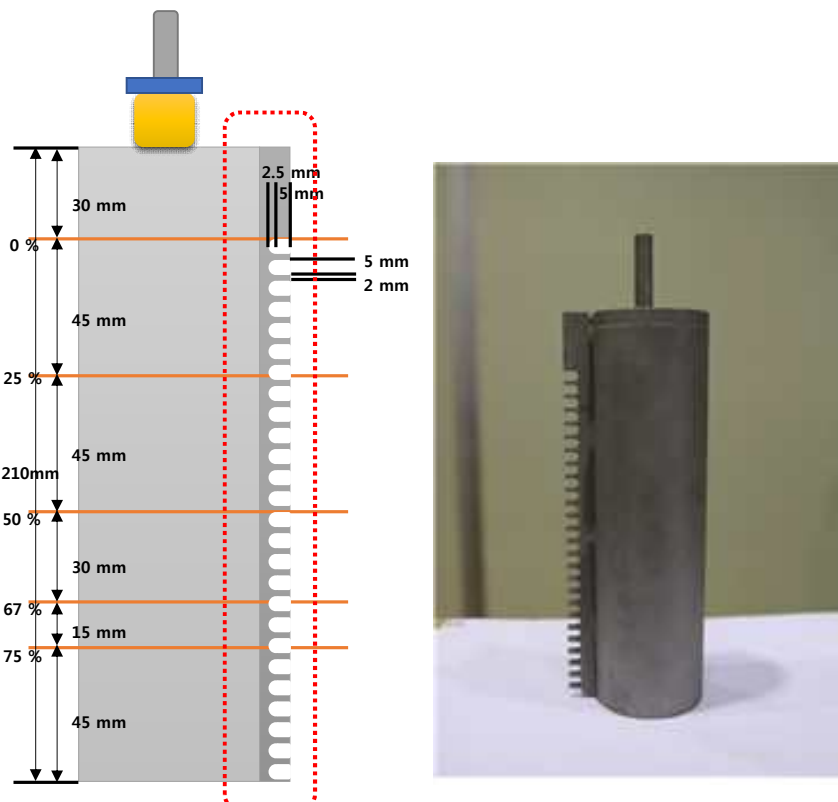


Fig. 3.30 Scheme of the final version of model pile

Fig. 3.31 Final version of model pile

This final type of model pile has been processed by aluminum plate having 5 mm thickness, cut holes having 7.5 mm depth, 5 mm width with 2 mm intervals. This type is lighter than previous ones and can be considered to minimize the penetration resistance. However, skillful techniques are needed to locate pile into the target loading depth. Thus, repeated tests were necessary in some cases.

### Group suction piles

In this study, group suction piles have been proposed newly as a foundation of huge floating offshore structure. This group model pile was made having same properties of single model pile. This has been contrived to reproduce the penetrating process of suction pile in sand (Fig. 3.32 ~ 3.33).



Fig. 3.32 Group suction piles (3D)

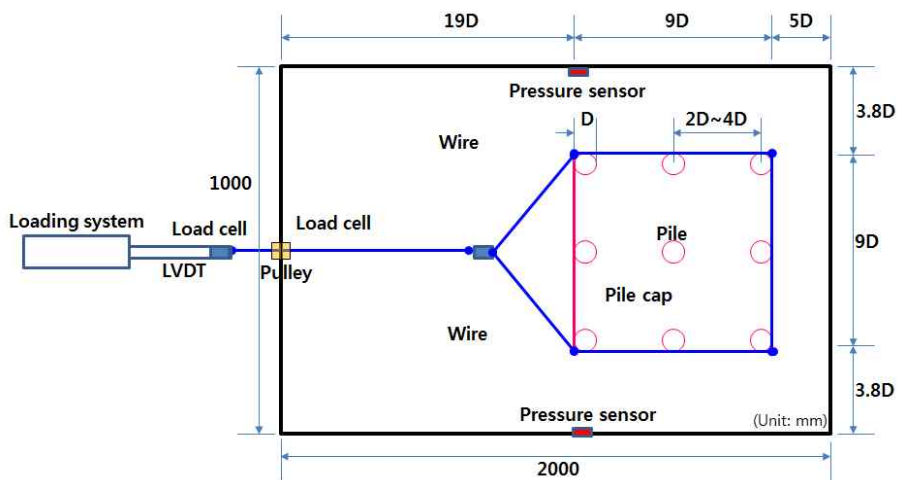


Fig. 3.33 Scheme of installed group suction piles (4D)

This processed group suction piles are the structure which connected pile cap and single model pile are connected firmly. By locating single suction pile under the pile cap having 2D, 3D, 4D spacing, respectively, the group model pile has been set up (Fig. 3.34 ~ 3.35). The group suction piles and the pile cap have been processed by the same materials as aluminum with single suction pile, for considering the stiffness or endurance of the pile, and for comparing to the behavior of single suction pile and group suction piles.

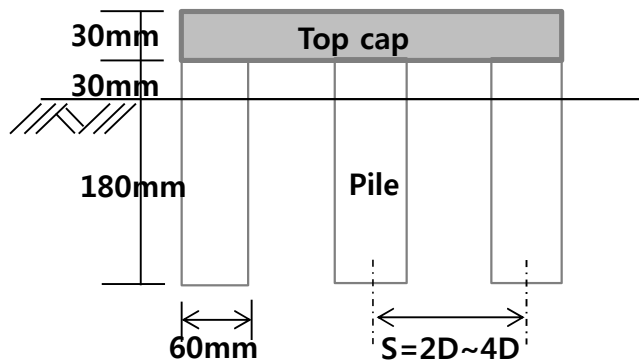


Fig. 3.34 Scheme of side view of group suction piles

(Unit: mm)

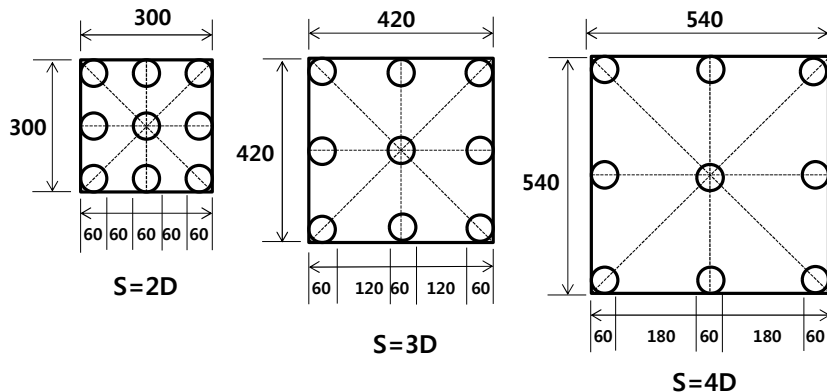


Fig. 3.35 Scheme of plain view of group suction piles

Total six earth pressure cells have been attached on each row's center or side, and analyzed relative distribution of earth pressure to draw 'group pile effect' and 'reduction coefficient of bearing capacity' over each pile according to the position (Fig. 3.36). Moreover, inducing jig has been attached onto the third row's wall to pull out the piles (Fig. 3.37).



Fig. 3.36 Attached earth pressure cell



Fig. 3.37 Attached inducing jig on third row

The group suction piles are the favorable structure for supporting large loading. Additionally, a rotation of the pile can be restrained by the pile cap in horizontal loading condition so that larger bearing capacity can be expected to be shown.

### 3.3.2 Surface roughness of model pile

The numbers of parameters that influence performance of a pile subjected to a vertical or horizontal load are widely and mostly interrelated. Leland and Kraft (1991) categorized these parameters into 4 main parameters: installation methods, load, soil and pile parameters. An equation of the following form (Eq. (3.1)) is usually used to estimate the ultimate skin resistance of a vertical circular pile in sand:

$$\tau_f = \sigma'_{rf} \tan \delta_f = K_o \sigma'_{v} \tan \delta_f \quad (3.1)$$

Parameters  $K_o$  and  $\delta_f$  are the most important ones that need to be determined. Several studies have been performed on the shear resistance at the interface between soil and foundation material (Potyondy 1961; Yoshimi and Khishida 1981; Acar et al. 1982; Bozozuk et al. 1979; Datta et al. 1980), and revealed that the interface friction is affected by surface roughness (Fig. 3.38).

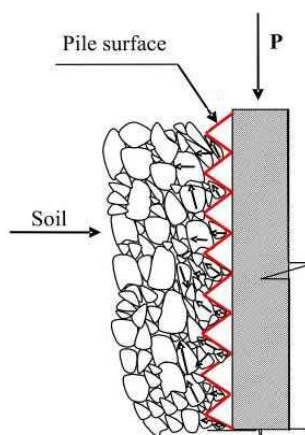


Fig. 3.38 Schematic expression of surface roughness  
(Leland and Kraft, 1991)

At this point, many researchers had been proposed that the ratio ( $R_n = R_a/D_{50}$ ; Eq. (3.2)) of the average surface roughness ( $R_a$ ) of a model pile to the mean particle size ( $D_{50}$ ) of the sand influences the interface friction characteristics between the model pile and sands (Uesugi et al., 1986; Subba et al., 1998; Porcino et al., 2003).

$$R_n = \frac{R_a}{D_{50}} \quad (3.2)$$

Where,  $R_n$ : relative roughness

$R_a$ : average surface roughness of model pile

$D_{50}$ : mean particle size

Firstly, parameters presented above had been investigated. Next, to improve the reliability of the this study's test, sand-blasting work had been performed to the model pile by reproducing the surface roughness of a prototype. The results is shown below (Table 3.3, Fig. 3.39 ~ 3.40).

Table 3.3 Test result of surface roughness

Parameter	Prototype	Model
$D_{50}$	0.35 mm	0.57 mm
$R_a$	8 $\mu m$ (Lehane et al., 1993)	12 $\mu m$ ~ 15 $\mu m$
$R_n$	0.229	0.211 ~ 0.263



Fig. 3.39 Original model pile



Fig. 3.40 Sand blasted model pile

Measured surface roughness of model pile shows similar value with the prototype's one. The roughness of steel piles varies based on the manufacturing company; however, the surface roughness and friction coefficient used in these model tests can be assumed to be reasonable.

## 3.4 Soil conditions

### 3.4.1 Engineering properties of the test sand

In general, standard sand is used to make up the soil condition in the model test using large scale soil chamber. Therefore, Joomunjin sand have been used in this study. A series of basic laboratory tests were performed to obtain the engineering properties of the test sand. The properties of Joomunjin sand is shown below (Fig. 3.41 ~ 3.43, Table 3.4 ~ 3.5).

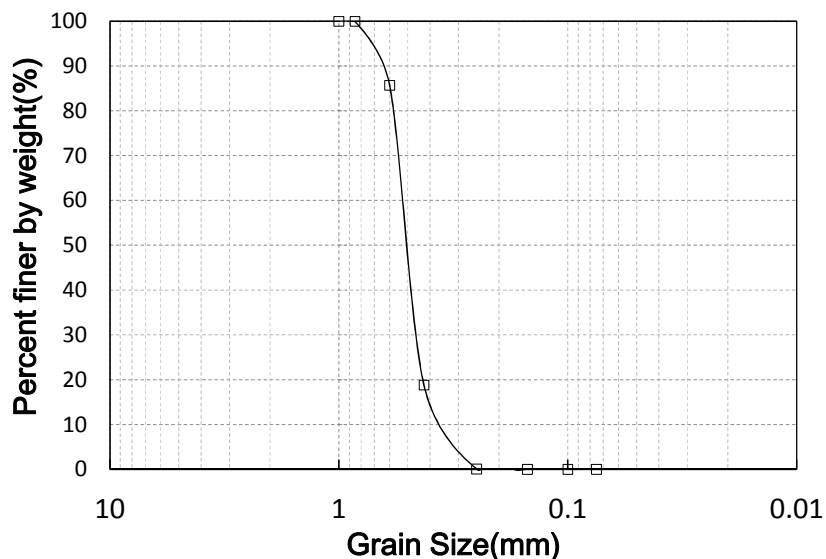


Fig. 3.41 Grain size distribution curve

Table 3.4 Soil properties

Description	Symbol	Property
USCS	SP	Poorly graded sand
Specific gravity	$G_s$	2.62
Max. void ratio	$e_{\max}$	0.92
Min. void ratio	$e_{\min}$	0.63
Max. dry unit weight	$\gamma_{d\max}$	15.8 $kN/m^3$
Min. dry unit weight	$\gamma_{d\min}$	13.4 $kN/m^3$
Effective particle size	$D_{10}$	0.42 mm
Particle size of 30 passing %	$D_{30}$	0.51 mm
Mean particle size	$D_{50}$	0.57 mm
Particle size of 60 passing %	$D_{60}$	0.63 mm
Uniformity coefficient	$C_u$	1.5
Coefficient of curvature	$C_c$	1.0
Average relative density	Avg. $D_r$	70%
Cohesion	c	0
Internal friction angle	$\phi$	37.5

Table 3.5 Internal friction angle ( $^\circ$ ) of Joomunjin Standard Sand

Relative density		70%
Principle stress ratio	$\sigma_3 = 50$ kPa	38.6
	$\sigma_3 = 100$ kPa	38.2
	$\sigma_3 = 200$ kPa	35.7
	Average	37.5

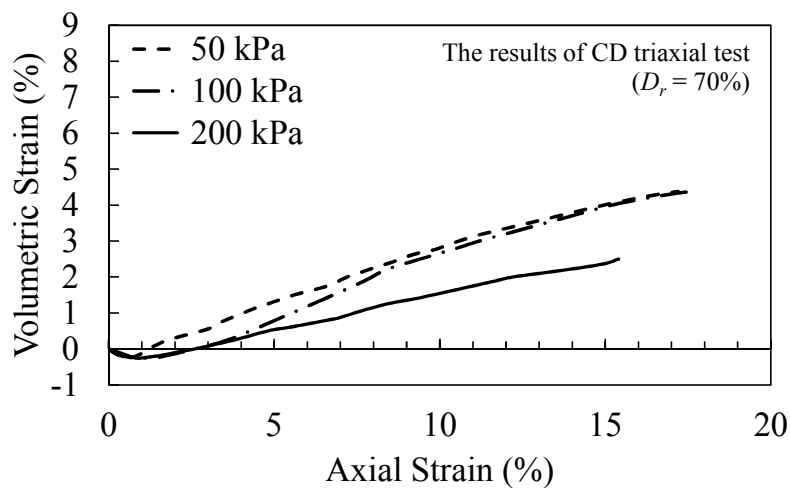


Fig. 3.42 Axial and volumetric strain Dr 70%

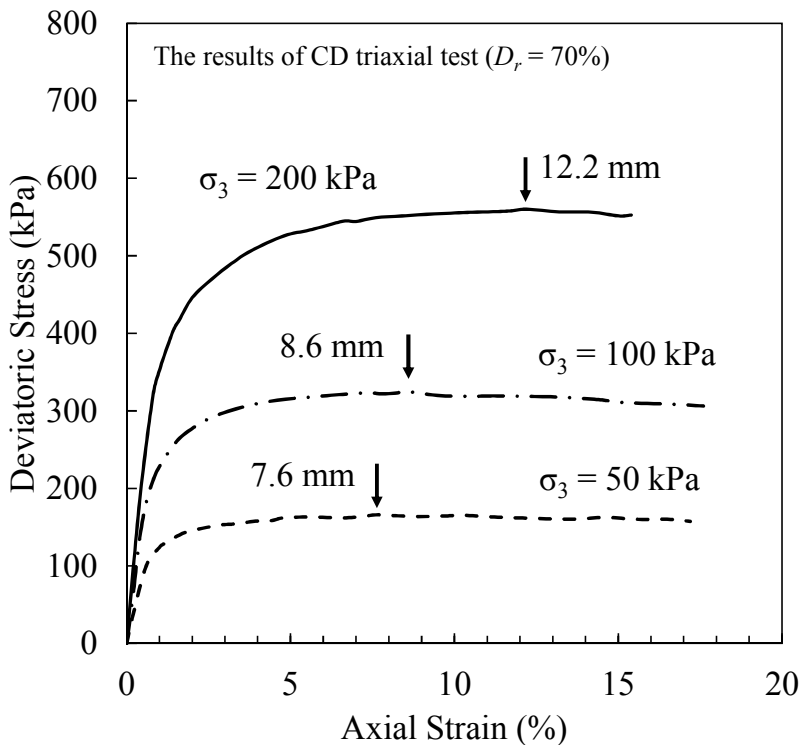


Fig. 3.43 Axial strain and deviatoric stress Dr 70%

### 3.4.2 Size effect

Tests on soil chambers or tanks cannot simulate perfectly full-scale field tests because of the boundary effects that result from limited chamber sizes. This is one of the limitations of soil chamber tests. There is, however, general agreement in the literature that the boundary effects can be neglected if the ratio of the pile diameter to the chamber diameter is above certain threshold values. Many researchers have investigated chamber boundary effects on pile or cone penetration resistance measured in chamber samples (Parkin et al., 1982; Been et al., 1986; Vipulanandan et al., 1989; Schnaid and Houlsby, 1991; Salgado et al., 1998).

Parkin and Lunne (1982) had been revealed that in normally consolidated sand, the ratio should be more than about 50 times, and in over consolidated sand, it should be more than about 100 times through two model piles having different diameters and model tests using pressed soil chamber. In addition, Salgado et al. (1998) had been obtained that the ratio should be more than 100 times in sand through numerical analysis to minimize the chamber size effect.

Tcheng (1996) had been reported that in case of rigid wall, the ratio of the pile diameter to the chamber diameter should be more than 200 times to neglect chamber size effect. Also, in case of flexible wall, the ratio of pile diameter and soil chamber's distance should be more than about 20 times to neglect chamber size effect.

On the other hand, according to the ‘cavity expansion theory’, plastic zone occurred on the point of penetrated model pile into dense sand is expanded 7.5 times of diameter horizontally, and 8 times of diameter vertically. Therefore, since this plastic zone is related to the penetrating resistance and bearing capacity, the soil chamber should be

larger than the plastic zone occurred on the point of the model pile to minimize the effect. Considering these points, Vipulanandan et al. (1989) had been proposed that the minimum size of soil chamber is 7.5 times of model pile, and maximum penetration depth is 4 times of model pile from the bottom of the soil chamber in dense sand.

The diameter ratio is an important factor in model pile testing because the proximity of the chamber boundary may cause an increase in the experimental pile capacities. In this study, the chamber-to-pile diameter ratio is approximately 17 since the soil chamber's the width and model pile diameter are equal to 1,000 mm and 60 mm, respectively, and penetration depth, 180 mm is approximately 1/5 times of the distance to the bottom, 820 mm (Fig. 3.44). Therefore, chamber size effect can be neglected.

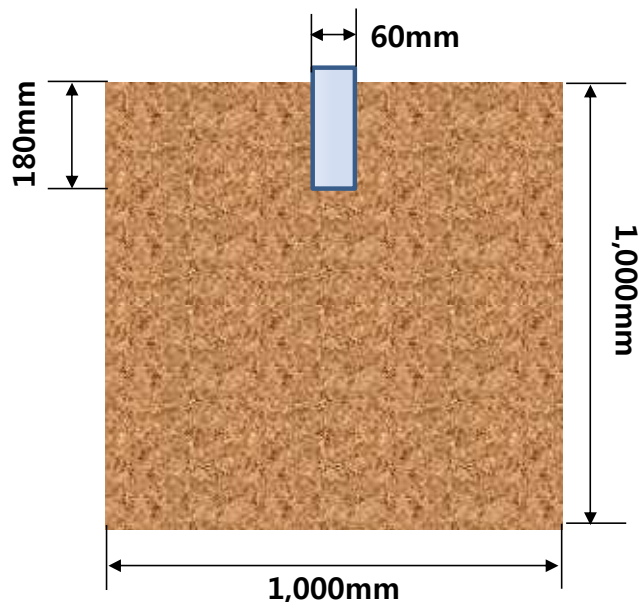


Fig. 3.44 Scheme of installed model pile

Before taking up the main subject, a numerical analysis had been performed to verify the boundary effect. The dimension of the soil box used in the tests is  $2\text{m}$  (length)  $\times$   $1\text{m}$  (width)  $\times$   $1.5\text{m}$  (height). The outer boundary of the foundation with  $4D$  center-to-center pile spacing is the  $0.36\text{m}$  (length)  $\times$   $0.36\text{m}$  (width)  $\times$   $0.06\text{m}$  (long). Therefore, the net distance between the side of the foundation and the soil box is  $3.8D$  (Ch.3.3.1 in detail). The Finite Element (FE) analysis was performed using a commercial ABAQUS/Standard (Simulia, 2010) program. Fig. 3.45 and Table 3.6 show the performed FE meshes and boundary conditions, and input properties.

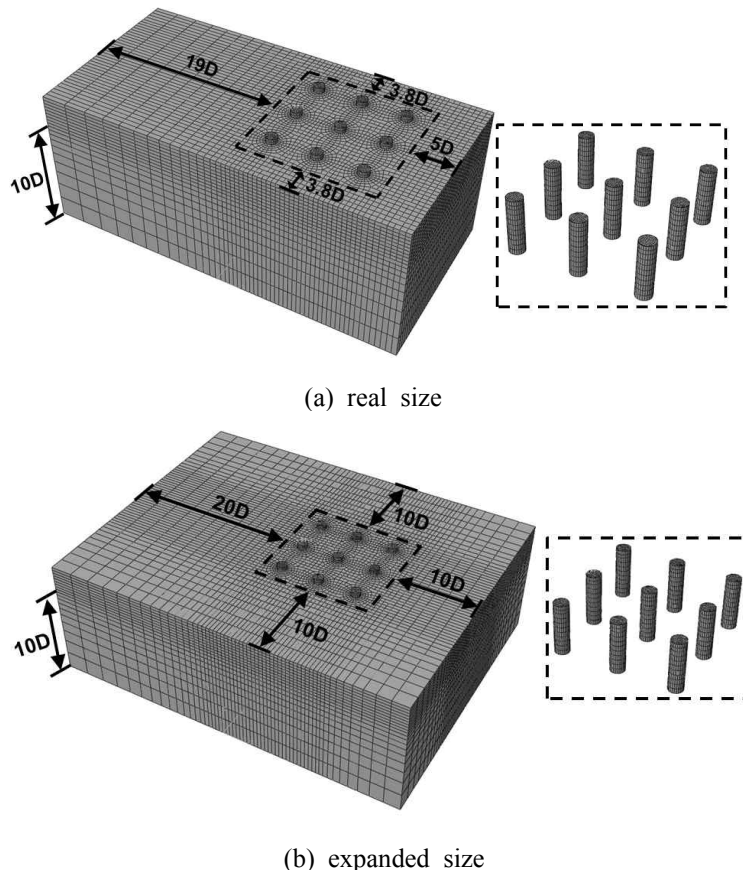
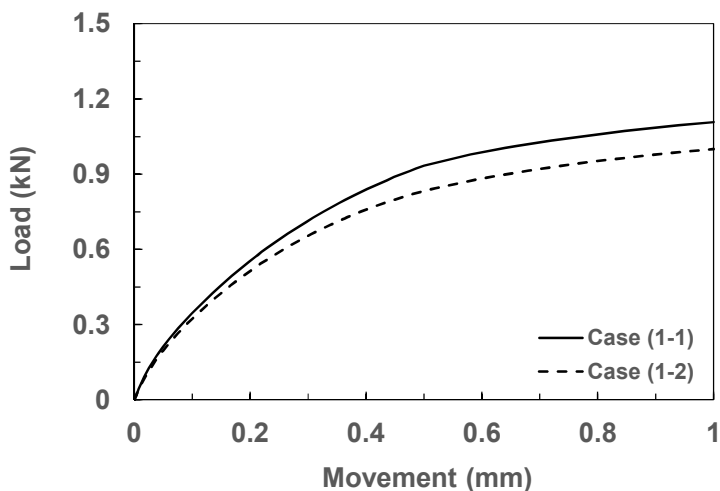


Fig. 3.45 FE meshes and boundary conditions

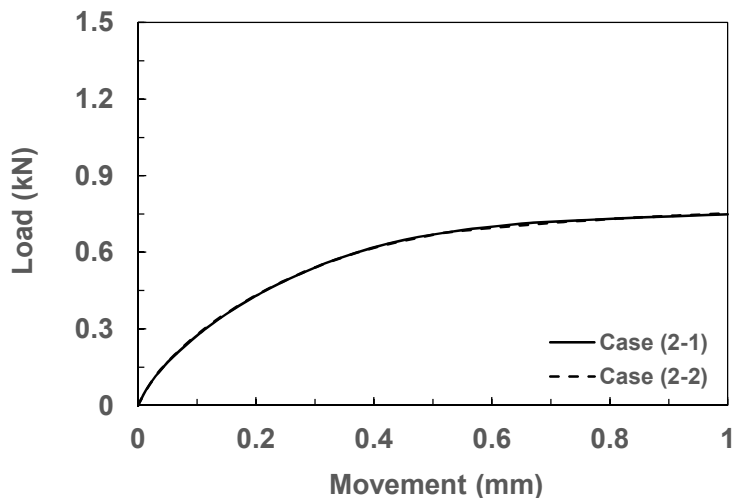
Table 3.6 Input properties

Type	Constitutive model	Young's modulus ( $kPa$ )	$\gamma'$ ( $kN/m^3$ )	Poisson ratio	Cohesion ( $kPa$ )	Internal friction angle ( $^\circ$ )	Dilation angle ( $^\circ$ )
Sand	Mohr-Coulomb	5,000	9	0.30	0.1	36	6
Pile	Elastic	$7.1 \times 10^7$	17	0.33	-	-	-

Fig. 3.46 shows the comparison of the load-movement curves. Case (1-1) (model with 4D pile spacing) showed about 10% larger resistance than that of Case (1-2) due to the restraint effect of the narrow boundary. However, Case (2-1) (model with 3D pile spacing) showed almost the identical resistance with Case (2-2), which means that there is no boundary effect in the model with 3D pile spacing.



(a) 4D pile spacing



(b) 3D pile spacing

Fig. 3.46 Horizontal load-movement curves at the top of the foundation

Thus, the results mean that some amount of bearing capacity in the group test can be estimated more slightly.

### **3.4.3 Internal scale effect**

There are two sources of internal scale effects: for tip resistance, if the particles become too large compared with the pile diameter, the particle's characteristics of soil chamber over and cone resistance becomes too dependent on the geometry of the particles and their arrangement (additionally, continuum mechanics cannot be assumed); for shaft resistance, the shear band that forms around the pile shaft during vertical loading becomes too thick with respect to the pile diameter if particles are large, and this causes to the development of excessive normal effective stress and thus excessively high shaft resistance.

In order to minimize these internal scale effects, the ratio of the pile or cone diameter to the soil particle diameter have been suggested by the literature for penetration tests in sand (Peterson, 1988; Vipulanandan et al., 1989).

Peterson (1988) had been conducted a laboratory investigation to estimate the influence of specimen density, grain size, penetrometer diameter, penetration rate, and pore water on penetration resistance in fine sand. Peterson suggested that it is desirable to maintain the ratio of the pile diameter to the soil particle diameter at 80 or larger to minimize the internal scale effect between a penetrated object and the used soil. By contrast, Vipulanandan et al. (1989) suggested that the pile-to-particle diameter ratio (soil particle diameter D<sub>10</sub>) should be at least 50.

In this study, the ratio of the model pile diameter (60mm) to the mean sand particle diameter (mean sand particle size,  $D_{50}=0.57$  mm) is approximately 105. This ratio is greater than the suggested values in the researches presented above; therefore, it can be considered that the soil particle size is small enough to avoid internal scale effect over model test.

### 3.4.4 Target relative density

Based on the report of the Korea Rural Community Corporation (KRC), the seabed of Saemanguem region at the West Sea in Korea consists of silty sand and silty clay having  $10 \sim 30$  of  $N$  value and  $15 \text{ m} \sim 25 \text{ m}$  of the depth. Skempton (1986) had been standardized the  $N$  value to  $N_1$  under effective overburden pressure  $1 \text{ kg/cm}^2$ , and to  $(N_1)_{60}$  having 60% of the blow energy. Then, by using previous studies proposed in USA, Japan, England, etc., standardized relationships between  $(N_1)_{60}$  and relative density on sand had been analyzed and suggested(Eq. (3.3) ~ (3.5)).

$$\frac{(N_1)_{60}}{Dr^2} = 55 \quad \text{for fine sand} \quad (3.3)$$

$$\frac{(N_1)_{60}}{Dr^2} = 60 \quad \text{for medium sand} \quad (3.4)$$

$$\frac{(N_1)_{60}}{Dr^2} = 65 \quad \text{for coarse sand} \quad (3.5)$$

Using equation for medium sand and  $N = 30$ , the relative density on the western sea is expected as  $Dr = 70\%$ . Thus, in this study, Dr 70% of Joomunjin standard sand has been set up for the test.

(Page intentionally left blank)

## **CHAPTER IV MODEL TESTS ON SINGLE SUCTION PILE**

### **4.1 Introduction**

The purposes of single suction pile model test are (a) to obtain reliability against test method and equipment operation in terms of results and repeatability of the experiment, (b) to analyze the effect of suction installation method on the horizontal behavior of the suction pile, and (c) to provide reference values for the verification of group suction piles behavior under various loading conditions from the examination of suction pile behavior.

The suction installation of suction pile into sandy soils induces seepage flow from outside to inside of suction pile; therefore, the downward seepage near the outside of suction pile increases the effective stress while the upward seepage inside the suction pile decreases the effective stress (Manh, 2005; Fig. 4.1). The seepage effect helps suction pile installation by reducing the penetration resistance during the installation, on the other hand, reduces the horizontal capacity of suction pile from the significant disturbance at the tip of the suction pile. Due to the complexity and difficulty in quantification of the suction installation effects (including seepage effect), many previous researchers neglect the effect of suction installation in their experiments. Therefore, in this study, the effect of suction installation on the horizontal suction pile capacity has been examined.

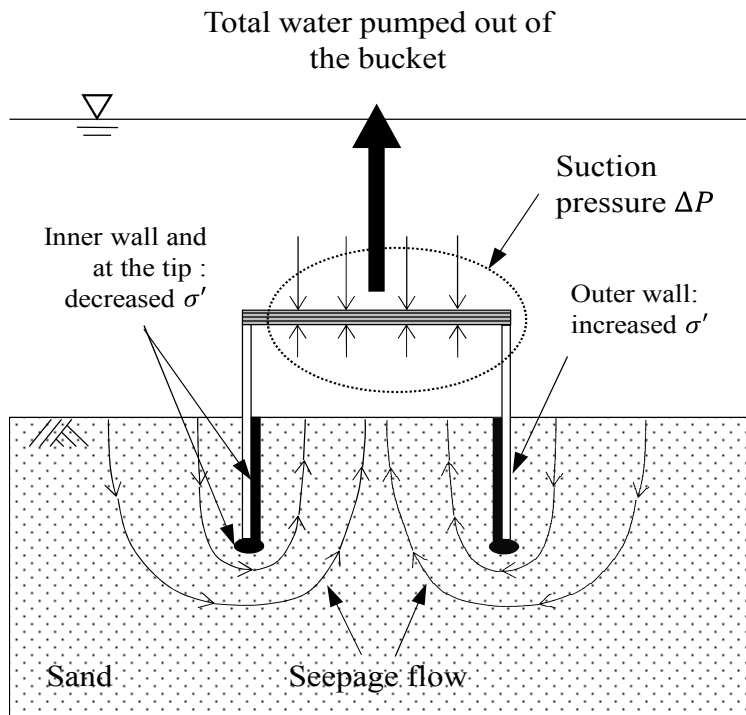


Fig. 4.1 Effect of seepage gradient on soil effective stress (Manh, 2005)

The reason of studying horizontal behavior of suction piles in the present research is as follows: The pulling direction of suction pile in the catenary type mooring system of a floating structure (Fig. 4.2) is  $0^\circ \sim 20^\circ$  to the horizontal under moderate sea depth (less than 50 m),  $30^\circ \sim 40^\circ$  under deeper sea depth more than 50 m (Randolph et al., 2005). The maximum pull-out capacities of suction piles installed on cohesive and frictional soils identified at the mooring locations of 55%  $\sim$  70% and 70%  $\sim$  80% of their embedded depths from their pile tops, respectively (Table 4.1). Therefore, in this study, suction behavior under different loading locations and loading inclinations has been analyzed from the references of literature review results.

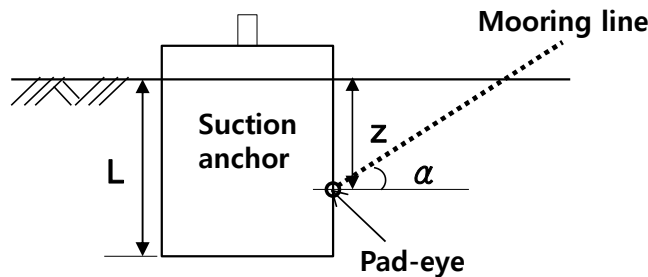
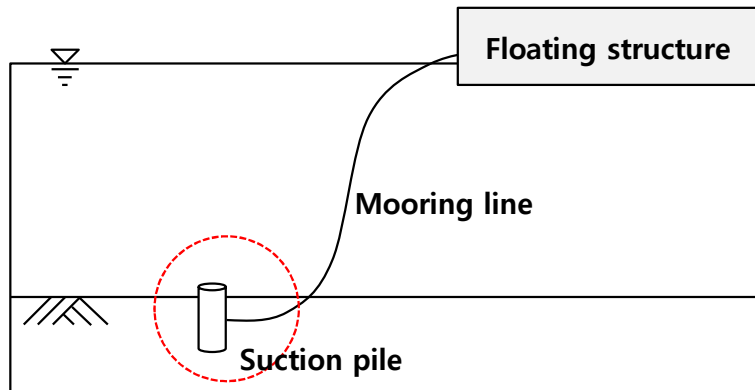


Fig. 4.2 Loading conditions of suction piles in Catenary mooring system

Table 4.1 Loading angle and loading location of suction piles in Catenary mooring system

Loading angle, $\alpha$ (Randolph et al., 2005)		Loading point, $z/L$	
Moderate sea depth (20m~50m)	Deeper sea depth (>50m)	Clay	Sand
$0^\circ \sim 20^\circ$	$30^\circ \sim 40^\circ$	65% ~ 70% (Andersen et al., 2005)	70% ~ 80% (Bang et al., 2001, 2011)
		55% (Bang et al., 2001)	

## 4.2 Test program

Prior to the main experiment, assurance of the reliability of the experiment system and method should be important. The reliability of experimental method can be obtained from repeatability of the test results. In this study, triplicate tests were performed for each test under the same test condition to validate the repeatability of the experiment. The horizontal loading location is determined at two third from the pile top along its shaft, which is the centroid of the triangular lateral earth pressure distribution proposed by Broms (1964). When a suction pile is horizontally loaded, both rotation and translation occur simultaneously, as explained in the earlier chapter (Ch. III).

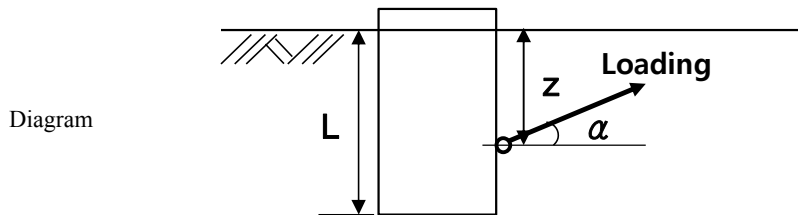
Ideally, if the horizontal loading location is at the centroid of the mobilized earth pressure distribution against the horizontal load, only translation occurs without any rotation. To test the repeatability of the experiment, a suction pile with embedded depth ( $L$ ) of 180 mm is installed using suction and is horizontally loaded at the depth ( $z$ ) of 67% of  $L$  from the pile top along the shaft.

To examine the effect of suction installation on a suction pile's horizontal behavior, the model pile was installed both by suction pressure and jacking force at the loading location of 67% of  $L$  ( $L = 180$  mm) from the pile top. For each test, a miniature cone penetration test was performed to examine the soil states of inside and outside the suction pile. The loading locations of single suction pile are as follows: Percentiles of normalized loading locations ( $z/L$ ) with respect to the embedded depth of suction pile are 25%, 50%, 67%, and 75% and loading inclinations are  $0^\circ$  and  $20^\circ$ . The tests were performed under displacement controlled with the loading rate of 100 mm/min, as

proposed by Coffman et al. (2004) and Bang et al. (2011). More details of the test program are summarized in Table 4.2.

Table 4.2 Test program for single suction pile

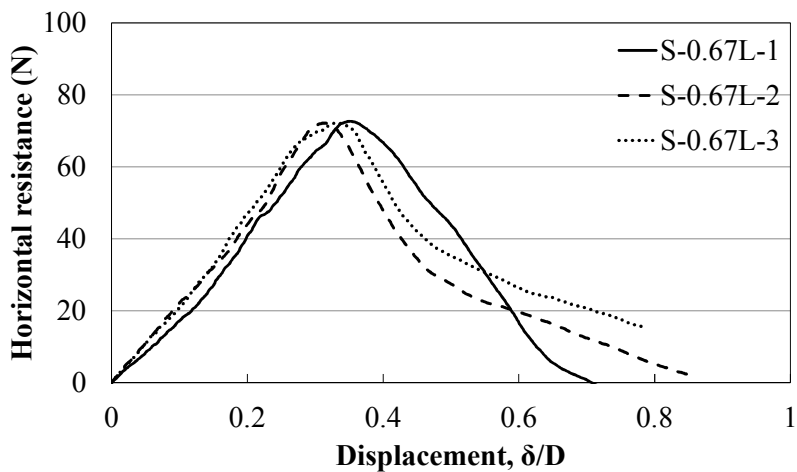
Case	Penetration depth, L (mm)	Loading point, z	Loading angle, $\alpha$ (degree)	Installation method	Loading rate (mm/min)
S-0.25L	180	0.25L	0, 20	Suction	100
S-0.50L	180	0.50L	0, 20	Suction	
S-0.67L	180	0.67L	0, 20	Suction	
			0	Jacking	
S-0.75L	180	0.75L	0, 20	Suction	



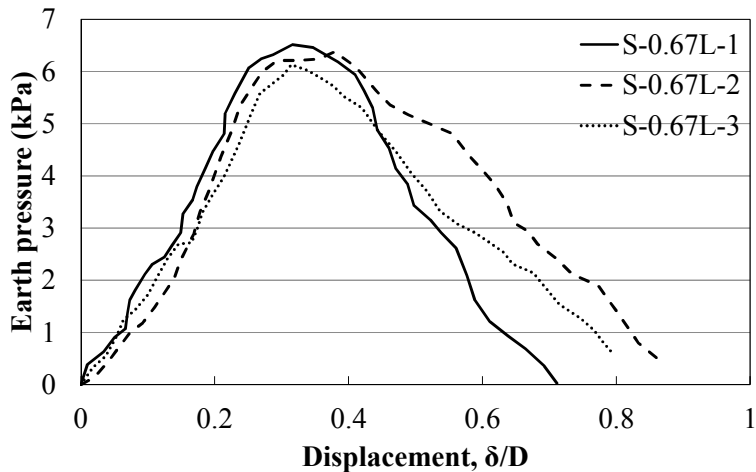
## 4.3 Test results and discussion

### 4.3.1 Repeatability of test results

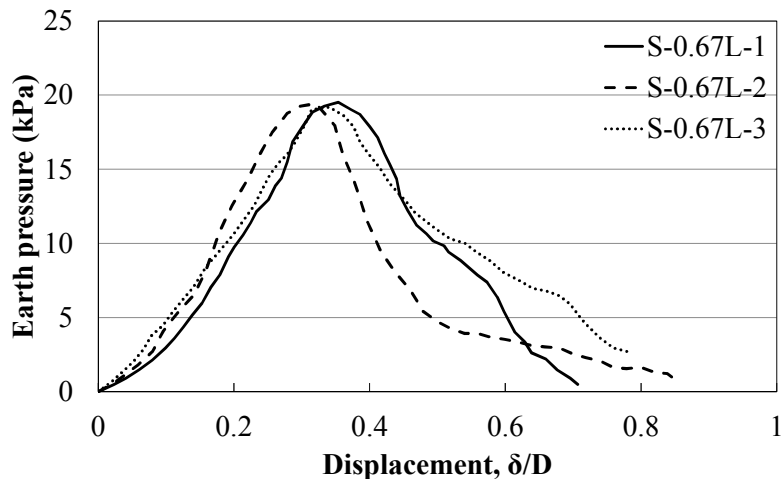
Fig. 4.3 represents the triplicate pull-out test results of the single suction pile with the normalized loading location ( $z/L$ ) of 67% and the loading inclination of  $0^\circ$ . Fig. 4.3(a) and 4.3(b) show the relationship between the horizontal pull-out force and displacement and that between the horizontal earth pressures from the earth pressure meter attached at the pile top, respectively. Fig. 4.3(c) indicates the earth pressure changes with increasing displacement based on the pressure measurement from the pressure meter at the pile bottom.



(a) Relationship between horizontal resistance and displacement



(b) Horizontal earth pressure at the pile top



(c) Horizontal earth pressure at the pile bottom

Fig. 4.3 Results of horizontal pull-out tests of a single suction pile

The relationships between the horizontal pull-out force and displacement from the triplicate tests (Fig. 4.3(a)) produced similar results. Especially, the ultimate (or maximum) pull-out forces of the triplicate tests converged within 2% in their magnitudes and the

maximum difference in their corresponding displacements was approximately 15%. The overall triplicate test results showed a reasonable repeatability.

From the comparison of change of horizontal pull-out force and pressure variations from two pressure meters attached on the pile top and bottom with an increasing displacement, overall increasing and decreasing trends of three curves (Fig. 4.3(a), (b), (c)) matched well. For example, the displacements corresponding to maximum pull-out force and pressures were similar. The overall shapes of the curves from Fig. 4.3(a) and 4.3(c) show better agreement than those from Fig. 4.3(a) and 4.3(b). However, it can be inferred that the reason of better agreement in overall shapes results from the closer distance between the load cell and the bottom pressure meter.

To examine the reliability of pressure meter measurements, the pressures were compared with the pressures (Table 4.3) back-calculated from the ultimate horizontal pressure Eq. (4.1) proposed by Broms (1964).

$$p_u = 3 K_p \sigma_v = 3 K_p \gamma' x \quad (4.1)$$

Where,  $p_u$ : ultimate horizontal pressure

$K_p$ : active earth pressure coefficient

$\sigma_v$ : vertical effective stress

$\gamma'$ : submerged unit weight of soil

$x$ : embedded depth of pressure meter.

From Table 4.3, the ultimate horizontal pressure from Broms'  $p_u$  equation was 30% less than that from the pressure measurement. The overestimation of lateral pressure from the Broms' equation in the

present study coincides with the experimental results from literature review. From the experimental findings in this section, it could be concluded that the experimental system and the methods used in the present study are effective and reliable in measuring pressure.

Table 4.3 Ultimate horizontal earth pressure by pressure sensor and Broms' equation

Case	Ultimate horizontal earth pressure (kPa)		Input parameter
	Pressure sensor	Broms (1964)	
Upper pressure sensor	6.5	5.0	$\phi = 37.5^\circ$ $\gamma' = 9.0 \text{ kN/m}^3$ $K_p = \tan^2(45 + \phi/2)$ $= 4.11$ $x = 0.045 \text{ m}$
Lower pressure sensor	19.2	15.0	$x = 0.135 \text{ m}$

### 4.3.2 Effect of installation method

Fig. 4.4 shows the experimental results of the horizontally-loaded suction model piles installed by suction pressure and jacking force. The horizontal loading locations placed at 67% from the piles' top without any loading inclination. In the Figure, the ultimate horizontal capacity and gradient (or stiffness) of "horizontal resistance-displacement curve" of pile installed by suction pressure were approximately 10% and 30% lower than those of pile installed by jacking force.

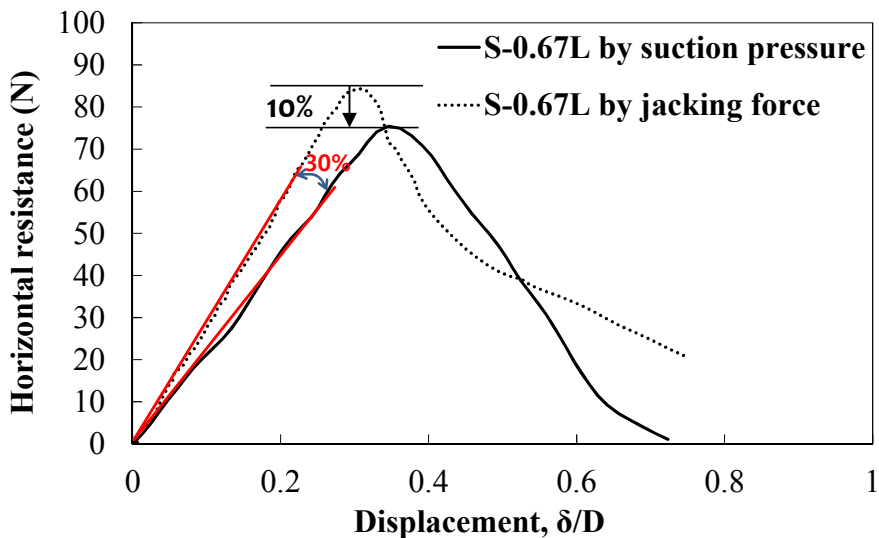


Fig. 4.4 Horizontal resistance-displacement curves of suction piles installed by suction pressure and jacking force

Fig. 4.5 represents the cone penetration test (CPT) results of inside and outside on suction piles for the measurement of effective stress difference resulting from suction pressure. The solid and dashed lines in the figure are the CPT test results of the suction piles installed by suction pressure and jacking force, respectively. The significant

difference in CPT results of the inside and outside of the suction pile results from the higher cone resistance due to the higher confinement inside of the pile shaft.

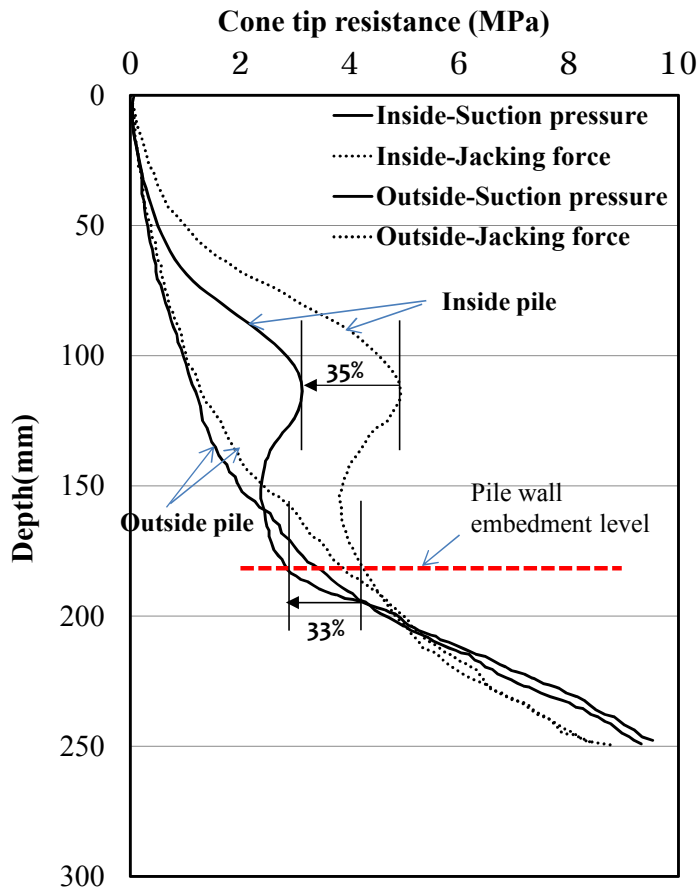


Fig. 4.5 CPT results of inside and outside on suction pile by different installations

The suction installation effect on the cone resistances inside of the suction pile is much greater than those outside of the pile. The CPT test results of outside on the suction pile indicated that the cone resistances at depths of 100 mm and 200 mm of the jacked pile were

2% ~ 15% higher than those of the suction-installed pile. As also mentioned by Mahn (2005), the downward seepage of outside on the suction pile within dense sand (relative density approximately equal to 70%) may not increase the effective stress significantly. Contrarily, the cone resistance of inside on the suction-installed pile was 35% lower than that inside on the jacked pile. The much lower cone resistance inside of the suction-installed pile may be caused from the decreased effective stress induced by the upward seepage, as also insisted by Mahn (2005). The cone resistance at the suction-installed pile tip was about 33% less than that at the jacked pile tip.

It can be inferred that the lower cone resistances for suction-installed pile compared to those for jacked pile at any depth contribute to the lower horizontal capacity (about 10% difference, as shown in Fig. 4.5) of the suction pile. However, more precise and extensive future research is required to identify the lower horizontal capacity for suction-installed pile.

In summary, to examine the actual horizontal behavior of a suction pile in sands, suction effect on the horizontal suction pile behavior plays an important role. Therefore, in this study, all the tests of group suction piles were designed to be installed by suction pressure.

### 4.3.3 Effect of loading conditions

#### Effect of loading location

Fig. 4.6 shows horizontal resistance-displacement curve of the single suction pile under different loading locations with no inclination of loads and Fig. 4.7 summarizes the ultimate horizontal resistances of the single suction pile for different loading locations. As mentioned in the earlier section, the maximum horizontal resistance was mobilized at 67% of the embedded depth from the pile top and the horizontal resistance linearly decreased as the distance of loading point increased from the maximum resistance location.

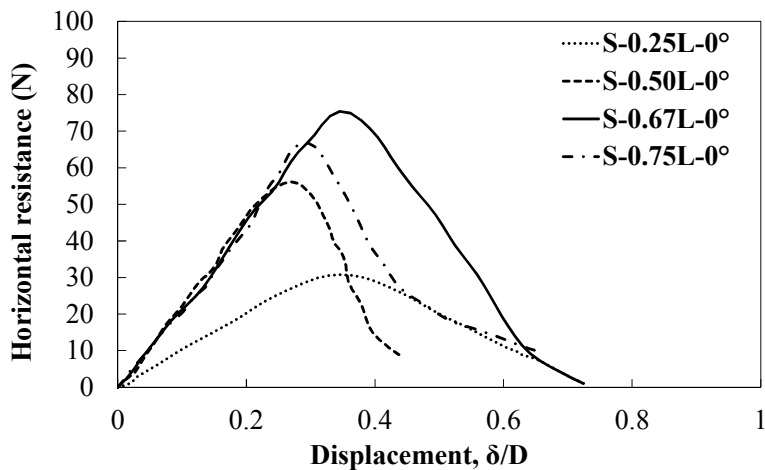


Fig. 4.6 Horizontal resistances and normalized displacements of single suction pile with different loading locations

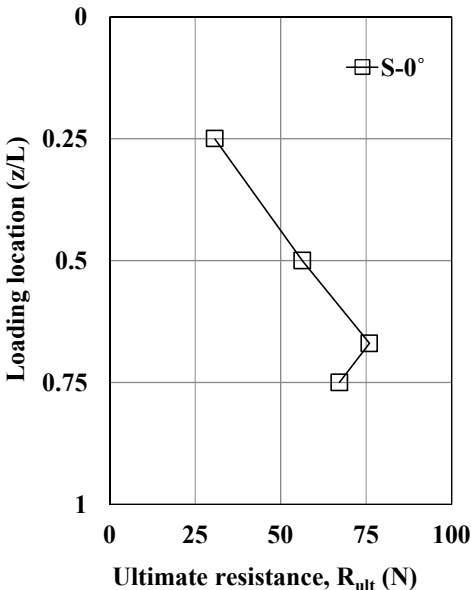


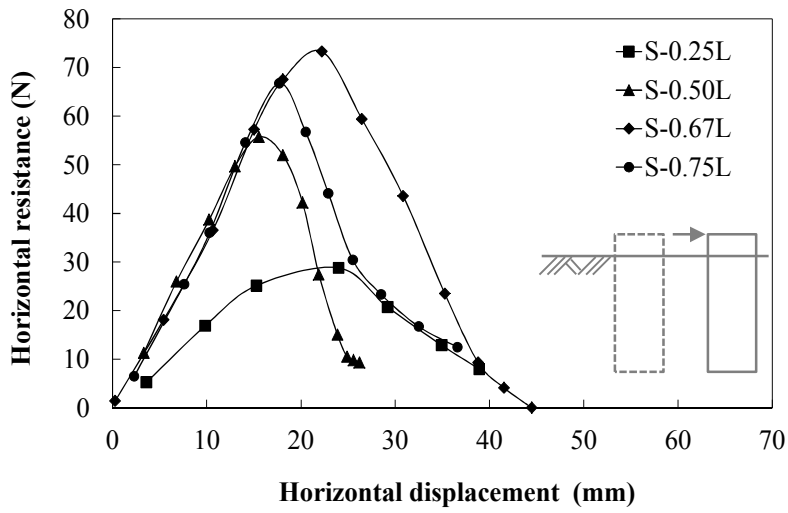
Fig. 4.7 Summarized ultimate resistances with different loading locations

The ultimate horizontal capacities of single suction piles were mobilized at displacements of about 30% of pile diameter. The interesting finding is that the horizontal resistance decreases stiffly after reaching its ultimate state; therefore, the use of single suction pile means unfavorable under a condition allowing large movement. In addition, the range of horizontal resistance variation with respect to loading locations (25% ~ 75% of pile embedded length from the pile top) is about 60% of its ultimate lateral capacity. Thus, it is difficult to determine an optimal loading point (producing ultimate capacity) and ultimate horizontal capacity of single suction pile in real fields, where multi-layered soils are presented.

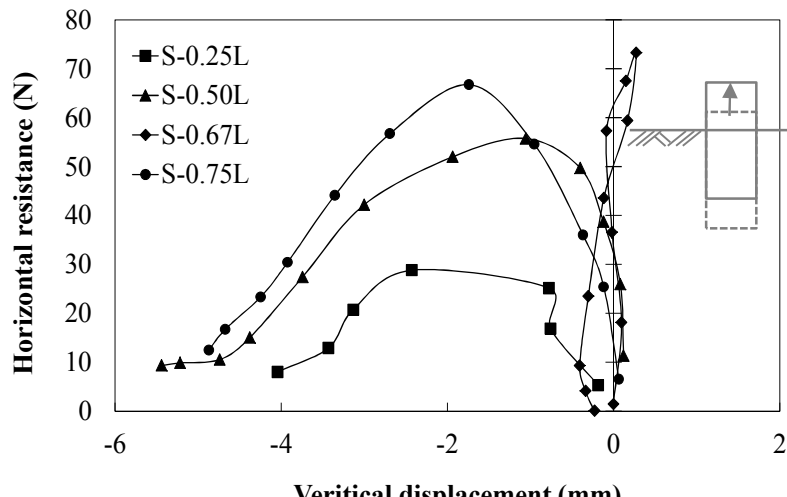
Particle Image Velocimetry (PIV) analysis technique has been implemented for an accurate analysis of the complex horizontal suction pile behavior which is represented by both rotation and translation. Fig. 4.8 shows the PIV analysis results of horizontal behavior of single

suction pile with different loading locations without any load inclination.

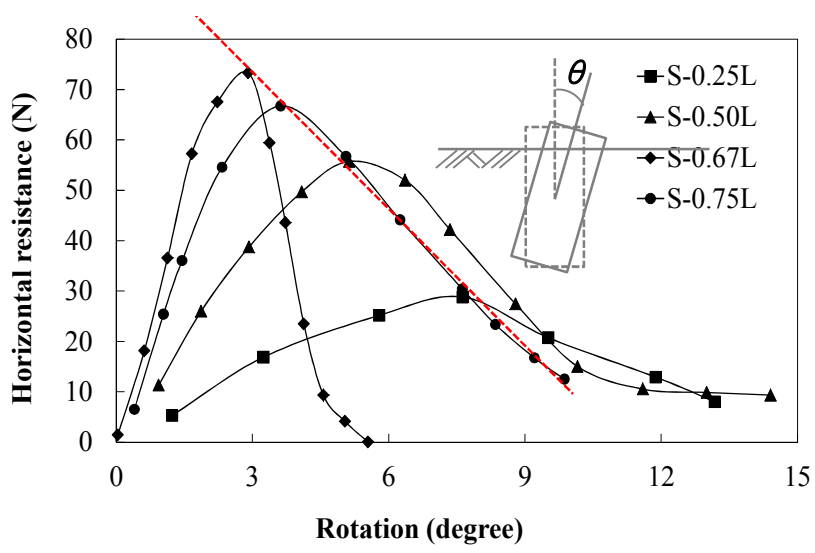
The PIV analysis enables to sort complex suction pile behavior in terms of rotation and displacement components: rotation and vertical and horizontal components of force and displacement. Fig. 4.8(a) and 4.8(b) show the variation of horizontal and vertical components of resistance with respect to horizontal and vertical displacements, respectively. Fig. 4.8(c) presents the relationship between horizontal resistance and pile rotation. The reference point of the suction pile for the PIV analysis locates at the center of pile top.



(a) Horizontal displacement



(b) Vertical displacement



(c) rotation

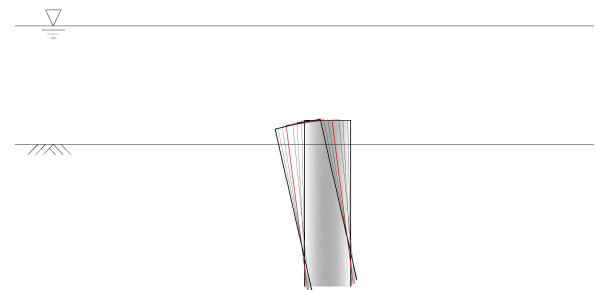
Fig. 4.8 The PIV analysis results of horizontal behavior on single suction pile with different loading locations with no inclination

The overall shape of “horizontal resistance-horizontal displacement

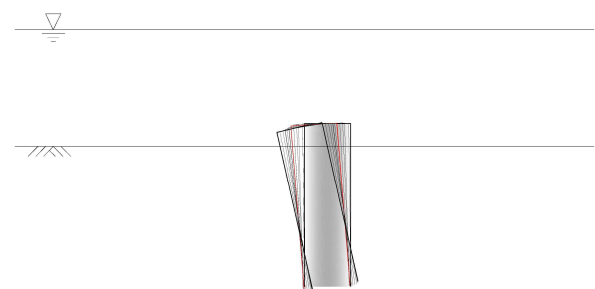
“curve” in Fig. 4.8(a) is very similar to that of ‘horizontal resistance – displacement curve’ given in Fig. 4.6. Fig. 4.8(b) indicated that small amount of vertical displacement was observed for the suction pile horizontally loaded only at 67% of the embedded depth from the reference ground. For the suction piles loaded at different locations (25%, 50%, and 75% of the embedded depth), considerable amount (1 mm ~ 2 mm) of downward vertical displacement occurred unit their ultimate capacities.

The reason of showing downward vertical displacements is the vertical downward movement of the reference point (center of pile top) due to pile rotation. The rotation direction of suction pile loaded at 75% of the embedded depth was different from those at 25% and 50% of their embedded depth. However, despite different rotation directions, only the amount of rotation was plotted in Fig. 4.8(c). As shown in the Figure, the ultimate capacity of a horizontally loaded suction pile has a clear linearly relationship between horizontal resistance and pile rotation. The horizontal ultimate resistance decreased with an increasing rotation. More details on the relationship between the ultimate horizontal capacity and the pile rotation will be dealt in Chapter VI.

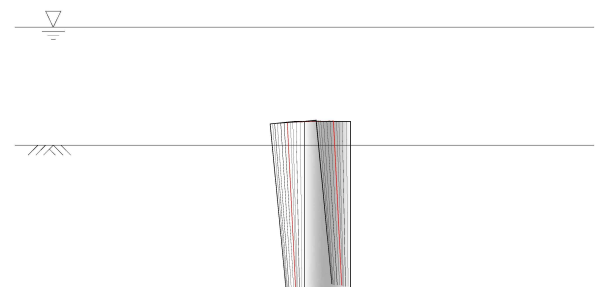
Fig. 4.9 is schematic figure on horizontal behavior of single suction pile based on PIV analysis results. Loading is applied from right to left. Red line means the ultimate horizontal resistance. From Fig. 4.9, the horizontal behavior of single suction pile can be figured out intuitively. In case of S-0.67L, which appears the maximum horizontal bearing capacity, the translation of the pile is dominant on the movement of the pile, and in case of other tests, the rotation of the pile is dominant on the behavior of the pile.



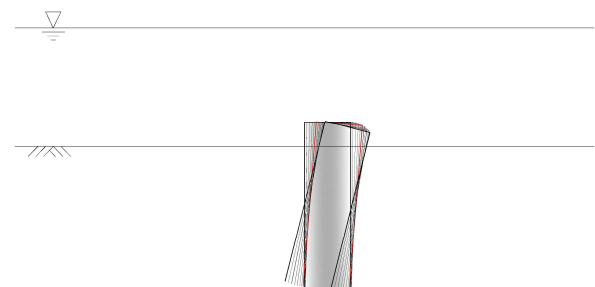
(a) S-0.25L



(b) S-0.50L



(c) S-0.67L



(d) S-0.75L

Fig. 4.9 Scheme of behavior on single suction pile

### **Effect of load inclination**

Fig. 4.10 represents the relationship between horizontal resistance and displacement for a single suction pile subjected to an inclined load with load inclination of  $20^\circ$ . Similarly to the case of horizontally loaded suction pile (load inclination of  $0^\circ$ ), the maximum pull-out resistance was mobilized with the loading location at 67% of the embedded depth, and the pull-out resistance approximately and linearly decreased as the distance between the loading point and the 67% of the embedded depth increased.

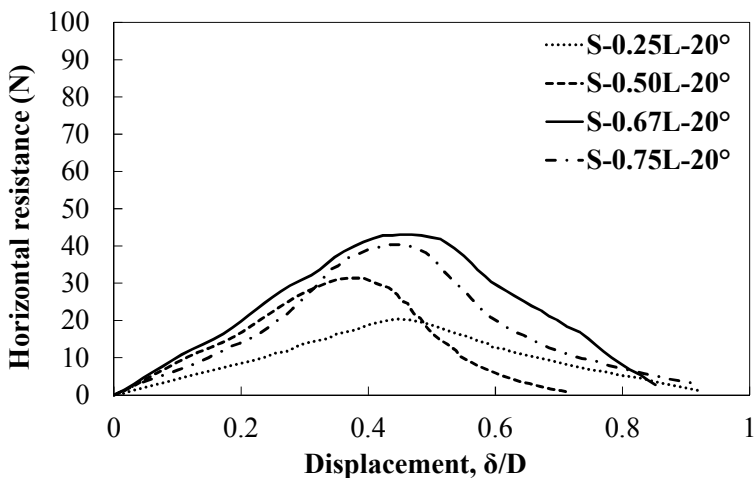


Fig. 4.10 Horizontal resistance and normalized displacement with different loading locations with  $20^\circ$  inclined

Fig. 4.11 compares the ultimate pull-out resistances of single suction piles subjected to  $0^\circ$  and  $20^\circ$ . Fig. 4.11(a) shows the ultimate resistances with different loading locations for load inclinations of  $0^\circ$  and  $20^\circ$ . Fig. 4.11(b) compares the ultimate resistances with different load inclinations of  $0^\circ$  and  $20^\circ$  by normalizing ultimate capacity with load inclination of  $20^\circ$  with that with no inclination for different

loading locations.

From Fig. 4.11(a), an ultimate capacity decrease rate with increasing distance between loading point and 67% of the embedded depth is lower for the loading location of 75% of the embedded depth than for the loading locations of 25% and 50%. When the pile pull-out force acts lower than the centroid of pressure distribution during the pullout, the pile rotation direction (counter-clockwise direction; rotation occurs opposite direction to the loading direction) for the loading location of 75% of the embedded depth is different from other cases.

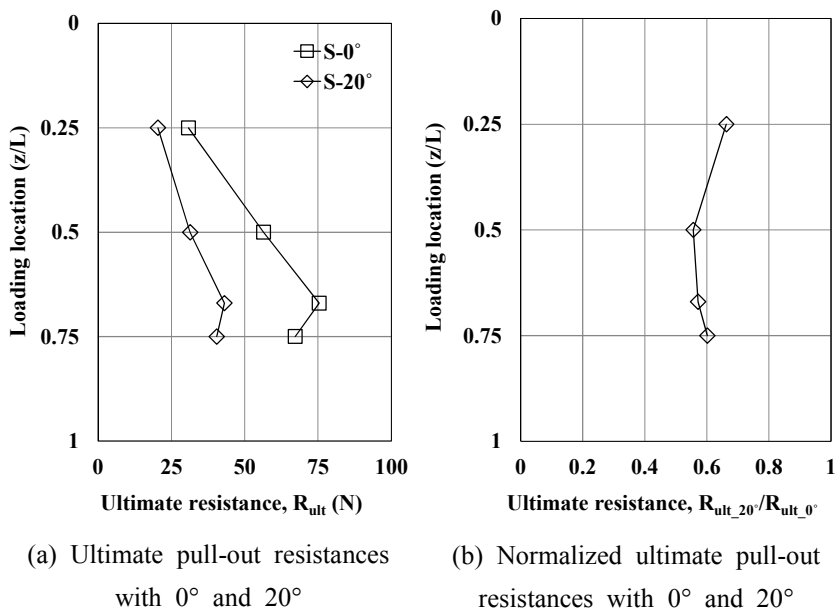


Fig. 4.11 Comparisons of the ultimate pull-out resistances of single suction piles with 0° and 20°

From Fig. 4.11(b) the ultimate capacity of suction pile subjected to inclined load of 20° was about 40% less than that subjected to the horizontal load. Therefore, it is concluded that the pull-out resistance of

single suction pile against horizontal load is much higher than that against inclined loads.

## 4.4 Summary

TriPLICATE tests were performed for each test condition to ensure the repeatability and reliability of experimental system and methods of model tests of single suction piles. From the examination of the suction installation effect on the horizontal pull-out resistance of a single suction pile in sands, an effective stress decrease inside the suction pile was identified. An estimation of the horizontal capacity of the single suction pile based on that from the jacked suction pile will overestimate the real horizontal capacity.

From the pull-out tests of a single suction pile with different loading locations and load inclinations, the pull-out resistance of the suction pile varies significantly with loading location and inclination. The maximum pull-out resistance was mobilized at the loading location of 67% of the embedded depth, and the pull-out resistance without load inclination is greater than those with load inclination.

# **CHAPTER V MODEL TESTS ON GROUP SUCTION PILES**

## **5.1 Introduction**

This chapter induces the detailed experimental methods and results of model group suction piles tests. Group suction model piles were accurately manufactured with different "center-to-center" pile spacings. All the group suction piles used in the experiment have nine component piles ( $3 \times 3$  pile matrix formation). A series of model tests was performed to examine static and cyclic pull-out behavior of group suction piles varying loading location and load inclination. In addition, pressure meters are attached to several selected component piles to evaluate load distributions on the selected component piles based on the measured earth pressure.

## **5.2 Test program**

The test conditions of series of group suction piles model tests are summarized in Table 5.1. Different center-to-center pile spacings (2D, 3D, 4D, D = pile diameter), loading locations (0%, 25%, 50%, 67%, and 75% of the embedded depth ( $D_f$ ) from the ground), load inclinations ( $0^\circ$  and  $20^\circ$ ) were considered. The tests were performed

under displacement-control condition with displacement rate of 100 mm/min. A cyclic pull-out test was performed at a loading point of 50%  $D_f$  and with pile spacing of 4D. Details of cyclic load test method will be dealt in the later section 6.3.

Table 5.1 Test program for group suction piles

Case	Pile spacing	Penetration depth, L (mm)	Loading point, z	Loading angle, $\alpha$ (degree)	Loading rate (mm/min)
G-2D-0L	2D	180	0L	0	100
G-2D-0.25L	2D	180	0.25L	0	
G-2D-0.50L	2D	180	0.50L	0	
G-2D-0.67L	2D	180	0.67L	0	
G-2D-0.75L	2D	180	0.75L	0	
G-3D-0L	3D	180	0L	0, 20	
G-3D-0.25L	3D	180	0.25L	0, 20	
G-3D-0.50L	3D	180	0.50L	0, 20	
G-3D-0.67L	3D	180	0.67L	0	
G-3D-0.75L	3D	180	0.75L	0, 20	
G-4D-0L	4D	180	0L	0, 20	
G-4D-0.25L	4D	180	0.25L	0, 20	
G-4D-0.50L*	4D	180	0.50L	0, 20	
G-4D-0.67L	4D	180	0.67L	0	
G-4D-0.75L	4D	180	0.75L	0, 20	

Diagram

\* G-4D-0.50L( $\alpha=0^\circ$ ) : cyclic loading test was performed in addition

## 5.3 Test results and discussion

### 5.3.1 Effect of loading conditions

#### Effect of loading location

Fig. 5.1 shows the relationship of horizontal resistance and displacement of a horizontally-loaded (load inclination of  $0^\circ$ ) group suction piles (9 component piles in each group suction piles) with pile spacing of  $2D$  under different loading locations ( $0\%$ ,  $25\%$ ,  $50\%$ ,  $67\%$ , and  $75\%$  of the embedded depth ( $D_f$ ) from the ground). From the figure, depending on the loading locations, the group suction piles behaviors are significantly different.

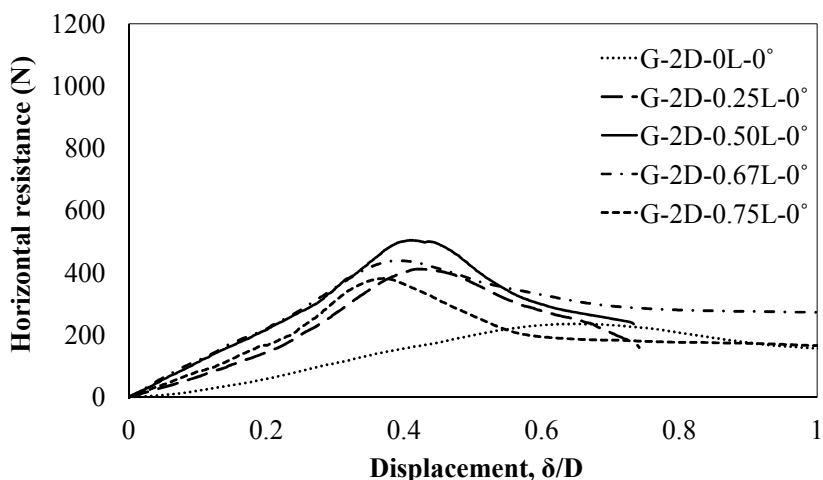


Fig. 5.1 Horizontal resistance of normalized displacement on  $2D$  with no inclination

Fig. 5.2(a) and 5.2(b) summarize the ultimate resistances and the ratios of residual resistance to ultimate resistance for different loading

locations. Unlike the single suction pile case, the loading location at 50%  $D_f$ , the group suction piles exhibited the highest ultimate horizontal capacity. The ultimate horizontal capacity decreased as the distance between a loading location and the location of 50%  $D_f$  increased. The interested finding from group suction piles behavior is the identification of significant residual resistance (at least 40% of its ultimate horizontal capacity), which was not seen from single suction pile behavior.

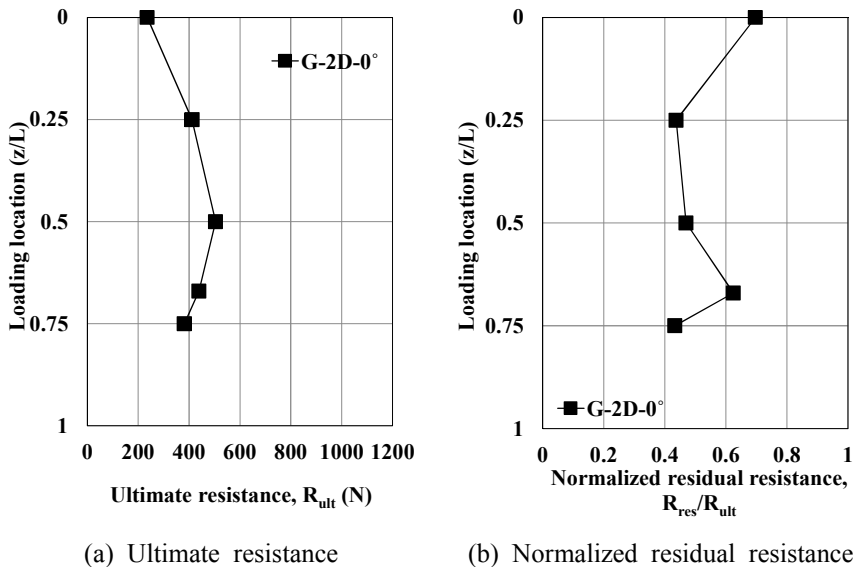


Fig. 5.2 Summarized horizontal resistance on different loading locations (2D)

Additional tests were performed with modified group suction piles with increased pile spacing (3D). Using the modified group suction piles, the group suction piles are horizontally pulled out varying loading location (0%, 25%, 50%, 67%, and 75% of  $D_f$ ). Their relationships between horizontal resistance and displacement from the test results are summarized in Fig. 5.3.

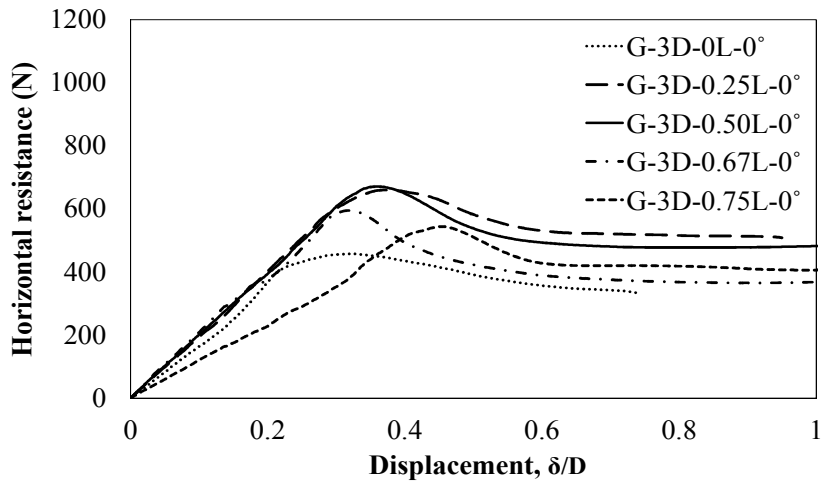


Fig. 5.3 Horizontal resistance of normalized displacement on 3D with no inclination

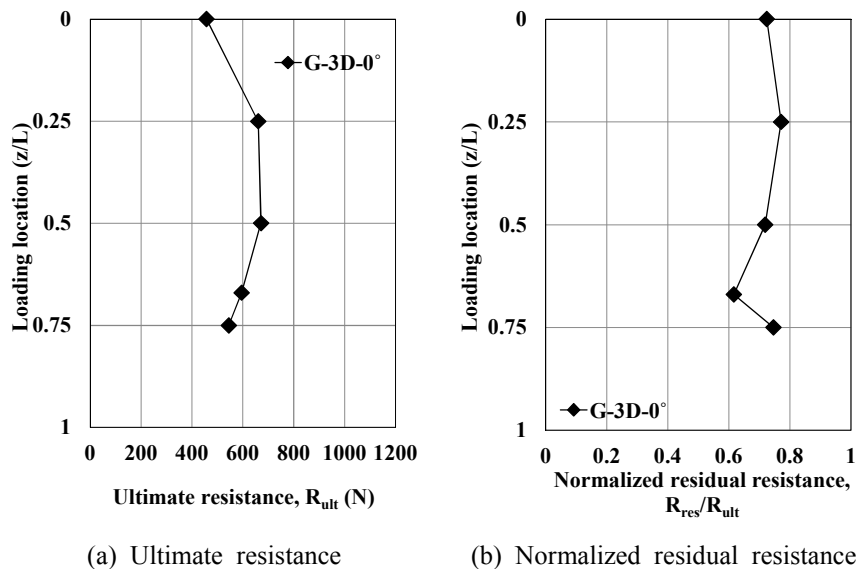


Fig. 5.4 Summarized horizontal resistance on different loading locations (3D)

Fig. 5.4(a) shows the ultimate resistance changes with respect to loading locations, and the ratios of residual resistance to ultimate resistance are summarized in Fig. 5.4(b).

Similarly to the group suction piles with pile spacing of 2D, the maximum ultimate capacity was observed at the loading location of 50%  $D_f$ . Interestingly, the ultimate capacity at the loading location of 25%  $D_f$  was almost the same as the maximum capacity at the loading location of 50%  $D_f$ . Furthermore, the ratios of residual resistance to ultimate resistance of all the tests were higher than 60%. Therefore, it is concluded that the group suction piles with pile spacing of 3D have more favorable behavior against pull-out force because the significant resistances are maintained even after a considerable movement.

Group suction piles with pile spacing of 4D are used for the tests. From the horizontal pull-out tests varying loading locations, horizontal resistances with increasing displacement are obtained (Fig. 5.5).

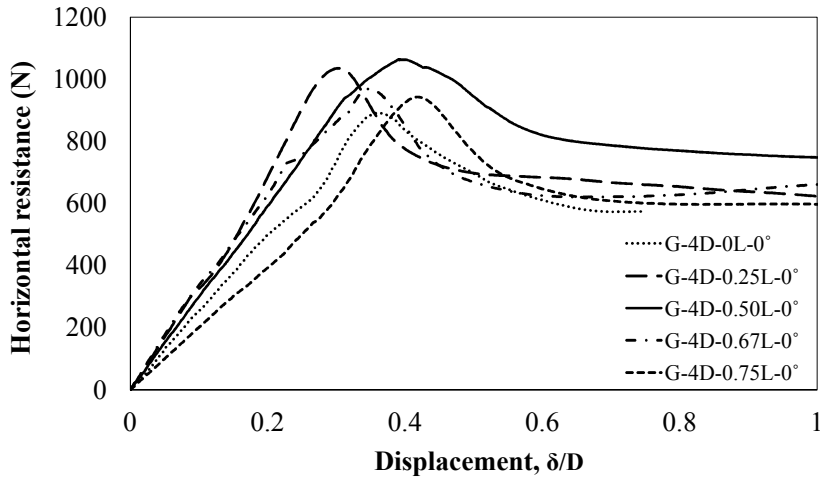


Fig. 5.5 Horizontal resistance of normalized displacement on 4D with no inclination

Fig. 5.6(a) and 5.6(b) show the ultimate horizontal capacities and ratios of residual resistance to ultimate resistance, respectively. In this set of experiment, the maximum ultimate capacity with respect to loading location was mobilized at the loading location of 50%  $D_f$ . Despite of different loading locations, the ultimate capacities do not show significant difference. The residual capacities of all the tests exceed at least 60% of their ultimate capacities.

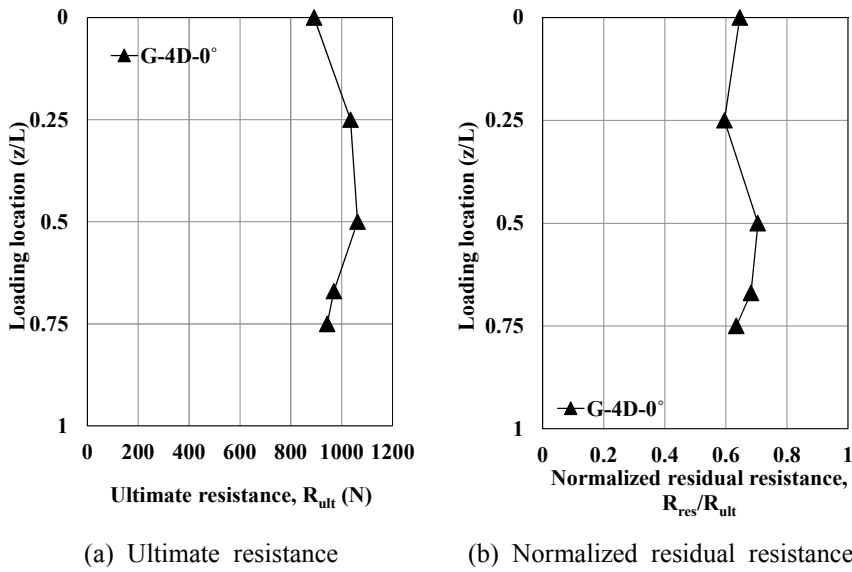
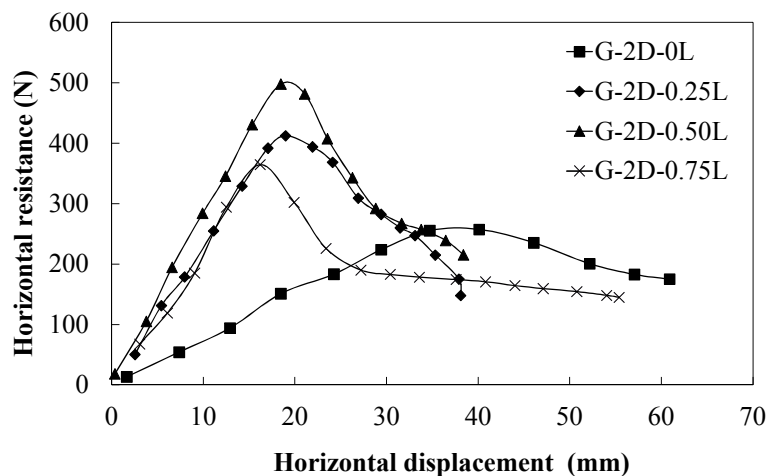
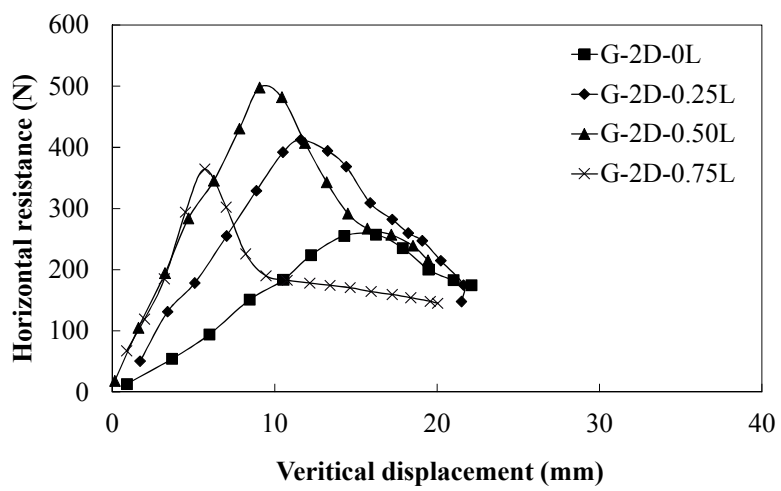


Fig. 5.6 Summarized horizontal resistance on different loading locations (4D)

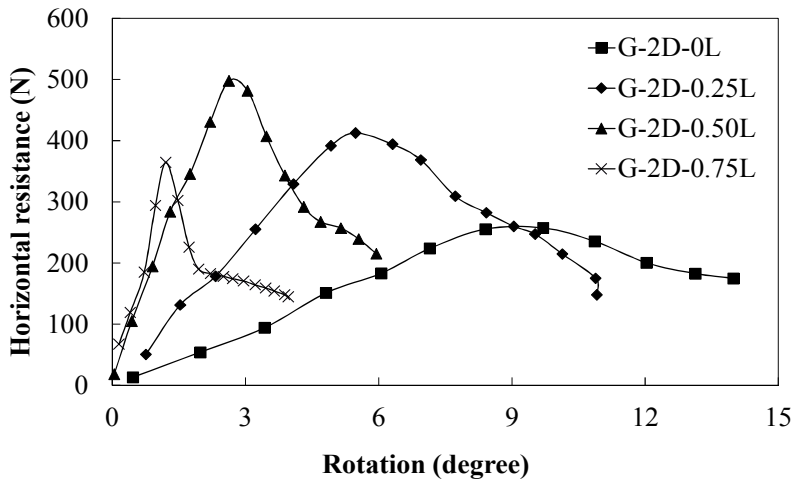
Particle Image Velocimetry (PIV) analysis is also conducted for group suction piles to examine their behavior in terms of rotation, horizontal displacement, and vertical displacement, respectively. Fig. 5.7(a), 5.7(b), 5.7(c) ~ 5.9(a), 5.9(b), 5.9(c) show the horizontal resistance changes of group suction piles against increasing horizontal displacement, vertical displacement, and rotation, respectively, for different loading locations based on the PIV analysis results.



(a) Horizontal displacement



(b) Vertical displacement



(c) rotation

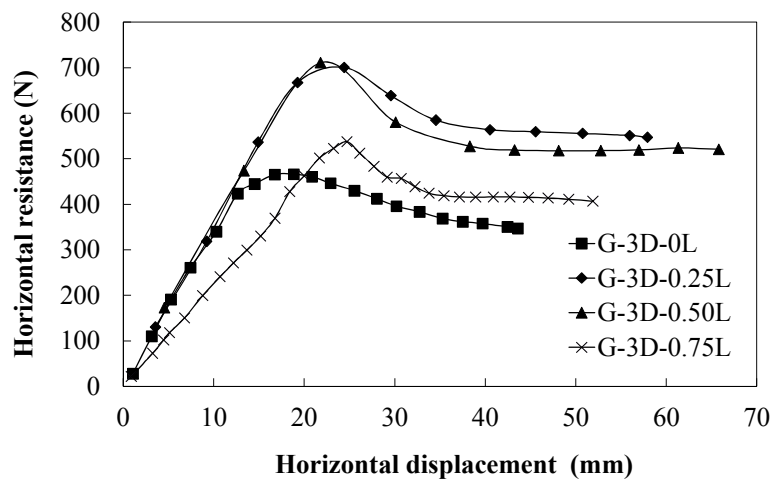
Fig. 5.7 PIV analysis on 2D

The reference point on the group suction piles for the PIV analysis is set at the center of top cap. Regardless of pile spacing of group suction piles, the overall trend of relationships of horizontal resistance and horizontal displacement is similar.

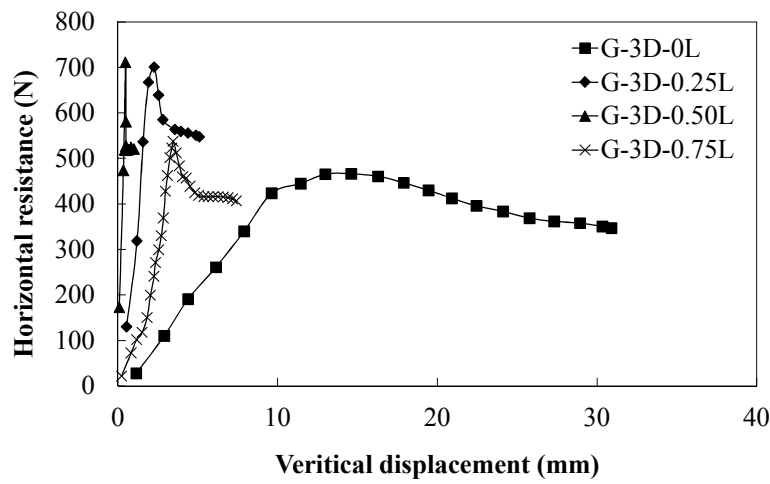
From the changes of horizontal resistance with increasing vertical displacement, Regardless of pile spacings considered in this study, the minimum vertical displacement was observed at the loading location of 50%  $D_f$ , at which the maximum ultimate capacity was identified. Moreover, the ultimate resistance decreased with increasing vertical displacement. It is inferred that the upward pull-out of group suction piles decreases its ultimate capacity.

The horizontal resistance changes with increasing rotation were evaluated. It was found that there exists a strong relationship between ultimate horizontal capacity and rotation, except the cases of the loading locations of 75%  $D_f$ . The ultimate horizontal capacity linearly decreases with increasing rotation. The inconsistent relationship between

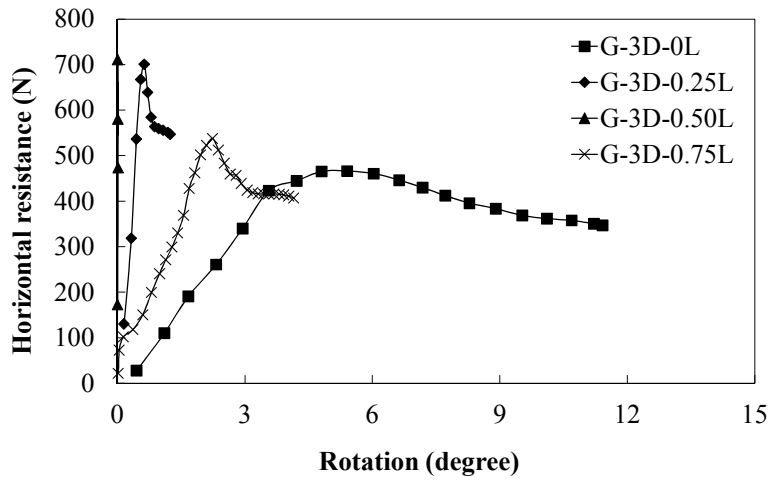
ultimate horizontal capacity and rotation for the loading location of 75%  $D_f$  may result from the different rotation direction compared with the rotation directions at other loading locations. Further explanation on the relationship between ultimate horizontal capacity and rotation will be dealt in Chapter VI.



(a) Horizontal displacement

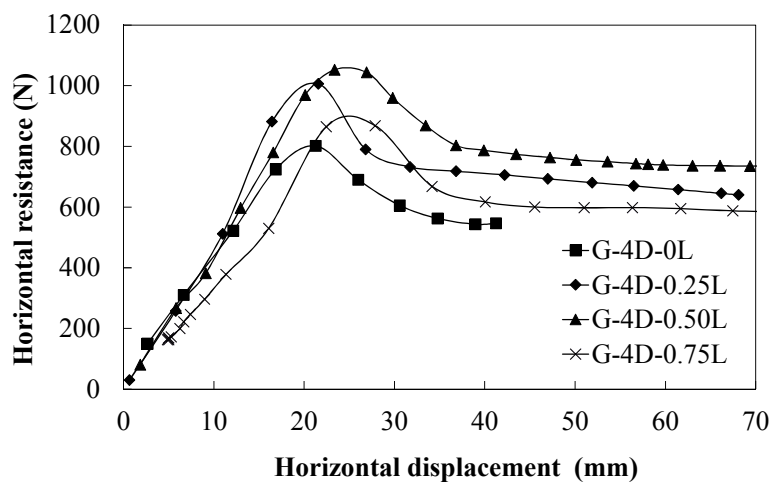


(b) Vertical displacement

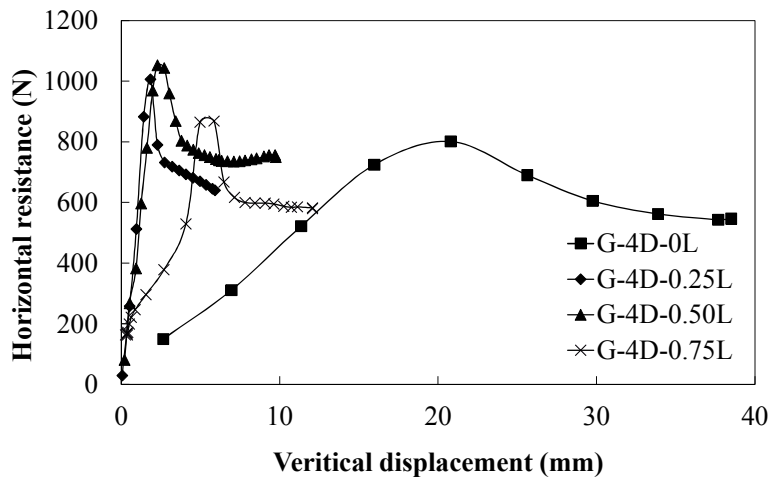


(c) Rotation

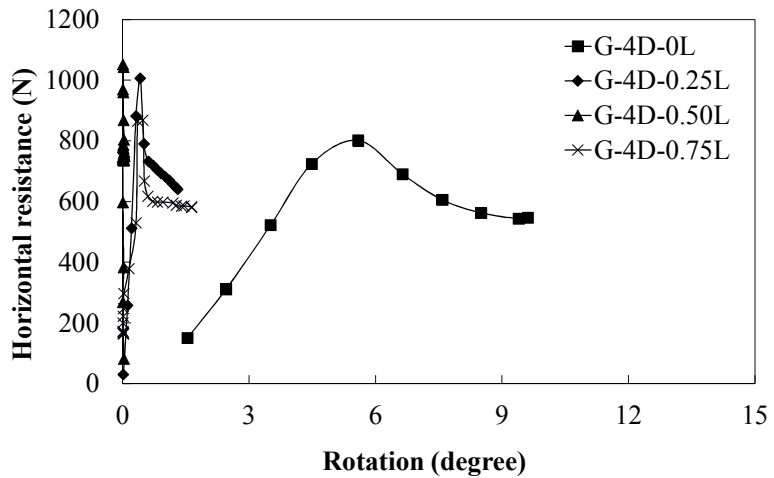
Fig. 5.8 PIV analysis on 3D



(a) Horizontal displacement



(b) Vertical displacement

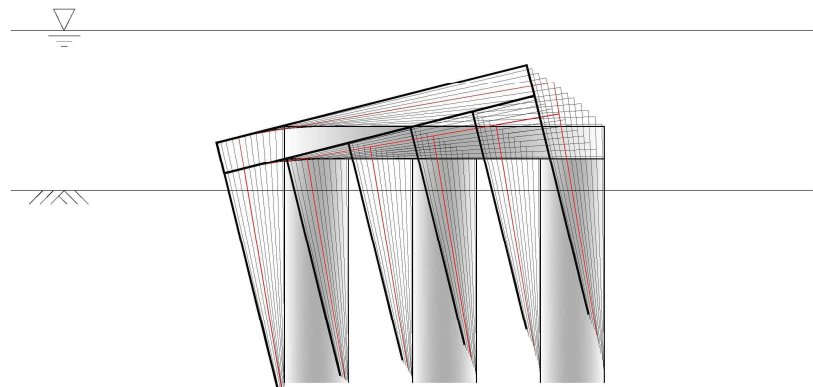


(c) Rotation

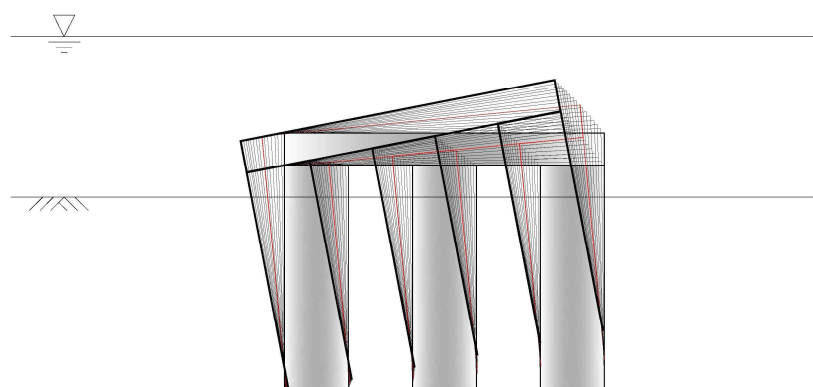
Fig. 5.9 PIV analysis on 4D

Fig. 5.10 ~ 5.12 are the scheme of horizontal behavior of group suction piles based on the PIV analysis by varying pile spacing. The loading direction is from right to left. Red line means the ultimate horizontal resistance. From these figures, the horizontal behavior of

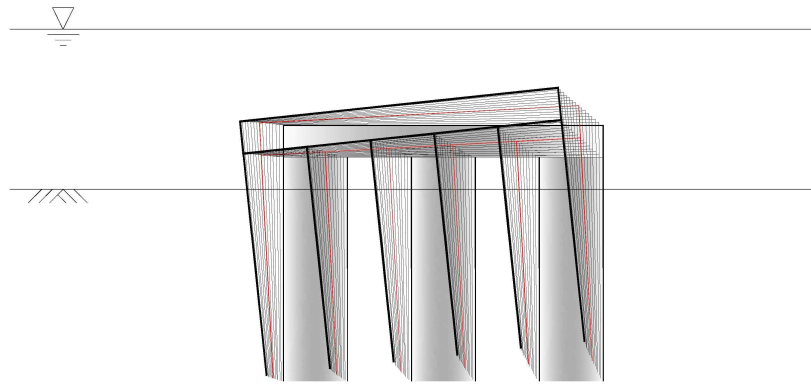
single suction pile can be figured out intuitively. In case of 2D spacing, all of the loading location occurred the rotation largely, and in case of 3D and 4D with 0.25L and 0.50L, the rotation of the pile has been restrained significantly.



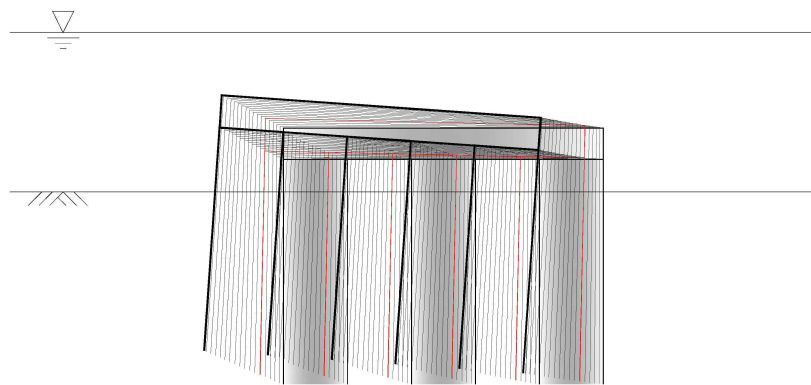
(a) G-2D-0L



(b) G-2D-0.25L

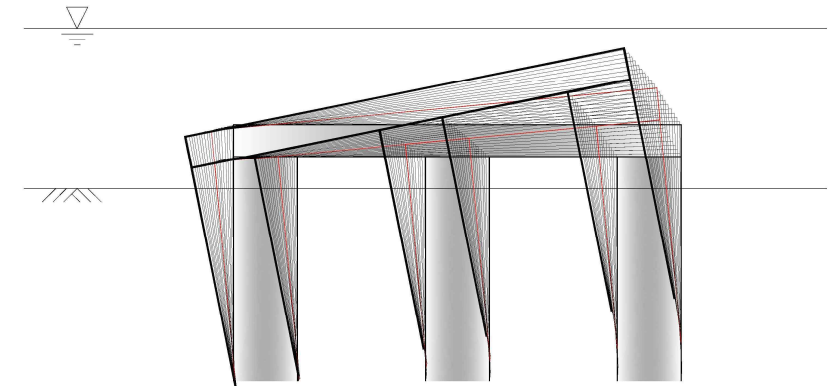


(c) G-2D-0.50L

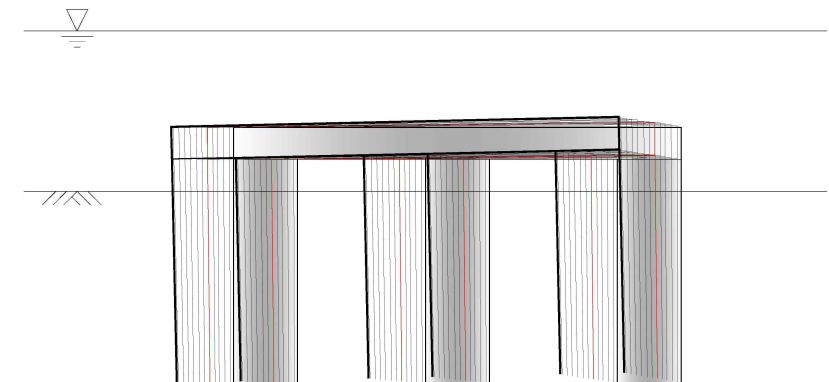


(d) G-2D-0.75L

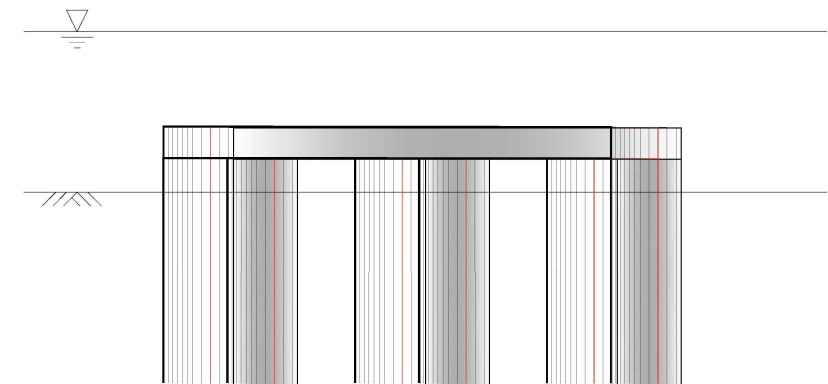
Fig. 5.10 Scheme of horizontal behavior on 2D spacing



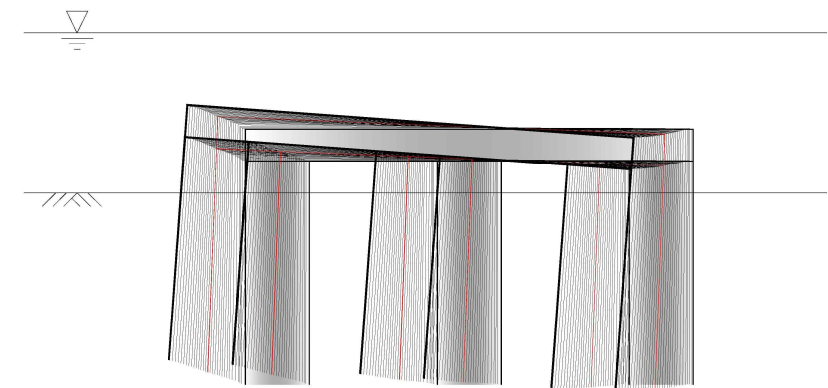
(a) G-3D-0L



(b) G-3D-0.25L

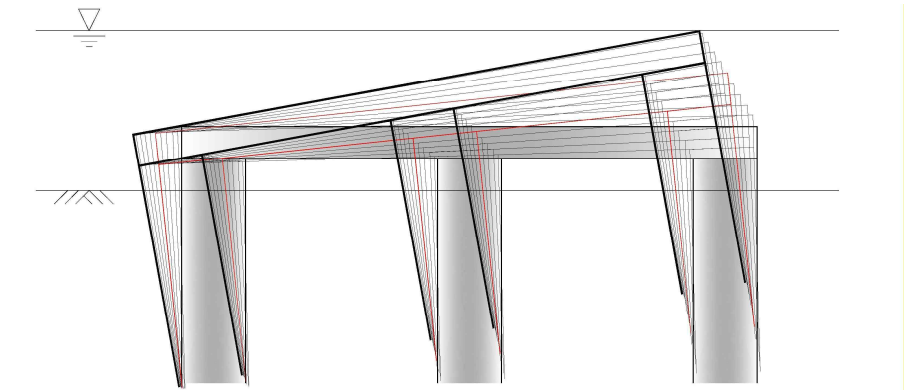


(c) G-3D-0.50L

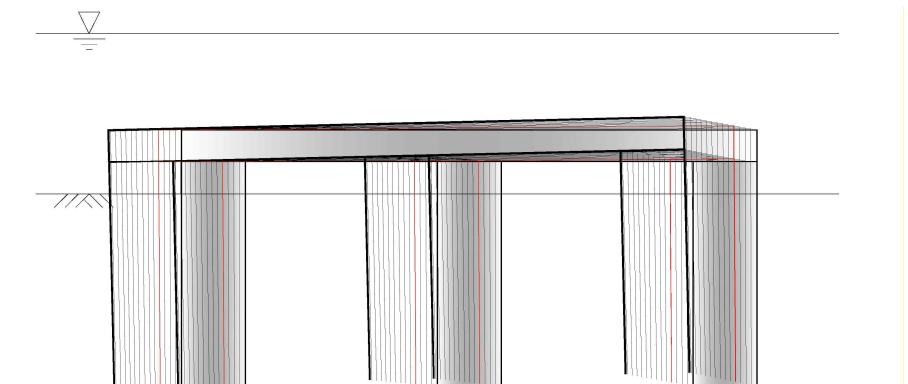


(d) G-3D-0.75L

Fig. 5.11 Scheme of horizontal behavior on 3D spacing



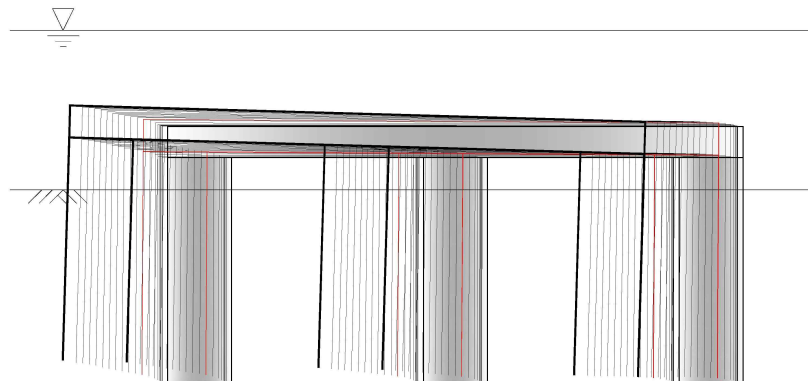
(a) G-4D-0L



(b) G-4D-0.25L



(c) G-4D-0.50L



(d) G-4D-0.75L

Fig. 5.12 Scheme of horizontal behavior on 4D spacing

### **Effect of load inclination**

Fig. 5.13 and 5.14 represent the relationships between horizontal resistance and displacement of group suction piles with different pile spacings (3D and 4D) and different loading locations (0%, 25%, 50%, and 75% of  $D_f$ ) under an inclined loading condition (load inclination of 20°). Similarly to the cases with no load inclination, the maximum horizontal ultimate capacities were found at the loading location of 50%  $D_f$  even under inclined loading (load inclination of 20°) condition. The ultimate horizontal capacity decreased as the distance between a loading location and the loading location of 50%  $D_f$  increased.

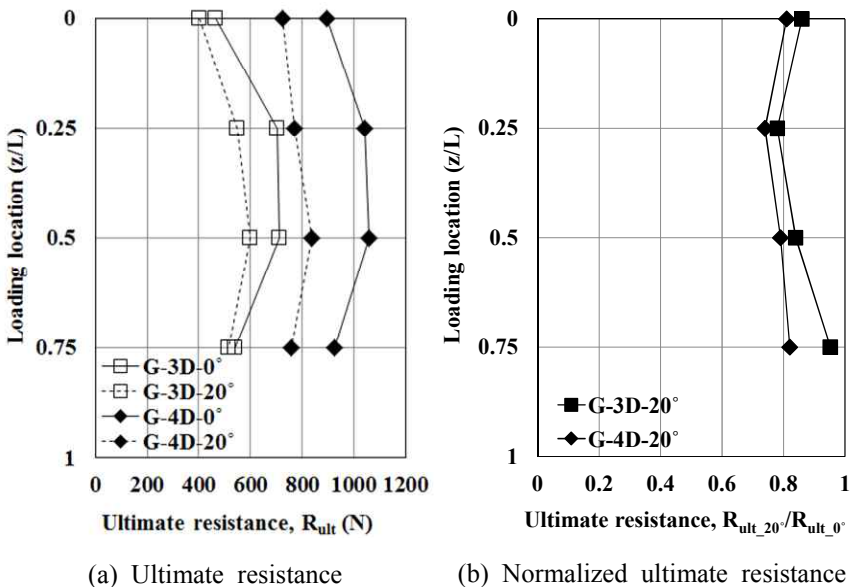


Fig. 5.13 Summarized ultimate horizontal resistance on different loading locations (3D and 4D) with 0° and 20°

Fig. 5.13(a) compares horizontal ultimate capacities of group suction piles by varying the loading location with different loading inclinations and pile spacings. Fig. 5.13(b) presents ultimate capacity

ratios of inclined load to horizontal loading conditions for different pile spacings and loading locations. As can be seen in Fig. 5.13(a), the reduction rate from ultimate capacity corresponding to horizontal loading condition to that with inclined load was more pronounced for the group suction piles with pile spacing of 4D than for that of 3D. For the loading locations of 0% and 75% of  $D_f$ , the load inclination effect on ultimate horizontal capacity was less significant. From Fig. 5.13(b), the ultimate capacity reduction for inclined loading condition was approximately 10% ~ 30% less than those for horizontal loading condition.

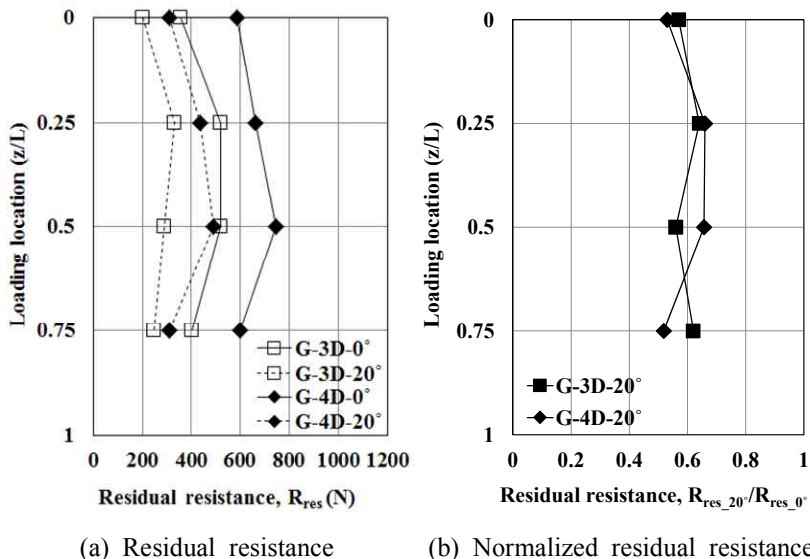


Fig. 5.14 Summarized residual horizontal resistance on different loading locations (3D and 4D) with 0° and 20°

Fig. 5.14 represents the load inclination effect on the residual resistance of group suction piles with pile spacings of 3D and 4D. Fig. 5.14(a) compares the residual resistances of group suction piles under

inclined loading and horizontal loading conditions varying loading location. In addition, Fig. 5.14(b) shows the comparison of ultimate capacity ratios of inclined loading to horizontal loading conditions to examine the load inclination effect on the residual resistance, for each loading location. The load inclination effect on the residual resistance of group suction piles was least pronounced at the loading location of 25%  $D_f$  for pile spacing of 3D and at the loading location of 50%  $D_f$  for pile spacing of 4D. For group suction piles with pile spacings of 3D and 4D, the residual resistances under inclined loading condition were 30%~50% less than those under horizontal loading condition.

In summary of the present experimental results, the inclined load (with load inclination of 20°) increase instability of group suction piles in terms of both ultimate and residual resistances. Therefore, special care is required to assess ultimate and residual resistance of both single and group suction piles.

#### **Effect of cyclic loading**

This study eventually focuses on the suction pile used as a foundation of floating structure. Generally, floating structures are exposed to significant forces from wave and tidal current and lateral movement is dominant over the vertical fluctuation; therefore, their foundations, suction piles, are also subjected to repetitive horizontal forces. The estimation of group suction piles behavior under cyclic horizontal load is important.

The magnitude of cyclic horizontal load is determined as 50% of the maximum ultimate pull-out capacity of group suction piles (G-4D-0.50L) with pile spacing of 4D. The specific magnitude, cycle, number of cycles used in the test are summarized in Table 5.2. The maximum number of cycles for a group pile is determined based on

the suggestions by Brown (1988).

Table 5.2 Cyclic testing program

Division	Cyclic loading conditions	Note
Size	50% of ultimate horizontal resistance	FS=2.0
Cycle	5.0 sec	
Count	1, 10, 100, 200	Brown, 1988

Fig. 5.15 and 5.16 show the cyclic load test results of the group suction piles with pile spacing of 4D. From Fig. 5.16, ultimate and residual horizontal resistances and initial stiffness decrease with increasing cyclic number. In addition, the displacement corresponding to the ultimate horizontal capacity increases as the number of cycle increases. After the number of cycle of 200, the ultimate and residual horizontal resistances decreased by approximately 10%, and the initial stiffness reduced by about 9%. The most of decreases of ultimate and residual horizontal resistances and initial stiffness occurred within the 10 times loading cycles, and their decrease rates per each cycle reduced with increasing loading cycle. In other word, the cyclic effect on group suction piles resistance diminishes as the number of cycle increases. Eventually, an estimation of resistances and initial stiffness of group suction piles under cyclic loads is important to determine their ultimate capacities and movement.

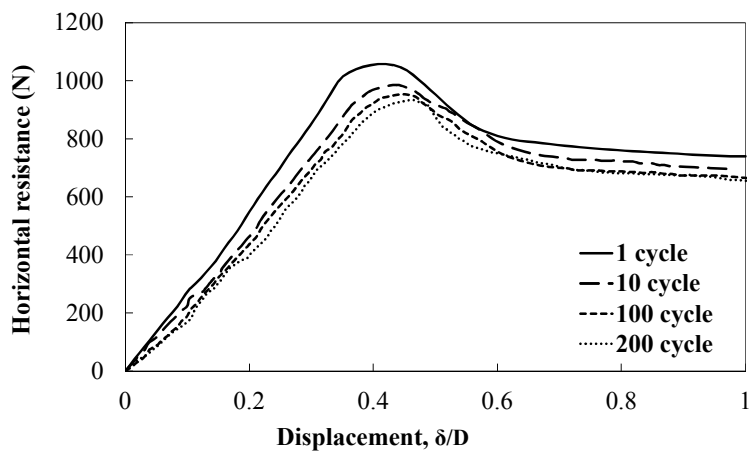


Fig. 5.15 Horizontal resistance and normalized displacement under diverse cyclic loadings

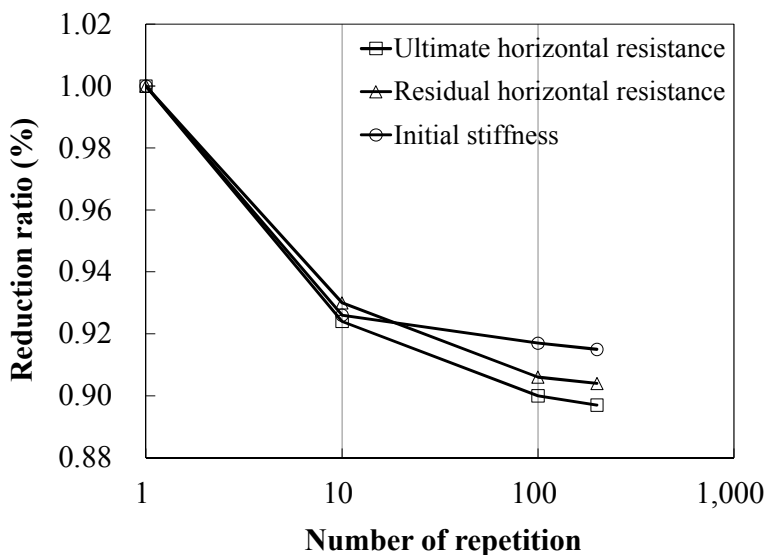
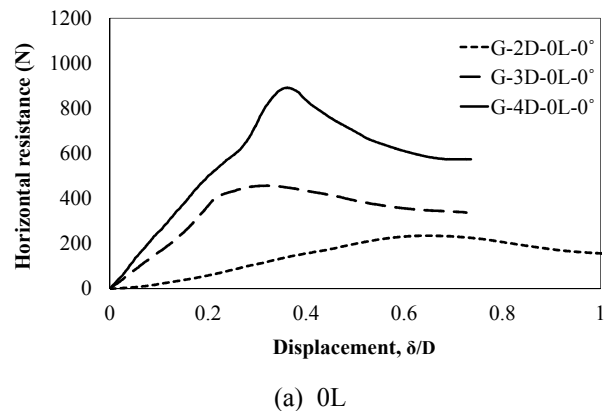


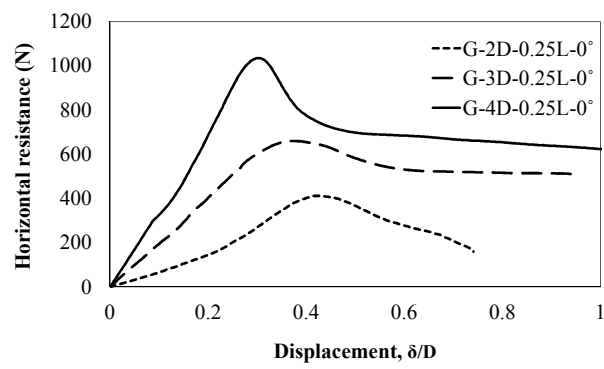
Fig. 5.16 Cyclic loadings and variations of stiffness

### 5.3.2 Effect of pile spacing

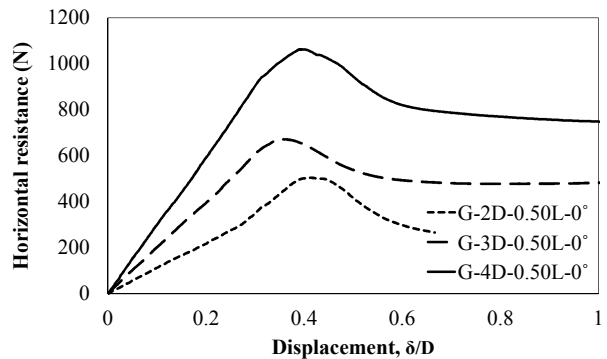
Fig. 5.17 represents the horizontal behavior of group suction piles with different pile spacings. Regardless of loading location, group suction piles with a higher pile spacing exhibit higher ultimate capacity, initial stiffness, and residual resistance. When group suction piles are exposed to a high horizontal load, similarly to ordinary group piles, there exists a group effect due to the overlapping failure regions. The overlapping failure regions by component piles increases with decreasing pile spacing; therefore, its ultimate horizontal capacity decreases.



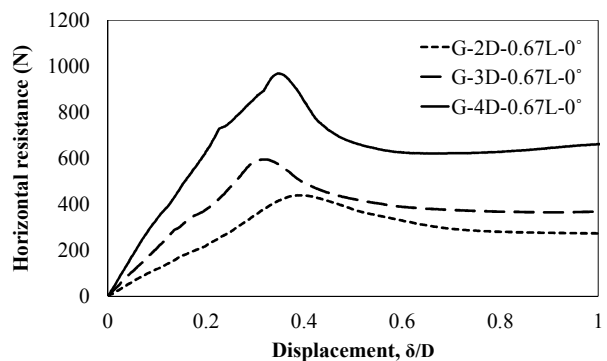
(a) 0L



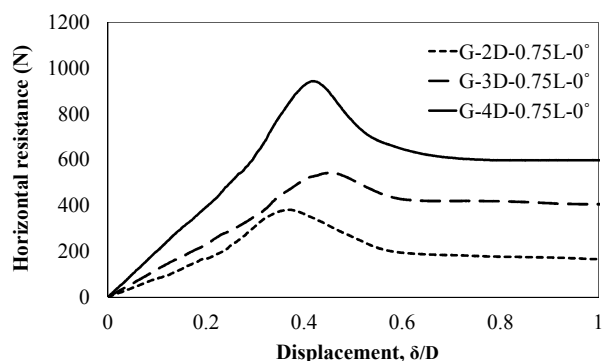
(b) 0.25L



(c) 0.50L



(d) 0.67L



(e) 0.75L

Fig. 5.17 Horizontal behavior of group suction piles with different pile spacings

For group suction piles case, the component suction pile has a large diameter; therefore, an increase of pile spacing requires a more significant pile cap as well as the high capacity equipment to handle the group suction piles. Practical limitation exists in the use of a longer pile spacing. As a result, a suction group pile's dimension should be determined with serious considerations of both group effect and economic efficiency.

### 5.3.3 Group effect

#### Load distribution factor

Load transfer ratios of all the component suction piles of group suction piles with different pile spacings (2D, 3D, and 4D) are analyzed based on the small pressure meters attached to the component piles (Table 5.3 ~ 5.5).

Table 5.3 Load distribution factor for 2D spacing

Loading point	Pile spacing = 2D		
	1 <sup>st</sup> row	2 <sup>nd</sup> row	3 <sup>rd</sup> row
0L	56.0	24.6	19.3
0.25L	59.0	22.6	18.4
0.50L	56.5	23.9	19.6
0.75L	54.4	19.7	25.9

Table 5.4 Load distribution factor for 3D spacing

Loading point	Pile spacing = 3D		
	1 <sup>st</sup> row	2 <sup>nd</sup> row	3 <sup>rd</sup> row
0L	49.7	29.1	21.2
0.25L	47.7	30.9	21.4
0.50L	45.3	30.6	24.1
0.75L	43.9	29.4	26.7

Table 5.5 Load distribution factor for 4D spacing

Loading point	Pile spacing = 4D		
	1 <sup>st</sup> row	2 <sup>nd</sup> row	3 <sup>rd</sup> row
0L	36.4	34.1	29.5
0.25L	36.3	34.8	28.9
0.50L	35.1	34.2	30.7
0.75L	36.7	33.1	30.2

The 1<sup>st</sup> row indicates three leading piles to the loading direction; the 2<sup>nd</sup> row consists of three piles behind the piles of 1<sup>st</sup> row; and the 3<sup>rd</sup> row has the rest of three piles (Fig. 5.18). From the analysis results of the measured load transfer ratios, the load transfer ratios of the piles in the 1<sup>st</sup> row of group suction piles range from 40% ~ 60% depending on the pile spacings. The load transfer ratio of the piles in the 1<sup>st</sup> row decreases and those in the 2<sup>nd</sup> and 3<sup>rd</sup> rows increase with increasing pile spacing. This is because of reduced group effect for increased pile spacing; therefore, relatively, the load transfer ratios of the 2<sup>nd</sup> and 3<sup>rd</sup> rows increase. The load transfer ratio results found in this study could be used as a reference in determination of effective selection of number of component piles and their arrangement.

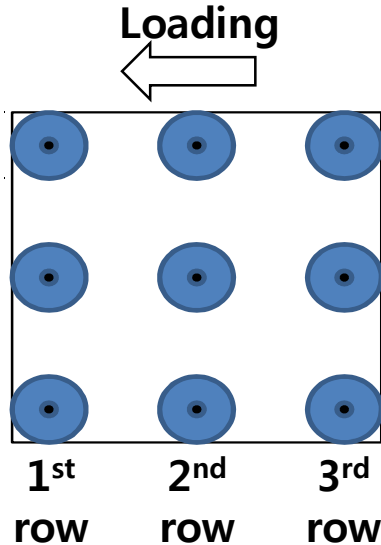


Fig. 5.18 Arrangement of piles

## 5.4 Summary

The horizontal behaviors of group suction piles with different pile spacings (2D, 3D, and 4D) are analyzed varying loading location and load inclination based on the mode test results. As suction piles are widely used as foundations of horizontally-moving floating structures, the suction piles are also subjected to horizontal cyclic loadings. Therefore, a cyclic horizontal load test was performed to examine the cyclic loading effect on the horizontal group suction piles behavior. In addition, load transfer ratios of component piles were assessed based on the earth pressures measured from pressure meters on the component piles.

The maximum ultimate horizontal capacities were found at the loading locations of 50%  $D_f$ . The residual resistances of group suction piles were higher than 40% of the corresponding ultimate horizontal capacities. The ultimate and residual horizontal resistances were lower for inclined loading condition than for horizontal loading condition.

The cyclic loading test results on the group suction piles with pile spacing of 4D show that ultimate and residual horizontal resistances and initial stiffness decrease with increasing number of cycle.

For the given loading locations, the horizontal resistance of group suction piles increases with increasing pile spacing. The average load transfer ratios of the 1<sup>st</sup> rows of the group suction piles fall within 40% ~ 60% of total resistance of the group suction piles. The average load transfer ratio of the 1<sup>st</sup> row piles decreases and those of the piles of the 2<sup>nd</sup> and 3<sup>rd</sup> rows increase with increasing pile spacing.

(Page intentionally left blank)

# **CHAPTER VI INTERPRETATION OF MODEL TEST RESULTS**

## **6.1 Introduction**

In this chapter, the measured ultimate horizontal capacity of single suction pile in this model experiment was compared with their calculated values using the equations for rigid piles proposed by the previous researches. From the examination of single and group piles' behavior, it was found that there exists a strong correlation between the ultimate horizontal capacity and the amount of rotation. In addition, based on the measured earth pressures of component piles of group suction piles, the group effect of the group suction piles was evaluated and the effect of pile spacing of group suction piles on the group effect was also examined.

The horizontal behavior of single and group suction piles was examined varying loading location, load inclination, spacing of component piles. The efficiency of group suction piles was verified under different loading conditions. Lastly, the efficiency of group suction piles derived from the model test results, comprehensive economic analysis was performed with considerations of manufacture, delivery, and construction (or installation) cost.

## 6.2 Ultimate horizontal resistance

### 6.2.1 Ultimate horizontal bearing capacity of rigid pile

An ultimate unit horizontal resistance happens by yielding the surrounding soil with occurring displacement simultaneously by applied horizontal load. In general, the top of a pile reaches the displacement which causes failure firstly, therefore, the ultimate horizontal bearing capacity shows the tendency of progressive failure into the depth direction of pile. When the ultimate unit horizontal bearing capacity occurs throughout the surface of pile, the pile is judged as an ultimate state. At this time, the horizontal bearing capacity getting from surrounding soils is ultimate bearing capacity.

The ultimate unit bearing capacity of pile,  $p_u$  and the ultimate horizontal bearing capacity,  $H_u$  can be calculated from the condition of static equilibrium as shown in Fig. 6.1. Also, from the condition of force equilibrium,  $\sum F_y = 0$ , Eq. (6.1) can be drawn.

$$H_u - \int_0^{x_r} p_{xu} D dx + \int_{x_r}^L p_{xu} D dx = 0 \quad (6.1)$$

Where,  $x_r$ : distance from the soil surface to rotation point of pile

$D$ : pile diameter

$L$ : pile length

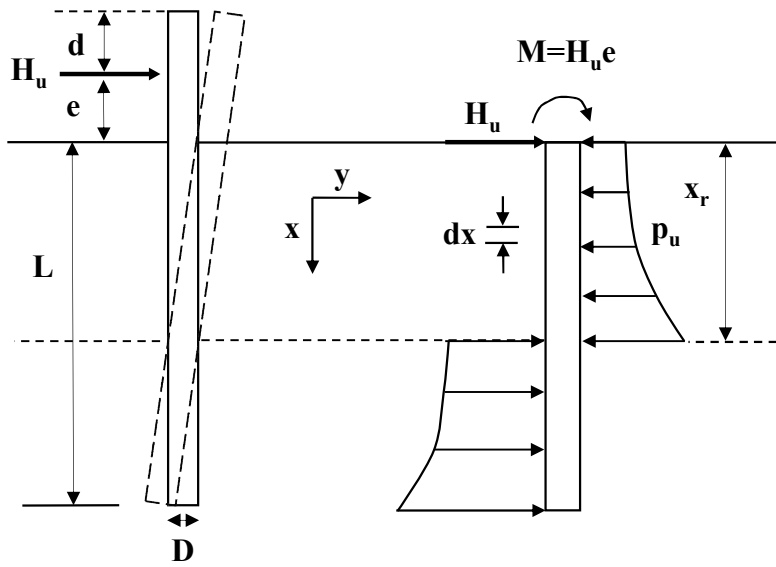


Fig. 6.1 Scheme of horizontal resistance of pile

Additionally, Eq. (6.2) can be drawn from moment equilibrium,  
 $\sum M = 0$ .

$$H_u e + \int_0^{x_r} p_{xu} D dx - \int_{x_r}^L p_{xu} D dx = 0 \quad (6.2)$$

Where  $e$ : distance from loading location to soil surface

If the distribution of the ultimate unit horizontal bearing capacity varying the depth is figured out, the distance to rotation point,  $x_r$ , and ultimate horizontal bearing capacity can be estimated from Eq. (6.1) and (6.2). Basically,  $x_r$  is estimated as the point, which the sum of moment is zero by trial and error method, but, according to the researcher who proposed the distribution of earth pressure, there can be several cases which  $x_r$  is fixed as constant value. The ultimate unit

horizontal bearing capacity can be generally estimated from the relationship between the earth pressure coefficient and vertical effective stress.

### ***Broms' method (1964)***

Broms (1964) assumed that, in the pile applied horizontal load, the tip of the pile is fixed bearing the horizontal load. The soil resistance caused by displacement accompanying the rotation is shown as simple triangle distribution of the ultimate unit horizontal bearing capacity as Fig. 6.2.

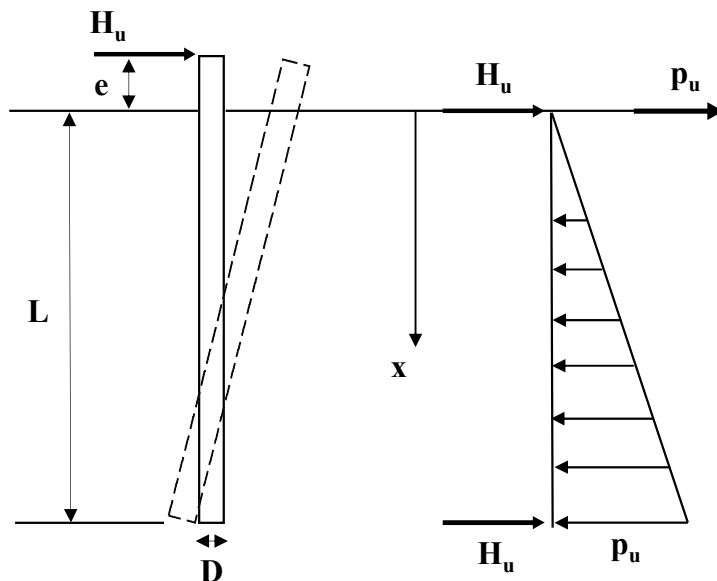


Fig. 6.2 Distribution of ultimate unit horizontal bearing capacity  
(Broms, 1964)

The resistance at ultimate state is the ultimate unit horizontal bearing capacity of the soil, and the ultimate unit horizontal bearing

capacity can be calculated by moment equilibrium (Eq. 6.3).

$$p_u = 3K_p \sigma'_v = 3K_p \gamma x \quad (6.3)$$

Where,  $K_p$ : coefficient of passive lateral earth pressure

$\sigma'_v$ : effective vertical stress

$\gamma$ : unit weight of soil

$x$ : depth from soil surface

The ultimate horizontal bearing capacity can be presented by adapting the triangle distribution of the ultimate unit horizontal bearing capacity as follow (Eq. 6.4)

$$H_u = \frac{1}{2}(3K_p \sigma'_v)L = 0.5P_u L \quad (6.4)$$

Where,  $L$ : embedded depth of pile

#### Petrasovits and Award's method (1972)

Petrasovits and Award (1972) assumed that, in horizontal loading, the pile is rotated at some amount of distance above from the tip of the pile, not at fixed tip of the pile, and passive lateral earth pressure occurs on opposite direction with rotation point as the center. Thus, the ultimate unit horizontal bearing capacity considered has been represented in Fig. 6.3.

At this time, the earth pressure occurs both active earth pressure and passive earth pressure according to the rotation point. Therefore, Petrasovits and Award (1972) presents the ultimate unit horizontal bearing capacity as Eq. (6.5) and the ultimate horizontal bearing

capacity as Eq. (6.6).

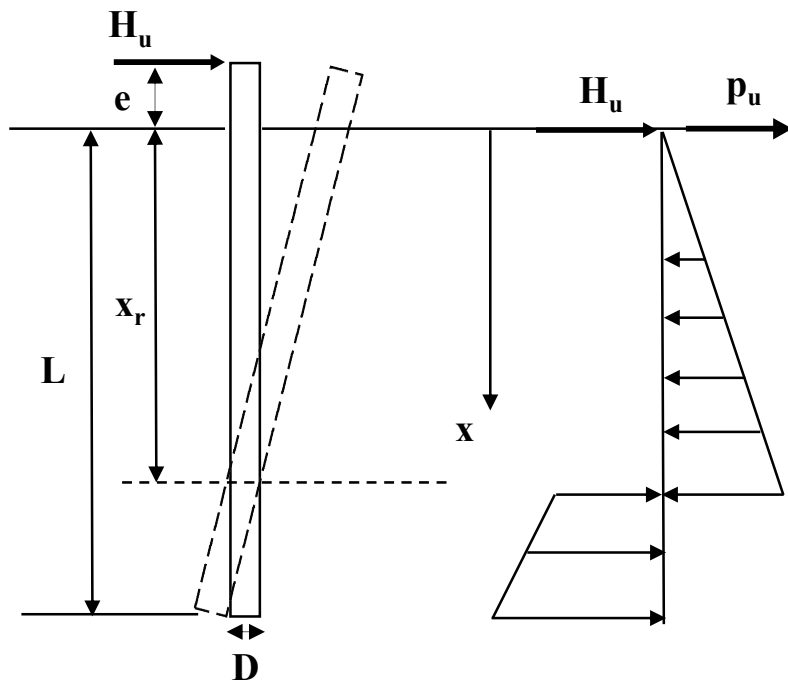


Fig. 6.3 Distribution of ultimate unit horizontal bearing capacity  
(Petasovits and Award, 1972)

$$P_u = (3.7K_p - K_a)\sigma_v' = (3.7K_p - K_a)\gamma x \quad (6.5)$$

$$H_u = P_u LD \left[ \left( \frac{L}{x_r} \right)^2 - \frac{1}{2} \right] \quad (6.6)$$

Where,  $K_a$ : coefficient of active lateral earth pressure

$x_r$ : distance from soil surface to rotation point

The  $x_r$  is estimated using Eq. (6.5) and (6.6) by trial and error method.

**Prasad and Chari's method (1999)**

Horizontally loaded pile is affected by different cross sectional shape of the pile (Prasad and Chari, 1999). Thus, Prasad and Chari (1999) brought some coefficients to estimate the ultimate unit horizontal bearing capacity according to the cross section of the pile shown as Fig. 6.4. and Eq. (6.7).

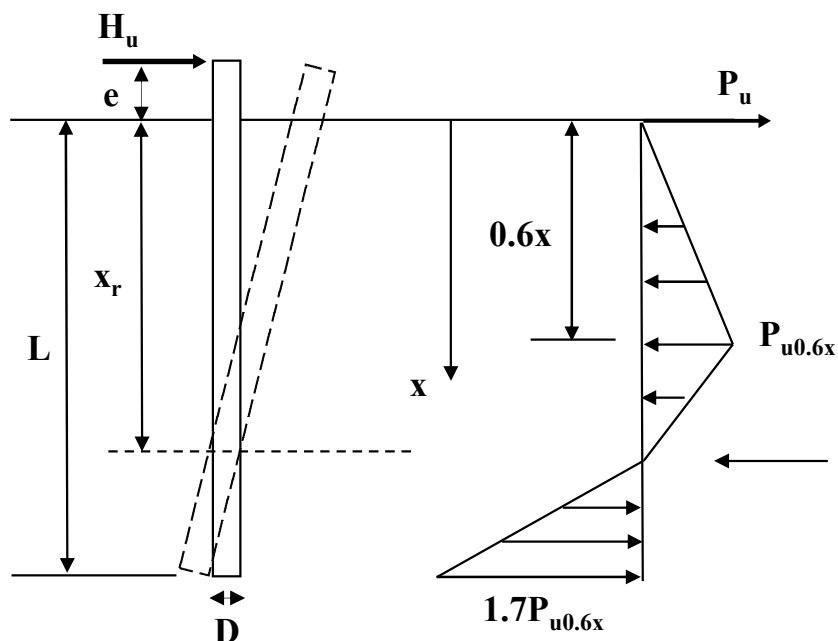


Fig. 6.4 Distribution of the ultimate unit horizontal bearing capacity  
(Prasad and Chari, 1999)

$$P_u = s K_p \sigma_{v,0.6x}' = 10^{(1.3\tan\phi + 0.3)} \gamma x \quad (6.7)$$

Where,  $s$ : cross section coefficient (circular=0.8, rectangular=1.0)

$\sigma_{v,0.6x}'$ : effective vertical stress at  $0.6x$  depth for soil surface

$\phi$ : internal friction angle

The ultimate horizontal bearing capacity can be represented by the distribution of the ultimate unit horizontal bearing capacity as shown in Fig. 6.4 as follows (Eg. (6.8) and (6.7)).

$$H_u = 0.4 [10^{(1.3\tan\phi + 0.3)}] \gamma x D (2.7x - 1.7L) \quad (6.8)$$

$$x_r = [-(0.567L + 2.7e) + (5.307L^2 + 7.29e^2 + 10.54eL)^{0.5}] / 2.1996 \quad (6.9)$$

Where,  $e$ : distance from loading location to soil surface

#### API RP2A's formular (1987)

P-y curve analysis method is typical nonlinear analysis to estimate a characteristic of load transfer by using the relationship between the response of the ground and horizontal displacement of the pile. This load transfer curve had been introduced by McClelland and Focht (1956). Reese and Matlock (1956) expanded this research, and this method had been adapted in API RP2A Standards for offshore structure of API (American Petroleum Institute).

The p-y curve can be estimated by following Eq. (6.10).

$$p = A p_u \tanh\left(\frac{k x}{A p_u} y\right) \quad (6.10)$$

Where,  $A$ : coefficient of frequency or static loading

$$\text{(cyclic loading: } A=0.9, \text{ static loading: } A=3.0 - 0.8 \frac{x}{b} \geq 0.9)$$

$k$ : initial ground response coefficient ( $kN/m^3$ ) (Fig. 6.5)

$p_u$ : smaller one between Eq. (6.11) and (6.12)

$$p_{us} = (C_1 x + C_2 D) \gamma' x \quad (6.11)$$

$$p_{ud} = C_3 D \gamma' x \quad (6.12)$$

Where,  $\gamma'$ : effective unit weight of soil

$C_1$ ,  $C_2$ ,  $C_3$ : function of internal friction angle (Fig. 6.6)

$\phi'$ : drained friction angle

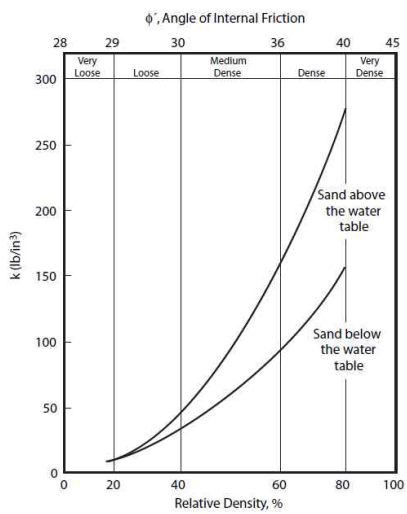


Fig. 6.5 initial ground response coefficient

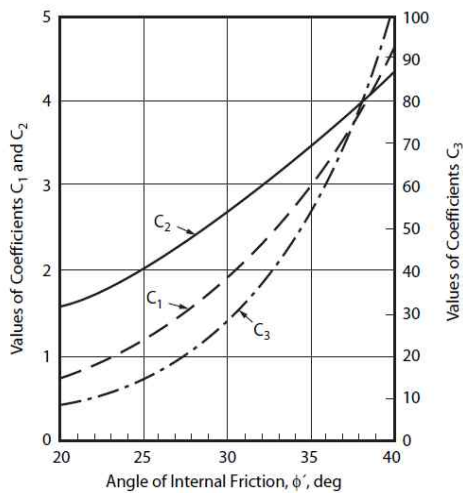


Fig. 6.6  $C_1$ ,  $C_2$ ,  $C_3$

### **6.2.2 Single suction pile**

Previous researchers (Broms 1964; Petrasovits and Award 1972; Prasad and Chari 1999; Reese and Matlock 1956) proposed different equations for determination of ultimate horizontal capacities piles. The measured ultimate horizontal capacities of single suction piles in this study were compared with their estimations from the previous research results, as shown in Fig. 6.7. The estimated ultimate horizontal capacities from the previous equations were much higher (approximately 30% higher) than those observed in the present experiment. The difference between the estimated and observed ultimate horizontal capacities varied with different loading locations. Therefore, it is difficult to clearly correlate the estimated ultimate horizontal capacities with the corresponding measured ones. The deviation of the ultimate horizontal capacity estimations from their observations lies in the assumption in their estimation that a rotation centroid exists inside of pile. In addition, it is assumed that the maximum horizontal resistance is mobilized within very small amount of movement. However, from the experiment of single suction piles, ultimate horizontal resistance is reached at a relatively large displacement and both translation and rotation occur simultaneously during the pile movement. In the experiment, the rotation centroid of single suction piles locates outside of pile. The rotation centroid of single suction pile exists below the suction pile if the loading point locates higher than the centroid of load distribution, and vice versa. Therefore, a more advanced ultimate horizontal capacity estimation method is required for the suction piles used as foundations of floating structures.

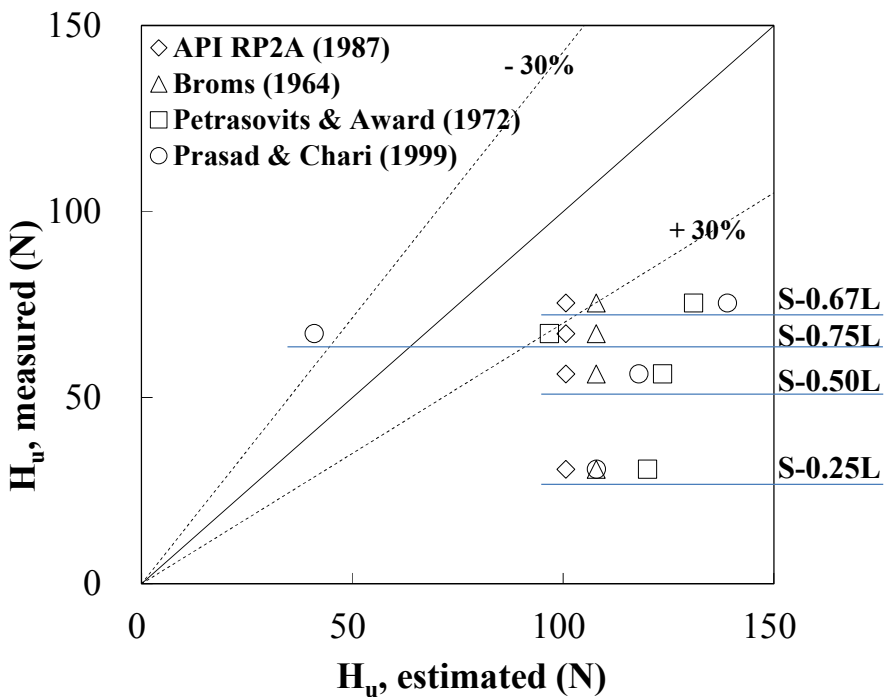


Fig. 6.7 Comparison of estimated  $H_u$  and measured  $H_u$

Fig. 6.8 shows the rotations corresponding to ultimate horizontal capacities of single suction piles under different loading locations. As seen in Fig. 6.8, a clear linear correlation exists between the ultimate horizontal capacity and rotation amount of single suction pile. It is inferred that the horizontal resistance of single suction pile is increased as the restraint against pile rotation is increased. Furthermore, the measured ultimate horizontal capacity of single suction pile shows high correlations with those estimated using the API and Broms' equations.

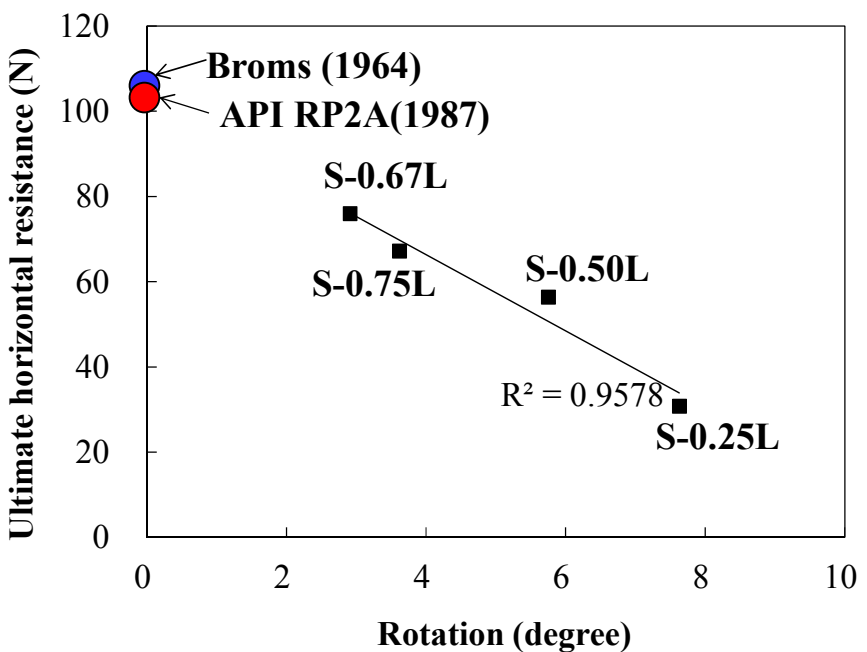


Fig. 6.8 Rotation of single suction pile at ultimate horizontal resistance

### 6.2.3 Group suction piles

Fig. 6.9 presents the ultimate horizontal capacities of group suction piles with increasing rotation under different loading locations. Similarly to the single suction pile cases, a strong linear correlation exists between ultimate horizontal capacity and pile rotation amount. The reduction rates in ultimate horizontal capacity for group suction piles with pile spacing of 2D and 3D with increasing rotation were similar; however, the reduction rate of ultimate horizontal capacity of the group suction piles with pile spacing of 4D was lower than those with less pile spacings (2D and 3D). It is inferred that the group suction piles with the highest pile spacing have the higher ultimate horizontal capacity that is less dependent on rotation.

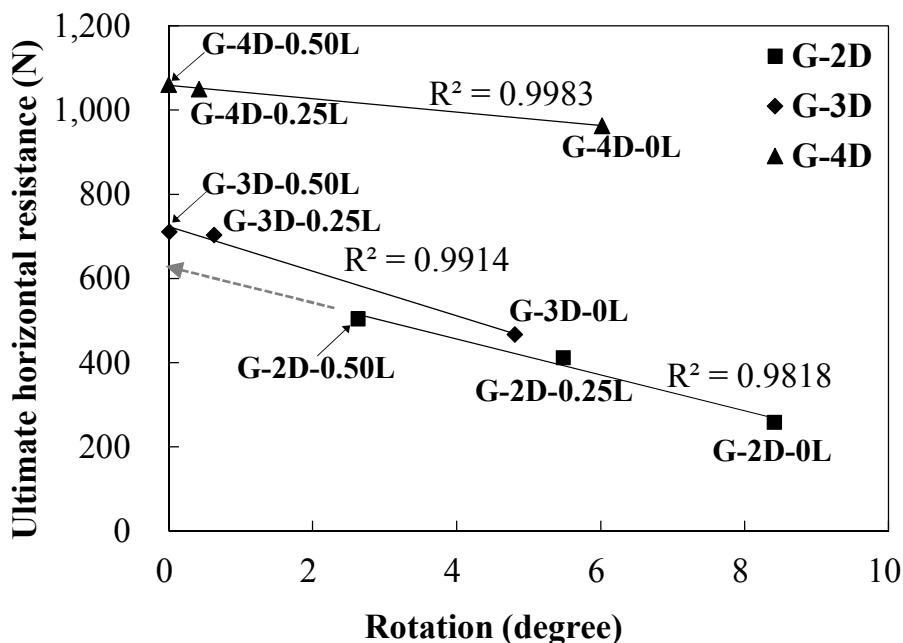


Fig. 6.9 Rotation of group suction piles at ultimate horizontal resistance

Based on the observed relationships between ultimate horizontal capacity and rotation for group suction piles with different pile spacings, expected rotation amount can be estimated for a known ultimate horizontal capacity, and vice versa. For example, the maximum ultimate horizontal capacity (corresponding to zero rotation) for the given group suction piles with pile spacing of 2D can be estimated by extending the lowest line to meet the y axis. The estimated maximum ultimate horizontal capacity is about 620 N, in model scale.

Generally, if the spacings between component piles are less than or equal to twice their diameters (2D), the group piles shows block behavior. From the experiments of group suction piles under the conditions that the loading locations are at 50% of the embedded depth (loading locations resulting ultimate horizontal resistances), comparisons was made between the test results and the calculations of ultimate horizontal resistances of the assumed blocks. When the group piles behaving as blocks are exposed to horizontal loadings (Figure 6.10), the total ultimate horizontal resistances of the group piles can be calculated as the sum of the passive resistances ( $H_u$ ) at the group pile facings and the frictional resistances ( $W\tan\delta$ ) against sliding, as shown in Table 6.1.

The measured ultimate resistance of the group pile with pile spacing of 2D was 17% less than the calculated value. The under-evaluation of the group pile's ultimate resistance from the experiment may result from the rotation observed during experiment. The ultimate resistance without any rotation, which can be estimated from the curve in Figure 6.9 showing the relationship between rotation and ultimate resistance, matched well with the calculated ultimate resistance of the equivalent block.

The ultimate resistance of group pile with pile spacing of 3D, the measured ultimate resistance was about 20% less than the calculated

resistance. The difference in ultimate resistances may result from the different behavior modes between the real group pile (showing considerable group effect) and block behaviors. Further experiment of the group pile with pile spacing of 4D showed that the measured and calculated ultimate horizontal resistances were very similar, which may result from negligible group effect (refer section 6.2.4 for group effect).

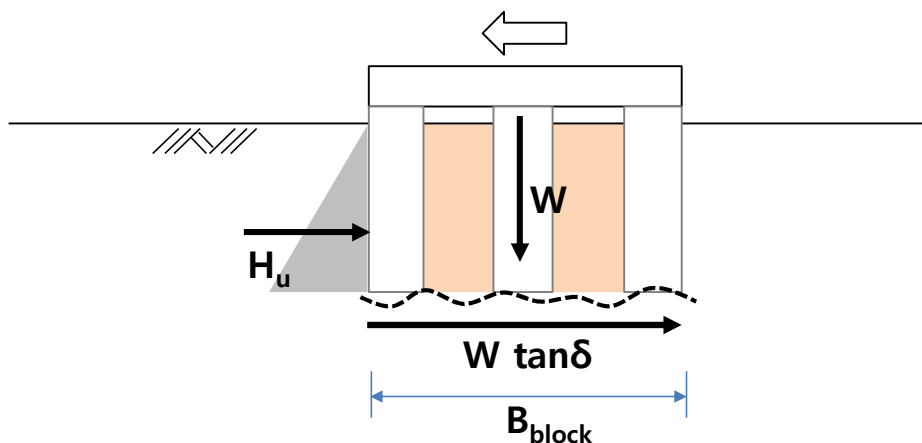


Fig. 6.10 Block resistance of group suction piles against sliding

Table 6.1 Comparison of the measured ultimate horizontal resistances with the calculated resistances of block-assumed group suction piles

Type	$B_{block}$ (m)	$H_u$ (N)	W (N)	$W \tan \delta$ (N)	Estimated $H_u + W \tan \delta$ (N)	Measured $R_{ult}$ (N)	Measured / Estimated
2D-0.50L	0.3	539.6	92.9	71.2	610.8	504.4	0.83
3D-0.50L	0.42	755.4	105.1	80.7	836.1	671.0	0.80
4D-0.50L	0.54	971.2	176.9	135.7	1106.9	1062.9	0.96

#### **6.2.4 Group effect**

For group suction piles with different pile spacings (2D, 3D, and 4D), the maximum ultimate horizontal capacities were observed when the loading location was at 50% of the embedded depth ( $D_f$ ). Based on the earth pressures measured from the small pressure meters attached to component piles of group suction piles with different pile spacings, group effects of component piles were examined for group suction piles with a loading location at 50%  $D_f$ . The group effect of group suction piles was evaluated following the p-multiplier factors of group piles proposed by Brown (1988). The measured horizontal resistances of component piles were normalized with the estimated ultimate horizontal capacity of single suction piles using the proposed analytical equation by API RP2A (1987).

The group effect of group suction piles was examined based on the measured earth pressures on all the component piles. The detailed calculation procedure is summarized in Table 6.2 and 6.3. The effect of component pile spacing on the group pile was also evaluated by increasing pile spacings. For the component pile spacing higher than 4D, it can be concluded that there exists negligible group effect.

From the comparison of group effect between the group suction piles with pile spacing of 3D and the literature review results (Table 2.3), for the given pile spacing of 3D, the comparison results show that the group effect is smaller for the group suction piles than for the conventional group piles.

Table 6.2 Calculation procedure for estimating group effect

Pile spacing	Loading point	Ultimate horizontal capacity (N)	Capacity by top cap (N)	Ultimate horizontal of only piles (N)	Load distribution factor		
					1 <sup>st</sup> row	2 <sup>nd</sup> row	3 <sup>rd</sup> row
2D	0.50L	504.4	92.9	411.5	0.57	0.24	0.20
		620.0*	92.9	527.1			
3D	0.50L	671.0	105.1	565.9	0.45	0.31	0.24
4D	0.50L	1062.9	176.9	886.0	0.35	0.34	0.31

\* Ultimate horizontal capacity of 2D group suction piles is derived from Fig. 6.9  
 Ultimate horizontal capacity of single suction pile (API RP2A(1987)) = 100.7 N

Table 6.3 Calculation results of group effect

Pile spacing	Loading point	Group effect*		
		(Horizontal capacity of group) / (Horizontal capacity of single)		
		1 <sup>st</sup> row	2 <sup>nd</sup> row	3 <sup>rd</sup> row
2D	0.50L	0.77	0.33	0.27
		0.99*	0.42*	0.35*
3D	0.50L	0.85	0.57	0.45
4D	0.50L	1.02	1.00	0.90

\* Ultimate horizontal capacity of 2D group suction piles is derived from Fig. 6.9

## 6.3 Comparison of single and group pile

### 6.3.1 Effect of loading conditions

#### Loading location

Fig. 6.11 compares ultimate horizontal capacities of single and group suction piles with different loading locations based on the model test results.

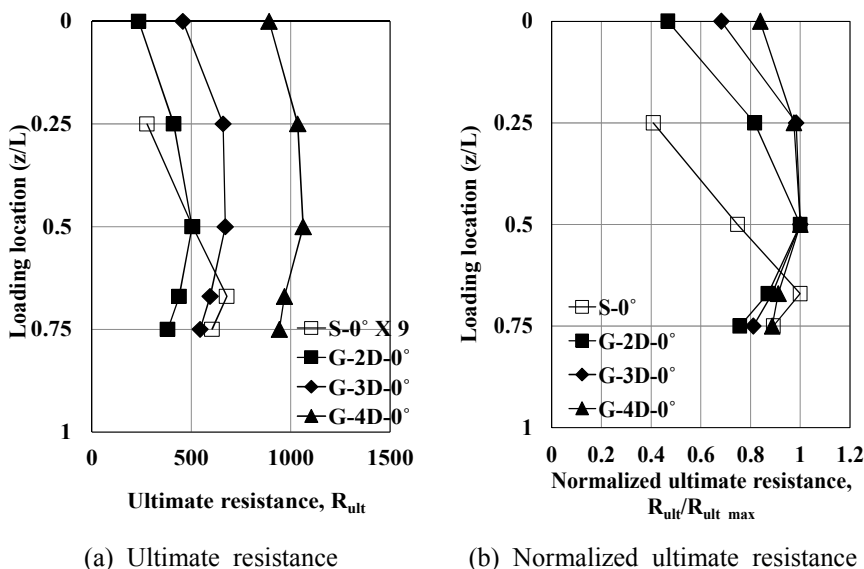


Fig. 6.11 Summarized ultimate horizontal resistance of single and group suction piles with different loading

Fig. 6.11(a) shows the ultimate horizontal capacities with respect to loading location on single and group pile, while Fig. 6.11(b) captures the ratios of the ultimate horizontal capacities at their measured loading locations to their maximum ultimate horizontal capacity to examine

ultimate horizontal capacity variation range with respect to loading location.

The ultimate horizontal capacity of the group suction piles with nine component piles is compared with nine times the ultimate horizontal capacity of a single suction pile. The ultimate horizontal capacities of the group suction piles with pile spacing of 3D at the loading locations of 25% and 50% were greater than the sum of ultimate capacities of nine single suction piles (Figure 6.11(a)). From Figure 6.11(b), the ultimate horizontal capacity ranges with respect to loading locations were 30% and 60% of their maximum ultimate capacities, respectively.

Fig. 6.12 compares the residual resistances of single and group suction piles with respect to loading locations.

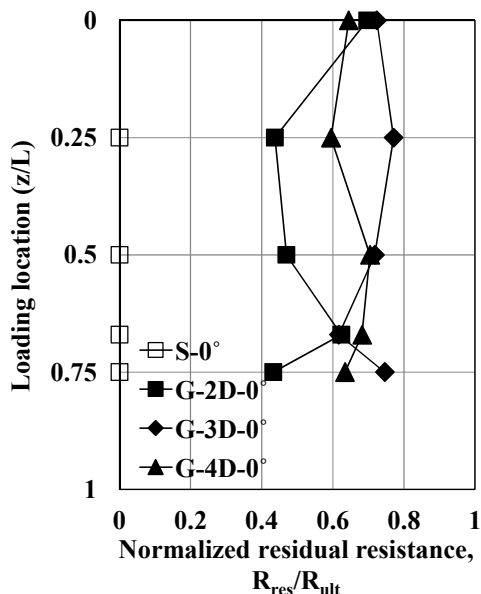
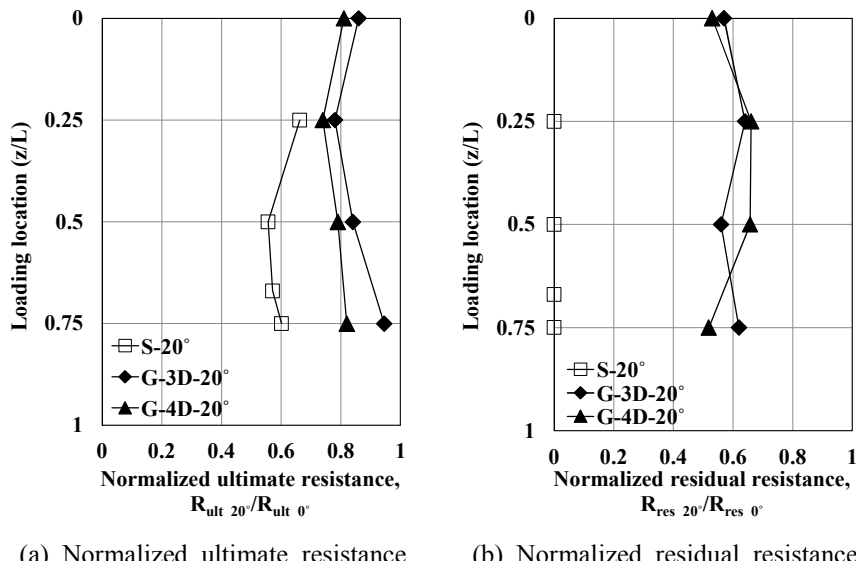


Fig. 6.12 Normalized residual resistance of single and group suction piles with different loading locations

The residual resistances of single suction pile is almost negligible while those of the group suction piles maintain within a range of 40% ~ 75% of their ultimate horizontal capacities. Therefore, it can indicate that group suction piles are considered superior over the single suction pile in terms of resistance against horizontal loads.

### Loading angle

Fig. 6.13 compares the reduction rates from the ultimate horizontal capacities to their corresponding residual horizontal resistances of single and group suction piles under different load inclinations.



(a) Normalized ultimate resistance      (b) Normalized residual resistance

Fig. 6.13 Summarized ultimate horizontal resistance of single and group suction piles with 20° inclination

Fig. 6.13(a) shows that the ultimate horizontal capacities of group suction piles decreased by 5% ~ 30% when load inclination become 20° from 0° while the ultimate capacity decreased 40% ~ 60% for

single suction pile. Under load inclination of  $20^\circ$ , the residual resistances of single suction piles were almost zero while those of group suction piles reached approximately 60% of their ultimate capacity (Fig. 6.13(b)).

### 6.3.2 Effect of pile spacing

Fig. 6.14 compares the ultimate horizontal capacities of single and group suction piles. For equivalent comparison of ultimate capacities of single and group suction piles, the ultimate capacity of single pile was multiplied by nine to match the number of component piles. The comparison results show that the ultimate horizontal capacity of group suction piles increases with increasing component pile spacing (maximum ultimate capacity was identified for pile spacing of 4D). The ultimate horizontal capacity of group suction piles with pile spacing of 4D was about 55% higher than that of nine single suction piles (Table 6.4).

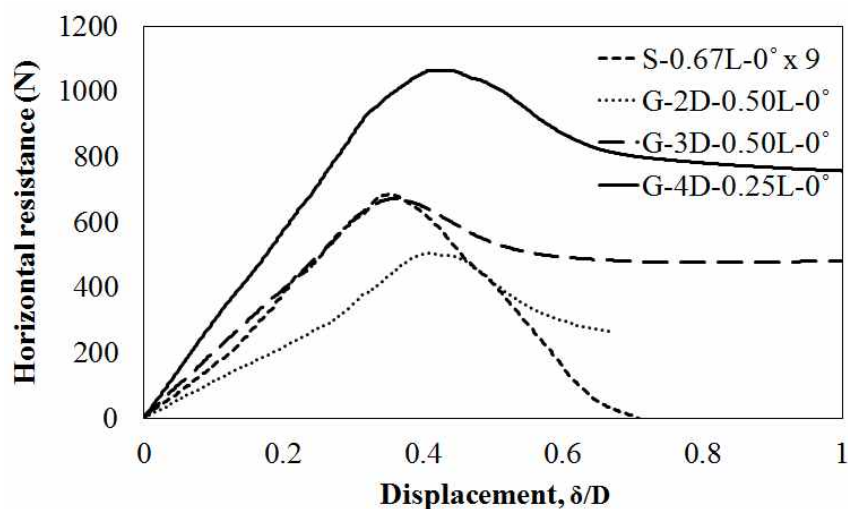


Fig. 6.14 Comparison on the ultimate horizontal resistance of single and group suction piles

Table 6.4 Summarized comparison results of ultimate horizontal resistance

Type	Ultimate horizontal resistance (N)	(Ultimate horizontal resistance of group) / (Ultimate horizontal resistance of single × 9EA) × 100 (%)
S	Single	76.0
	Single×9EA	684.0
G	2D-0.50L	504.4
	3D-0.50L	671.0
	4D-0.50L	1062.9

## 6.4 Cost analysis

Cost analysis was performed based on the comparison of the ultimate horizontal capacities of single and group suction piles. The ultimate horizontal capacities of group suction piles were measured varying component pile spacing, loading location, load inclination. The maximum horizontal resistance of group suction pile was found at pile spacing of 4D and loading location of 50% of its embedded depth. Despite that the number of component piles of the group suction pile is nine, its ultimate capacity was comparable with the fourteen times of the ultimate capacity of single pile. In other word, for the site that requires 14 times of ultimate capacity of single suction pile, the number of required component piles can be reduced by 5 if group suction pile with 4D pile spacing and loading location at the mid-length is implemented (Table 6.5).

Table 6.5 Equivalent number of piles based on the comparison of the ultimate horizontal capacities

Type		Ultimate horizontal resistance (N)	Equivalent number of piles (Ultimate resistance of group) / (Ultimate resistance of single)
S	Single	76.0	1 EA
	Single × 9EA	684.0	9 EA
G	2D-0.50L	504.4	7 EA
	3D-0.50L	671.0	9 EA
	4D-0.50L	1062.9	14 EA

For the cost analysis, the hydraulic and geotechnical conditions were fit to the conditions of Saemanguem region at the West Sea side

of Korea. From the comparison results, comprehensive cost analysis was performed reflecting manufacture, transportation, and installation costs. The pile cap of the group suction pile is fabricated using H beam, as shown in Fig. 6.15.

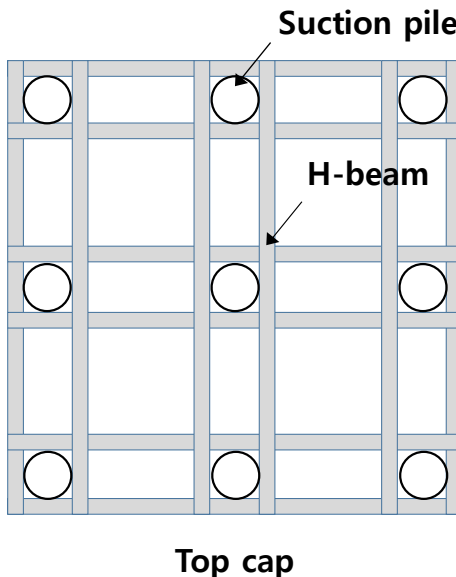


Fig. 6.15 Scheme of top cap using H beam

Tables 6.6 and 6.7 summarize the total construction cost analysis results of single and group suction piles. From the previous analysis, the group suction pile's ultimate capacity was assumed to be equivalent to 14 times of single suction pile's ultimate capacity. Construction cost analysis results with respect to ultimate horizontal capacity of suction pile are presented in Fig. 6.16. From Fig. 6.16(b), the use of group suction pile pays off against the use of single suction piles when the ultimate horizontal capacity exceeds 30 MN. In other words, group suction pile is more economical than sum of single suction piles for which the required ultimate capacity is higher than 30 MN. In addition,

to have ultimate capacity of 30 MN, the required single suction pile's diameter is approximately 9.0 m. In this case, use of the group pile with component suction pile's diameter of 4.0 m is more economical.

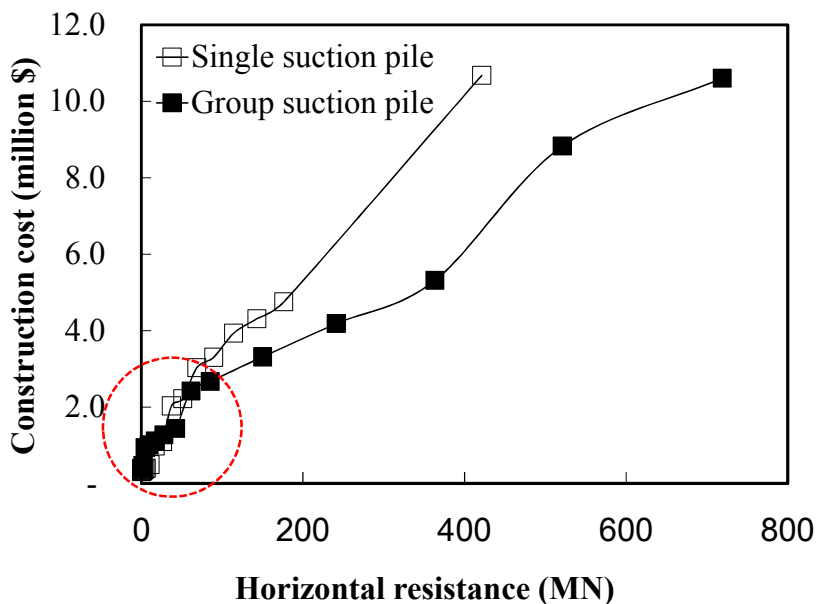
When single suction pile's diameter increases, the self-weight of the pile increases geometrically; therefore, construction cost is significantly increased due to the tremendous expense required to use offshore cranes. On the other hand, the component piles of group suction piles are not too heavy and are installed individually. Installation of each component pile does not require heavy offshore cranes. However, the cost analysis in this study was performed with simplified assumptions without considerations of certified installation method and procedure. Further study is required for better cost analysis after establishment of detailed construction methods of suction group piles.

Table 6.6 Calculation table of economic analysis

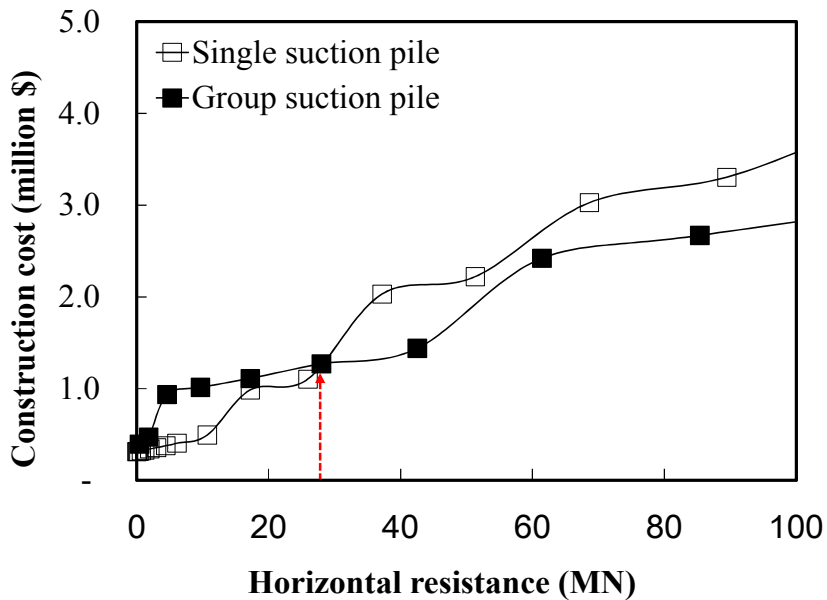
Single pile					Installation (\$)	Total construction cost (\$)	Horizontal resistance (MN)
D (m)	L (m)	t (mm)	Self weight (ton)	Manufacturing and shipping (\$)			
1.0	3.0	6	0.48	601	313,000	313,601	0.03
1.5	4.5	9	1.62	2,029	313,000	315,029	0.13
2.0	6.0	12	3.85	4,809	313,000	317,809	0.33
2.5	7.5	15	7.51	9,393	313,000	322,393	0.69
3.0	9.0	18	12.98	16,230	313,000	329,230	1.23
3.5	10.5	21	20.62	29,897	313,000	342,897	2.00
4.0	12.0	24	30.78	44,627	313,000	357,627	3.04
4.5	13.5	27	43.82	63,542	314,000	377,542	4.39
5.0	15.0	30	60.11	87,163	318,000	405,163	6.10
6.0	18.0	36	103.87	150,618	345,000	495,618	10.72
7.0	21.0	42	164.95	239,175	748,000	987,175	17.23
8.0	24.0	48	246.22	357,020	748,000	1,105,020	25.96
9.0	27.0	54	350.58	508,335	1,524,000	2,032,335	37.22
10.0	30.0	60	480.90	697,304	1,524,000	2,221,304	51.34
11.0	33.0	66	640.08	928,112	2,100,000	3,028,112	68.66
12.0	36.0	72	830.99	1,204,941	2,100,000	3,304,941	89.48
13.0	39.0	78	1056.54	1,531,977	2,400,000	3,931,977	114.13
14.0	42.0	84	1319.59	1,913,402	2,400,000	4,313,402	142.95
15.0	45.0	90	1623.04	2,353,401	2,400,000	4,753,401	176.24
20.0	60.0	120	3847.19	5,578,432	5,100,000	10,678,432	421.29

Table 6.7 Calculation procedure of economic analysis

Group pile (Single pile * 9 EA)					Top cap		Installation (\$)	Total construction cost (\$)	Horizontal resistance (MN)
D (m)	L (m)	t (mm)	Self weight (ton)	Manufacturing and shipping (\$)	Self weight (ton)	Manufacturing and shipping (\$)			
1.0	3.0	6	4.3	5,410	68.04	72,514	318,000	395,924	0.42
1.5	4.5	9	14.6	18,259	102.06	108,770	345,000	472,030	1.82
2.0	6.0	12	34.6	43,281	136.08	145,027	748,000	936,308	4.62
2.5	7.5	15	67.6	84,533	170.10	181,284	748,000	1,013,817	9.66
3.0	9.0	18	116.9	146,073	204.12	217,541	748,000	1,111,614	17.22
3.5	10.5	21	185.6	269,072	238.14	253,798	748,000	1,270,870	28.00
4.0	12.0	24	277.0	401,647	272.16	290,055	748,000	1,439,702	42.56
4.5	13.5	27	394.4	571,876	306.18	326,311	1,524,000	2,422,188	61.46
5.0	15.0	30	541.0	784,467	340.20	362,568	1,524,000	2,671,035	85.40
6.0	18.0	36	934.9	1,355,559	408.24	435,082	1,524,000	3,314,641	150.08
7.0	21.0	42	1484.5	2,152,577	476.28	507,595	1,524,000	4,184,173	241.22
8.0	24.0	48	2216.0	3,213,177	544.32	580,109	1,524,000	5,317,286	363.44
9.0	27.0	54	3155.2	4,575,011	612.36	652,623	3,600,000	8,827,634	521.08
10.0	30.0	60	4328.1	6,275,736	680.40	725,136	3,600,000	10,600,872	718.76



(a) Construction cost with increasing horizontal resistance



(b) Enlarged plot of (a) : horizontal resistance less than 100 MN

Fig. 6.16 Construction cost analysis results with respect to horizontal resistance

## 6.5 Summary

The ultimate horizontal capacities of single suction piles measured from model tests were compared with those estimated from the lateral capacity equations of rigid piles by many researchers. There exists no strong correlation between the measured and estimated ultimate horizontal capacities, and an accurate estimation method is required to evaluate the ultimate horizontal capacity of single suction pile, which are often used as an anchor.

For both single and group suction piles, a strong corrections between ultimate horizontal capacity and rotation was found. The measured ultimate horizontal capacities of single suction piles also showed a high correlation with those predicted by previous researchers. The group effect of group suction piles is examined based on the measured earth pressures on all the component piles. The effect of component pile spacing on the group effect is also evaluated by increasing pile spacings. For the component pile spacing higher than 4D, there exists negligible group effect.

The efficiency of group suction piles were evaluated by examining horizontal behavior of single and group suction piles under different loading location, load inclinations, and pile spacings. The horizontal behavior of group suction pile is less sensitive against loading location and load inclination compared with those of single piles. Moreover, the residual horizontal resistances of group suction piles range within 40%~75% of their ultimate horizontal capacities.

The comprehensive cost analysis was performed considering manufacture, transportation, and installation cost. Based on cost analysis, use of group suction pile with component pile spacing of 4D is more economical than use of single suction piles when the required ultimate

capacity is higher than 30 MN.

(Page intentionally left blank)

# CHAPTER VII SUMMARY AND CONCLUSIONS

## 7.1 Summary

In this study, a new type of suction pile as a foundations of a floating structure, group suction piles were proposed to improve the shortcomings of conventional single suction piles. Small-scaled model tests were performed to estimate horizontal behavior of single suction piles and group suction piles with different pile spacings (2, 3 and 4 times of the pile diameter) under various loading conditions in terms of loading locations and inclinations. In addition, load distributions of component piles of group suction piles were evaluated.

### *Model tests on single suction piles*

To avoid any possible significant uncertainties associate with a single suction pile model test result, triplicate tests were performed for each test condition to ensure the repeatability and reliability of experimental system and methods of model tests. The results of triplicate test shown consistence reasonably. The suction installation effect on the horizontal resistance of a single suction pile in sands was examined. The ultimate horizontal resistance and initial stiffness of a single suction pile installed by suction pressure were approximately 10% and 30% lower than those of the pile installed by jacking force. Due to the lower effective stress from suction installation, it can be said that an estimation of the horizontal resistance from the single

suction pile installed by jacking force in dense sands may overestimate the true in-situ horizontal resistance.

The effect of different loading locations and load inclinations on the horizontal resistance of the suction pile was evaluated. Based on the test results, the horizontal behavior of the suction pile varied significantly with loading locations and inclinations. The maximum horizontal resistance was identified at the loading location of 67% of the embedded depth, and the horizontal resistance without load inclination is greater than those with load inclination.

### ***Model tests on group suction piles***

The horizontal behavior of group suction piles with different pile spacings is analyzed for various loading locations and load inclinations based on the model tests. For the given group pile configurations (a group pile having 9 component piles with pile formation of  $3 \times 3$ ), the horizontal resistance increases with increasing pile spacing. The maximum ultimate horizontal resistances were found at the loading locations of 50% of the embedded depth. Unlike the single suction pile case, the significantly maintained residual resistances were found for group suction piles. The residual resistances of group suction piles were at least higher than 40% of the corresponding ultimate horizontal resistances. The ultimate and residual horizontal resistances were lower for loading condition (20 degrees) than for no inclined loading condition.

A cyclic horizontal load test was performed to examine the cyclic loading effect on the horizontal behavior of group suction piles. The cyclic test was performed only for group suction piles with pile spacing of 4 times of pile diameter. When cyclic load (50% of the ultimate

horizontal resistances) is applied on the group suction piles, its ultimate and residual horizontal resistances and initial stiffness decrease; however, their decremental rates also reduce with increasing number of cycles.

For the examination of load distributions on each component pile, earth pressures were attached on the component piles. For smaller pile spacings of component piles, considerable amount of horizontal load were resisted by the piles at the first row. The average load distribution ratios of the 1<sup>st</sup> rows of the group suction piles fall within 40% ~ 60% of total resistance of the group suction piles. When the pile spacing is increased, it was found that the horizontal load is more evenly distributed to each component piles. The average load transfer ratio of the 1<sup>st</sup> row piles decreases and those of the piles of the 2<sup>nd</sup> and 3<sup>rd</sup> rows increase with increasing pile spacing.

### ***Interpretation of model test results***

The ultimate horizontal resistances of single suction piles measured from model tests were compared with the estimations based on the typically used equations proposed by other researcher. The estimated ultimate horizontal resistances were approximately 30% higher than those measured from the experiment. There exists no strong correlation between the measured and estimated ultimate horizontal capacities. A need of accurate estimation method should be developed for the suction piles, which behave as rigid piles subjected to large translation and rotation. In this study, a strong correlation between ultimate horizontal capacity and rotation was observed from the experiment for both single and group suction piles. The ultimate horizontal capacity increased with decreasing rotation.

The effect of component pile spacing on the group effect was also evaluated by increasing pile spacings from the experiment. For the component pile spacing higher than 4 times their pile diameters, there exists negligible group effect from pile spacing.

The efficiency of group suction piles was evaluated by examining horizontal behavior of single and group suction piles under various loading location and load inclinations, and pile spacings. The horizontal resistance of group suction piles is less sensitive against loading location and load inclination compared with those of single piles. Unlike the single suction pile case, the residual horizontal resistances of group suction piles were maintained within a range of 40% ~ 75% of their ultimate horizontal capacities.

Based on the model test results, the comprehensive cost analysis was performed considering manufacture, transportation, and installation costs. It was found that the use of group suction pile with pile spacing of 4D is superior to that of multiple single piles in terms of economics when horizontal loading exceeds 30 MN.

## **7.2 Conclusions and recommendations**

### **7.2.1 Conclusions**

Based in the findings of this study, the following main conclusions are drawn:

1. For dense sand layers, the loading locations along the suction piles shafts producing maximum horizontal resistances differ from suction pile types, single and group suction piles. The loading locations (50% of embedded length from the pile top) corresponding to the maximum horizontal resistances for group suction piles were closer to the seabed than those for single suction piles (67% of embedded length from the pile top), which is favorable condition to install suction piles from lower resistance induced by the pad-eye during installation.
2. Regardless of suction pile types and loading locations, the maximum horizontal resistance was greater for load inclination of 0 degree than for that of 20 degrees. It is beneficial for design suction piles and mooring systems to produce more horizontal loadings on the suction piles by implementing sinkers and buoy techniques.
3. The significant residual horizontal resistances were observed only for the group suction piles. This significant residual horizontal resistances could be still mobilized against an unexpected significant loading which exceeds the design load. More importantly, the residual horizontal resistance induces ductile failure of foundation, therefore,

the ductile behavior enables designers to provide an indication of foundation failure if monitoring of a large deformation of group suction piles is possible.

4. The ultimate and residual horizontal resistances of the group suction piles after cyclic loading with cyclic number of 200 under their magnitudes of 50% of their ultimate horizontal resistances were roughly 10% smaller than those under static loading conditions. This cyclic loading effect on horizontal resistances should be reflected in the group suction piles designs because the actual loading condition of the foundations for floating structures is closed to cyclic loading conditions.
5. The horizontal resistances of group suction piles are less sensitive against loading location and load inclination compared with those of single piles. Moreover, the residual horizontal resistances of group suction piles range 40% ~ 75% of their ultimate horizontal capacities. On the other hand, there observed no residual resistances for single suction pile. Such horizontal behavior of group suction piles can reduce uncertainties of horizontal ultimate and residual resistances resulting from unexpected soil conditions and spatial variation of soil parameters.
6. For both single and group suction piles, there exists a strong linear corrections between ultimate horizontal capacity and rotation. The ultimate horizontal capacity increased with decreasing rotation. It seems that the higher horizontal resistances of the group suction piles are offered by the group suction piles structure restraining suction pile rotation.

7. The load distributions among component piles of the group suction piles are highly dependent on pile spacing. For the component pile spacing higher than 4 times their pile diameters, there exists negligible group effect. For the smallest pile spacing (pile spacing of 2 times the pile diameter) in this study, the piles located at the first (leading) row takes more than half of the horizontal load. The significantly high load distribution ratios of the piles at the first row decrease with increasing pile spacing. Therefore, for the given direction of horizontal load, group pile geometry, and smaller pile spacing, a rectangular formation of component piles ( $3 \times 3$  component pile formation) may not be a desirable. Future research is required for further analysis of horizontal behavior of the  $2 \times 2$  group suction piles, including their group effects.
8. The cost analyses were performed considering manufacture, transportation, and installation costs based on the model test results. The suction pile installation cost took most of the suction pile construction cost. From the detailed cost analysis results with increasing horizontal resistance, the use of group suction pile with sufficient component pile spacing may not be economical for lower horizontal resistance; however, it becomes more economical with increasing horizontal resistance, compared to the use of single suction piles. It should be noted that the cost analysis in this study is conducted with simplified assumptions due to the absence of certified installation methods and procedures. Advanced and accurate qualitative cost analysis is possible after establishment of detailed construction methods or specifications of suction group piles.

### **7.2.2 Recommendations**

The following engineering contributions are presented, as well as recommendations for future studies to clarify the problems discussed.

1. Need of massive floating offshore structure constructions is steeply increasing internationally for the purpose of the wide use of offshore space, development of marine resources including the power generation using offshore wind turbines. In this study, a new type of suction pile, group suction piles were proposed to replace the large single suction piles for the use as anchor foundations of the massive floating offshore structures. Construction of the conventional large diameter single suction pile requires huge equipment due to its enormous dimension and significant self-weight; therefore, the cost for the installation of the single suction pile is no longer cost efficient. The group suction piles types suggested in this paper could be a good and reasonable alternative as foundations of floating structures, which require substantial horizontal capacities. In this study, cost analysis was conducted considering group suction piles' manufacturing, transporting, and installation cost in a real site (a site in the Western coastal area) and revealed that the group suction piles are superior over the single suction pile in terms of construction cost. For the cost analysis, the horizontal load was compared with the capacities of group piles varying diameter of component piles.
2. Horizontal behavior of the newly developed group suction piles in dense sands was qualitatively analyzed based on a series of model tests under different loading conditions. Based on the test results,

structural safeties of horizontally loaded group suction piles were evaluated and their residual horizontal resistances were identified. Even though the experimental study on horizontal behavior of the developed group suction piles has not been expanded to the practical field implementation, detailed experimental results themselves have an experimental value, which provides conceptual information for further practical implementation.

3. A unique relationship was observed between the ultimate horizontal resistance and the suction pile rotation, regardless of loading location along the pile shaft for both single and group piles. The unique relationship would provide a relative estimation of the ultimate horizontal resistances of suction piles if the rotation can be measured in the fields. In addition, it is noted that more horizontal resistance of a rigid pile, such as suction piles, can be obtained by restraining pile rotation.
4. The group effect of the  $3 \times 3$  group suction piles in dense sands is quantitatively analyzed in this study. As a result, the minimum component pile spacing of having no group effect is recommended. The findings will be beneficially useful for the estimation of horizontal capacities and the optimal designs of group suction piles after the verification by numerical analysis results and real scale field experiments.
5. The scope of this study is to analyze horizontal behavior of  $3 \times 3$  group suction piles having nine component piles. The purpose of the study on the  $3 \times 3$  group suction piles is to analyze effectively the many effects including pile spacing, load distributions of component

piles and the group effect on their horizontal behavior. In reality, the use of  $2 \times 2$  group suction piles varying their component pile diameters is more practical and cost efficient due to the reduced top cap size. Future research is required for further analysis of horizontal behavior of the  $2 \times 2$  group suction piles, including their group effects.

6. In this study, horizontal behavior of group suction piles is examined based on the small scaled model test results. For reliable implementation of the developed suction group pile type in construction practices, verification of horizontal behavior of the group suction piles is necessary through future centrifuge or field tests. Furthermore, the newly developed group suction piles have a complex structure compared to those of single suction piles; therefore, it is difficult to propose verified design or construction methods. Future research on the group suction piles is a priority for the development of their verified design and construction methods and implementations in construction practices.

## References

- Aas, P. M., Sparrevik, P., Hylen, S. (2002). "SAL suction anchor in shallow water and layered soil - a competitive alternative," The 12<sup>th</sup> International Offshore and Polar Engineering Conference, Kitakyushu, Japan, presented-only paper.
- Acar, Y. B., Durgunoglu, H. T., Tumay, M. T. (1982). "Interface properties of sand," Journal of Geotechnical Engineering, ASCE, Vol. 108, No. 4, pp.648-654.
- Allersma, H. G. B., Brinkgreve, R. B. J., Simon, T. (2000). "Centrifuge and Numerical Modelling of Horizontally Loaded Suction Piles," International Journal of Offshore and Polar Engineering, Vol. 10, No. 3.
- Allersma, H. G. B., Kierstein, A. A., Maes, D. (2001a). "Centrifuge modeling on suction piles under cyclic and long term vertical loading," Proceedings of the 10<sup>th</sup> International Offshore and Polar Engineering Conference, Seattle, USA, May 28-June 2.
- Allersma, H. G. B., Hogervorst, J. R., Pimouille, M. (2001b). "Centrifuge modelling of suction pile installation in layered soil by percussion method," Proceedings of the 20<sup>th</sup> International Conference on Offshore Mechanics and Arctic Engineering, Rio de Janeiro, Brazil. OMAE2001/OFT-1036.
- Allersma, H. G. B., Jacobse, J. A., Krabbendam, R. L. (2003). "Centrifuge Tests on Uplift Capacity of Suction Caissons with Active

Suction," Proceedings of the 13<sup>th</sup> (2003) International Offshore and Polar Engineering Conference, pp.724-739.

Andersen, K. H., Jostad, H. P. (1999). "Foundation design of skirted foundations and anchors in clay," Proceedings of the 31<sup>st</sup> annual Offshore Technology Conference, Houston, Texas, OTC 10824, May 3-6, Vol. 1, pp.383-392.

Andersen, K. H. and Jostad, H. P. (2004). "Shear strength along inside of suction anchor skirt wall in clay," Proceeding, Paper 16844, Offshore Technology Conference, Houston, May.

Andersen, K. H., Murff, J. D., Randolph, M. F., Clukey, E., Erbrich, C., Jostad, H. P., Hansen, B. Aubeny, C., Sharma, P., Supachawarote, C. (2005). "Suction anchors for deepwater applications," Proceedings of the International Symposium on Frontiers in Offshore Geotechniques (ISFOG), Perth, Australia, Sep. 19-21, pp.1-30.

API (1987). "Recommended practice for planning, designing and constructing fixed offshore platforms," American Petroleum Institute, API RP 2A, 17<sup>th</sup> Edition.

Bang, S., Cho, Y., Preber, T., Thomason, J. (1999). "Model testing and calibration of suction pile in sand," Proceedings of the 11<sup>th</sup> Asian Regional Conference of the International Society of Soil Mechanics and Geotechnical Engineering ISSMGE, Seoul, Korea, 1, pp.253-256.

Bang, S., Cho, Y. (2001). "Ultimate Horizontal Loading Capacity of Suction Piles," Proceedings of the 11<sup>th</sup> International Offshore and Polar

Engineering Conference, pp.552-559.

Bang, S., Cho, Y. (2003). "Investigation on Suction Pile Retrieval," International Conference on Foundations, Dundee, Scotland, Sep.

Bang, S., Cho, Y., Kwag, D. J. (2005). "Design and installation of suction piles for breakwater foundation." OCEANS, 2005. Proceedings of MTS/IEEE, Vol. 1, pp.1-6.

Bang, S., Leahy, J. C., Cho, Y., Kwon, O. (2006). "Horizontal Bearing Capacity of Suction Piles in Sand," Transportation Research Record, Journal of the Transportation Research Board, No. 1975, Transportation Research Board of the National Academies, Washington, D.C., pp.21-27.

Bang, S., Jones, K. D., Kim, K. O. (2011). "Inclined loading capacity of suction piles in sand," Ocean Engineering, 38, pp.915-924.

Been, K., Crooks, J. H. A., Becker, D. E., Jefferies, M. G. (1986). "The cone penetration test in sands: part I, state parameter interpretation," Geotechnique, pp.239-249.

Bienen, B., Gaudin, C., Cassidy, M. J., Rausch, L., Purwana, O. A., Krisdani, H. (2012). "Numerical modelling of a hybrid skirted foundation under combined loading," Computers and Geotechnics 45, pp.127-139.

Bozozuk, M., Keenan, G. H., Pheeney, P. E. (1979). "Analysis of load tests on instrumented steel test piles in compressible silty soils," Behavior of Deep Foundations, ASTM STP 670, ASTM, Philadelphia,

PA., pp.153-180.

Broms, B. B. (1964). "Lateral Resistance of Piles in Cohesionless Soils," Journal of the Soil Mechanics and Foundation Division, American Society of Civil Engineers, Vol. 89, No. SM3, May, pp.123-157.

Brown, G. A., Nacci, V. A. (1971). "Performance of hydrostatic anchors in granular soils," Proceedings of the 3<sup>rd</sup> annual Offshore Technology Conference, Houston, Texas, OTC 1472, pp. II 533-542.

Brown, D. A., Morrison, C., Reese, L. C. (1988). "Lateral Load Behavior of Pile Group in Sand," Journal of Geotechnical Engineering, Vol. 114, No. 11, p.1261-1276.

Bye, A., Erbrich, C., Earl, K. (1995). "Geotechnical design of bucket foundation," Proceedings of the Offshore Technology Conference, Houston, OTC7793, pp.869-883.

Byrne, B. W. (2000). "Investigation of Suction Caissons in Dense Sand," DPhil Thesis, The University of Oxford.

Byrne, B. W., Houlsby, G. T., Martin, C. M., Fish, P. M. (2002). "Suction caisson foundations for offshore wind turbines," Journal of Wind Engineering, Vol. 26, No. 3, pp.145-155.

Byrne, B. W., Houlsby, G. T. (2004). "Experimental investigations of the response of suction caissons to transient combined loading," Proceedings of the ASCE, Journal of Geotechnical and

Geoenvironmental Engineering 130, No. 3, pp.240-253.

Cao, J., Phillips, R., Popescu, R., Audibert, J. M. E., Al-Khafaji, Z. (2002). "Numerical Analysis of the Behavior of Suction Caissons in Clay," Proceedings of The 12<sup>th</sup> International Offshore and Polar Engineering Conference, Kitakyushu, Japan, May 26-31, pp.795-799.

Chairat, S., Randolph, M., Gourvenec, S. (2004). "Inclined pull-out capacity of suction caissons," Proceedings of the 14<sup>th</sup> International Offshore and Polar Engineering Conference.

Chen, W., Randolph, M. F. (2004). "Radial stress changes around caissons installed in clay by jacking and by suction," The 14<sup>th</sup> International Offshore and Polar Engineering Conference, California, USA, 2, pp.493-499.

Christensen, N. H., Haahr, F. (1992). "A computer program to analyse suction effects," Offshore Technology Conference, Houston, USA. OTC 6845.

Chung, S. H., Jeong, S. S. (2001). "Model test of pile groups in sand," Journal of Geotechnical Engineering, Vol. 17, No. 6, pp.193-205.

Coffman, R. A., Fugro-McClelland Marine Geosciences, Inc.; El-Sherbiny, R. M., Rauch, A. F., Olson, R. E. (2004). "Measured Horizontal Capacity of Suction Caissons," Offshore Technology Conference, Houston, Texas U.S.A., OTC 16161.

Clukey, E. C., Templeton, J. S., Randolph, M. F., Phillips, R. (2004).

"Suction caisson response under sustained loop current loads," Proceedings of the 36<sup>th</sup> annual Offshore Technology Conference, Houston, Texas, OTC 16843.

Colliat, J-L., Boisand, P., Gramet, J-C., Sparrevik, P. (1996). "Design and installation of suction anchor piles at a soft clay site in the Gulf of Guinea," Proceedings of the annual Offshore Technology Conference, Houston, Texas, pp.8150.

Datta, M., Gulhati, S. K., Rao, G. V. (1980). "An appraisal of the existing practice of determining the axial load capacity of deep penetration piles in calcareous sands," Proceedings of the 12<sup>th</sup> Annual Offshore Technology Conference, May, pp.119-125.

Deng, W., Carter, J. P. (2000). "A theoretical study of the vertical uplift capacity of suction caissons," Proceedings of the 10<sup>th</sup> International Offshore and Polar Engineering Conference, pp.342-349.

Deng, W., Charter, J. P. (2002). "A theoretical study of the vertical uplift capacity of suction caisson," Proceedings of the 12<sup>th</sup> International Offshore and Polar Engineering Conference, Kitakyushu, Japan, No. 2, p.89-97.

Dyvik, R., Andersen, K. H., Hansen, S. B., Christophersen, H. P. (1993). "Field tests of anchors in clay," Journal of Geotechnical Engineering, Vol. 119, No. 10, pp.1515-1531.

El-Ghabawwy, S. L., Olson, R. E., Scott, A. (1999). "Suction Anchor Installations for Deep Gulf of Mexico Applications," Proceedings of the

Offshore Technology Conference, Paper 10992, Houston, May.

Fakharian, K., Rismanchian, A. (2004). "A new method for reduction of trial and error in design of suction piles and its application in the Caspian Sea," Proceedings of the 14<sup>th</sup> International Offshore and Polar Engineering Conference, Toulon, France, 2, pp.545-551.

Feld, T., Rasmussen, J. L., Sorensen, P. H. (1999). "Structural and economic optimization of offshore wind turbine support structure and foundation," Proceedings of the 18<sup>th</sup> International Conference on Offshore Mechanics and Artic Engineering, St John's, Canada.

Feld, T. (2001). "Suction buckets, a new innovative foundation concept, applied to offshore wind turbines," Ph.D thesis, Aalborg University, Demark.

Fines, S., Stove, O. J., Guldberg, F. (1991). "Snorre TLP tethers and foundation," Offshore Technology Conference, Houston, USA, OTC 6623.

Fuglsang, L. D., Steensen-Bach, J. O. (1991). "Breakout resistance of suction piles in clay," Proceedings of the International Conference: Centrifuge 91, A.A. Balkema, Rotterdam, Netherlands, pp.153–159.

Goodman, L. J., Lee, C. N., Walker, F. J. (1961). "The feasibility of vacuum anchorage in soil," Geotechnique, Vol. 1, No. 4, pp.356-359.

Helfrich, S. C., Brazill, R. L., Richards, A. F. (1976). "Pullout characteristics of a suction anchor in sand," Proceedings of the 8<sup>th</sup>

annual Offshore Technology Conference, Houston, Texas, OTC 2469, May 3-6, pp.501-506.

Hogervorst, J. R. (1980). "Field trials with large diameter suction piles," Offshore Technology Conference, Houston, USA, OTC 3817.

Housby, G. T., Byrne, B. W. (2000). "Suction caisson foundations for off-shore wind turbines and anemometer masts," Wind Engineering, Vol. 24, No. 4, pp.249–255.

Housby, G. T., Byrne, B. W. (2005). "Design procedures for installation of suction caissons in sand," Geotechnique Engineering, Vol. 158, No. 3, pp.135–144.

House, A. R., Randolph, M. F., Borbas, M. E. (1999). "Limiting aspect ratio for suction caisson installation in clay," Proceedings of the 9<sup>th</sup> International Offshore and Polar Engineering Conference, Brest, France, pp.676-683.

House, A. R. (2002). "Suction caisson foundations for buoyant offshore facilities," Ph.D thesis, University of Western Australia, Australia.

Iskander, M., El-Gharbawy, S., Olson, R. (2002). "Performance of suction caisson in sand and clay," Canadian Geotechnical Journal, Vol. 39, pp.576-584.

Ishihara, K., Yoshimine, M. (1992). "Evaluation of settlements in sand deposits following liquefaction during earthquake," Soils and Foundations. Vol. 32, No. 1, pp.29-44.

Jang, Y. S., Kim, Y. S. (2013). "Centrifugal Model Behavior of Laterally Loaded Suction Pile in Sand," KSCE Journal of Civil Engineering, Vol. 17, No. 5, pp.980-988.

Jee, S. H., Yoon, J. U., Kim, D. J., Choi, J. Y. (2013). "Development of technique for installation of deep sea offshore plant," Korea Geo-environmental Society, Vol. 14, No. 3, pp.2-9.

Kim, B. T., Yoon, G. L. (2011). "Laboratory modelling of laterally loaded pile groups in sand," KSCE Journal of Civil Engineering, Vol. 15, No. 1, pp.65-75.

Kim, J. H., Kim, S., Kim, D. S., Youn, J. U., Kim, D. J., Jee, S. H. (2014). "Centrifuge model test on load capacity of hybrid suction foundation for vertical and horizontal loading," KGS Spring National Conference, pp.423-430.

Lade, P. V., Yamamuro, J. A. (1997). "Effects of nonplastic fines on static liquefaction of sands," Canadian Geotechnical Journal, Vol. 24, No. 6, pp.918-928.

Larsen, P. (1989). "Suction anchors as an anchoring system for floating offshore constructions," Proceedings of the Offshore Technology Conference, Houston, Texas, paper 6029, pp.535-540.

Lehane, B. M., Jardine, R. J., Bond, A. J., Frank, R. (1993). "Mechanisms of shaft friction in sand from instrumented pile tests," Journal of Geotechnical Engineering, Vol. 119, No. 1, pp.19-35.

Leland, M., Kraft, Jr. (1991). "Performance of axially loaded pipe piles in sand," ASCE, Vol. 117, No. 2, pp.832-835.

Lu, X., Wu, Y., Jiao, B., Wang, S. (2007). "Centrifugal experimental study of suction bucket foundations under dynamic loading," Acta Mech Sin, Vol. 23, pp.689-698.

Li, Y., Zhang, J. (2012). "On the Suction Pile Relocation Distance," Proceedings of the 22<sup>nd</sup> International Offshore and Polar Engineering Conference, pp.650-657.

Mackereth, F. J. H. (1958). "A Portable Core Sampler for Lake Deposits," Limnology and Oceanography, 3, pp.181-191.

Manh, N. T. (2005). "Installation of Suction Caissons in Dense Sand and the Influence of Silt and Cemented Layers," Ph.D thesis, The University of Sydney.

Masui, N., Ito, M., Inoue, A., Shimada, Y., Hermstad, J. (2004). "Recovery of wall friction after penetration in skirt suction foundation," The 14<sup>th</sup> International Offshore and Polar Engineering Conference, 23-28 May, Toulon, France.

Masui, N., Yoneda, H., Zenda, Y., Ito, M., Iida, Y., Hermstad, J. (2001). "Installation of offshore concrete structure with skirt foundation," Proceedings of the 11<sup>th</sup> International Offshore and Polar Engineering Conference, Stavanger, Norway, 2, pp.626-630.

McClelland, B., Focht, J. A. (1956). "Soil modulus for laterally loaded piles," Journal of Soil Mechanics and Foundation Engineering, ASCE, Vol. 82, No. SM4.

Parkin, A. K., Lunne, T. (1982). "Boundary effects in the laboratory calibration of a cone penetrometer for sand," Proceedings of the 2<sup>nd</sup> European Symposium, Penetration Testing, Amsterdam, Vol. 2, pp.761-768.

McVay, M., Casper, R., Shang, T. (1995). "Lateral response of three-row groups in loose to dense sands at 3D and 5D pile spacing," Journal of Geotechnical Engineering, Vol. 121, No. 5, pp.436-441.

McVay, M., Zhang, L., Molnit, T., Lai, P. (1998). "Centrifuge testing of large laterally loaded pile groups in sands," Journal of Geotechnical and Geoenvironmental Engineering, Vol. 124, No. 10, pp.1016-1026.

North Sea report (1972). "Submersible sounding tools to test North Sea floor," The Oil and Gas Journal, pp.74-77.

Parkin, A. K., Lunne, T. (1982). "Boundary effects in the laboratory calibration of a cone penetrometer in sand," Proceedings of the 2<sup>nd</sup> Europe Symposium on Penetration Testing, Vol. 2, pp.761-768.

Petrasovits, G., Award, A. (1972). "Ultimate lateral resistance of a rigid pile in cohesionless soil," Proceedings of the 5<sup>th</sup> European Conference on SMEF, Vol. 3, pp.407-412.

Peterson, R. W. (1988), "Laboratory investigation of the penetration

resistance of fine cohesionless materials," Proceeding of the International Symposium on Penetration Testing, ISOPT-1, Orlando, 2, pp.895-902.

Potyondy, J. G. (1961). "Skin friction between various soils and construction materials," Geotechnique, Vol. 11, No. 4, pp.339-353.

Porcino, D., Fioravante, V., Chionna, V. N., Pedrono, S. (2003). "Interface behavior of sands from constant normal stiffness direct shear tests," Geotechnical Testing Journal, Vol. 26, No. 3, pp.74-86.

Prakash, S. (1962). "Behavior of pile groups subjected to lateral loads," Thesis presented to the University of Illinois, at Urbana, Ill., in partial fulfillment of the requirements for the degree of Doctor of Philosophy.

Prasad, Y. V. S. N., Chari, T. R. (1999). "Lateral capacity of model rigid piles in cohesionless soils," Journal of Soil Mechanics and Foundation Engineering, Vol. 39, No. 2, pp.21-29.

Randolph, M., O'Neill, M., Stewart, D. (1998). "Performance of suction anchors in fine-grained calcareous soils," Proceedings of the Offshore Technology Conference, OTC 8831, pp.521-529.

Randolph, M. F. (2002). "Analysis of suction caisson capacity in clay," Proceedings of the 34<sup>th</sup> annual Offshore Technology Conference, Houston, Texas, OTRC-14236, May 6-9, pp.2145-2155.

Rauch, A. F., Olson, R. E., Luke, A. M., Mecham, E. C. (2003). "Measured response during laboratory installation of suction caissons," Proceedings of the 13<sup>th</sup> International Offshore and Polar Engineering

Conference, Honolulu, Hawaii, May 25-30, pp.1327-1334.

Reese, L. C., Matlock, H. (1956). "Non-dimensional solutions for laterally-loaded piles with soil modulus assumed proportional to depth," Proceedings of the 8<sup>th</sup> Texas Conference on Soil Mechanics and Foundation Engineering, Austin, Texas, pp.1-41.

Rollines, K. M., Peterson, K. T., Weaver, T. J. (1998). "Lateral load behavior of full-scale pile group in clay," Journal of Geotechnical and Geoenvironmental Engineering, Vol. 124, No. 6, pp.468-478.

Rollines, K. M., Lane, J. D., Gerber, T. M. (2005). "Measured and computed lateral response of a pile group in sand," Journal of Geotechnical and Geoenvironmental Engineering, Vol. 131, No. 1, pp.103-114.

Salgado, R., Mitchell, J. K., Jamiolkowski, M. (1998). "Calibration chamber size effects on penetration resistance in sand," Journal of Geotechnical and Geoenvironmental Engineering, ASCE, Vol. 124, No. 9, pp.878-888.

Schnaid, F., Houlsby, G. T. (1991). "An assessment of chamber size effects in the calibration of in situ tests in sand," Geotechnique, Vol. 41, No. 3, pp.437-445.

Senpere, D., Auvergne, G. A. (1982). "Suction anchor piles - a proven alternative to driving or drilling," Proceedings of the 14<sup>th</sup> annual Offshore Technology Conference, Houston, Texas, OTC 4206, May 3-6, pp.483-493.

Skempton, A. W. (1986). "Standard penetration test procedures and the effects in sands of overburden pressure, relative density, particle size, ageing and overconsolidation," *Geotechnique*, Vol. 36, No. 3, pp.425-477.

Sohota, B. S., Wilson, Q. (1982). "The break-out behaviour of suction anchors embedded in submerged sands," *Offshore Technology Conference*, Houston, USA, OTC 4175.

Sparrevik, P. (2002). "Suction pile technology and installation in deep water," *Offshore Technology Conference*, Houston, USA, OTC 14241.

Steensen-Bach, J. O. (1992). "Recent model tests with suction piles in clay and sand," *Proceedings of the 24<sup>th</sup> annual Offshore Technology Conference*, Houston, Texas, OTC 6844, May 4-7, pp.323-330.

Stevenson, P. R. (2003). "Large scale instrumented offshore suction caisson tests to study set-up around suction caissons," *Suction caisson research report*, Fugro-McClelland Geosciences, Inc.

Stove, O. J., Bysveen, S., Christophersen, H. P. (1992). "New foundation systems for the snorre development," *Offshore Technology Conference*, Houston, USA, OTC 6882.

Subba, R. K. S., Allam, M. M., Robinson, R. G. (1998). "Interfacial friction between sands and solid surfaces," *Proceedings of International Civil Engineers Geotechnical Engineering*, London, Vol. 131, pp.75-82.

- Supachawarote, C., Randolph, M., Gourvenec, S. (2004). "Inclined pull-out capacity of suction caissons," Proceedings of the 14<sup>th</sup> International Offshore and Polar Engineering Conference, pp.500-506.
- Tjelta, T.L., Hermstad, J., Andenaes, E. (1990). "The skirt piled gullfaks C platform installation," Proceedings of the Offshore Technology Conference, Houston, OTC 6473, pp.453-462.
- Tjelta, T. I. (1995). "Geotechnical experience from the installation of the Europipe jacket with bucket foundations," Proceedings of the 27<sup>th</sup> annual Offshore Technology Conference, Houston, Texas, OTC 5103, May 5-8, pp.201-212.
- Tjelta, T. I. (2001). "Suction piles: their position and applications today," Proceedings of the 11<sup>th</sup> International Offshore and Polar Engineering Conference, Stavanger, Norway, June 17-22, Vol. 2.
- Uesugi, M., Kishida, H. (1986). "Frictional resistance at yield between dry sand and mild steel," Soils and Foundations, Vol. 26, No. 4, pp.139-149.
- Vipulanandan, C. (1989). "Modeling of displacement piles in sand using a pressure chamber," Proceedings of the Foundation Engineering Congress, ASCE, pp.526-541.
- Wang, M. C., Demars, K. R., Nacci, V. A. (1977). "Breakout capacity of model suction anchors in soil," Canadian Geotechnical Journal, Vol. 15, pp.246-257.
- Wang, M. C., Nacci, V. A., Demars, K. R. (1975). "Behavior of

underwater suction anchors in soil," Ocean Engineering, Vol. 3, No. 1, pp.47-62.

Wang, Y., Lu, X., Wang, S., Shi, Z. (2006). "The response of bucket foundation under horizontal dynamic loading," Ocean Engineering 33, pp.964-973.

Watson, P. G., Randolph, M. F. (1997). "Vertical capacity of caisson foundations in calcareous sediments," Proceedings of the 7<sup>th</sup> International Offshore and Polar Engineering Conference, Honolulu, USA, pp.784-790.

Watson, P. G. (1999). "Performance of Skirted Foundations for Offshore Structures, Ph.D Thesis, The University of Western Australia.

Wilson, Q., Sohota, B. S. (1980). "Pull-out parameters for buried suction anchors", Offshore Technology Conference, Houston, USA, OTC 3816.

Yoon, H. J., Jang, I. S., Oh, M. H., Kwon, O. S., Jung, S. J. (2010). "Trend in suction bucket foundation for offshore wind turbine," KGS Fall National Conference, pp.494-0503.

Yoshimi, Y., Kishida, T. (1981) "Friction between sand and metal surface." Proceedings of the 10<sup>th</sup> International Conference on Soil Mechanics and Foundation Engineering, International Society of Soil Mechanics and Foundation Engineering, 1, pp.831-834.

Zdravkovic, L., Potts, D. M., Jardine, R. J. (2001). "A parametric study

of the pull-out capacity of bucket foundations in soft clay," Geotechnique, Vol. 51, No. 1, pp.55-67.

Zhang, J. H., Zhang, L. M., Lu, X. B. (2007). "Centrifuge modelling of suction bucket foundations for platforms under ice-sheet-induced cyclic lateral loadings," Ocean Engineering 34, pp.1069-1079.

(Page intentionally left blank)

## 초 록

본 연구에서는 최근 국내에서도 많은 연구가 추진되고 있는 부유식 구조물의 기초로서 기존 석션파일의 단점을 보완한 그룹형 석션파일을 새롭게 제안하고, 그룹형 석션파일의 수평방향 거동특성을 파악하기 위하여 축소모형실험을 수행하였다.

축소모형실험의 한계를 극복하기 위하여 상사비는 물론 휨강성과 측강성을 고려한 모형말뚝을 제작하였으며, 지반과 말뚝의 상대적인 거칠기를 고려하였다. 또한, 입자영상분석기법의 일종인 PIV(Particle Image Velocimetry) 기법을 도입하여 석션파일의 복잡한 수평방향 거동을 정밀하게 분석하였다. 그리고 단일형 석션파일의 경우 기존 연구자들의 제안식과 모형실험 결과를 비교하였다.

실험방법에 대한 신뢰성 확보와 그룹형 석션파일의 효율성 검증을 위하여 다양한 하중조건에 대한 단일형 석션파일의 모형실험을 수행하였다. 단일형 석션파일에 대한 모형실험을 통하여 석션관입이 파일의 수평저항력에 미치는 영향을 규명하였으며, 하중재하위치와 하중재하각도에 따른 수평저항력의 변화를 관찰하였다.

그룹형 석션파일에 대한 모형실험에서는 하중재하위치, 하중재하각도, 말뚝의 간격에 따른 수평방향거동을 분석하였다. 또한 부유식 구조물의 수평방향 반복운동을 고려하여 반복하중이 수평지지력에 미치는 영향을 분석하였다. 개별 말뚝이 받는 수평토압 측정결과를 통하여 말뚝 배열에 따른 하중분담비율을 결정하고 그룹형 석션파일의 무리말뚝효율을 분석하였다.

단일형 석션파일과 그룹형 석션파일의 모형실험 결과의 비교분석을 통하여 석션파일의 수평저항력은 회전량과 밀접한 관련이 있음을 확인하였으며, 그룹형 석션파일이 단일형 석션파일에 비해 수평하중에 대한 회전량이 작게 발생함을 확인하였다. 또한 단일형 석션파일은 파괴이후 잔류수평저항력이 거의 없는데 반해 그룹형 석션파일은 극한 수평저항력의 40% ~ 75% 정도의 잔류수평저항력을 가지는 것으로

나타나 그룹형 석션파일이 싱글석션파일에 비해 수평하중에 대한 저항성이 뛰어남을 알 수 있었다. 그리고 말뚝간격이 말뚝직경의 4배 이상인 그룹형 석션파일에서는 무리말뚝 효과가 나타나지 않았으며, 동일한 말뚝개수를 가지는 단일형 석션파일에 비해 더 큰 수평저항력이 가지는 것을 알 수 있었다.

결론적으로, 본 연구에서 새롭게 제안된 그룹형 석션파일은 기존의 단일형 석션파일에 비해 수평하중에 대한 회전발생량이 작고, 수평하중에 유리한 기초형식임을 알 수 있었다.

**주요어:** 석션파일, 그룹형 석션파일, 수평거동, 모형실험, PIV분석, 무리말뚝 효과

**학 번:** 2010-31010